Table 1-2 Key Evidence contributing to "causal" and "likely to be causal" causality determinations for $PM_{2.5}$ exposure and health effects evaluated in the current draft Integrated Science Assessment for Particulate Matter.

Key Evidence	Health Effect Category[a] and Causality Determination	$PM_{2.5}$ Concentrations Associated with Effects
Respiratory Effects and Short-Term $PM_{2.5}$ Exposure (Section 5.1.12): Likely to be Causal Relationship *No change in causality determination from the 2009 PM ISA; new evidence further supports the previous determination.*		
Section 5.1.12 Table 5-18	Epidemiologic evidence, consisting mainly of hospital admissions and emergency department visits, strongly supports a relationship with asthma exacerbation, COPD exacerbation, and combinations of respiratory-related diseases. Evidence for associations with respiratory symptoms and medication use are coherent with other findings for asthma exacerbation and COPD exacerbation. Some epidemiologic studies examined copollutant confounding and reported that results are robust in models with gaseous pollutants (i.e., O_3, NO_2, SO_2, and with more limited evidence for CO) and other particle sizes (i.e., $PM_{10-2.5}$), especially for asthma exacerbation, aggregated respiratory conditions, and respiratory mortality. There is a large body of experimental evidence, some of which is coherent with epidemiologic study results, demonstrating respiratory effects due to short-term $PM_{2.5}$ exposure. These experimental studies provide evidence for biologically plausible pathways by which $PM_{2.5}$ exposure can impart a respiratory effect. Specifically, animal toxicological studies provide biological plausibility for asthma exacerbation, COPD exacerbation and respiratory infection and some evidence of an independent effect of $PM_{2.5}$ on respiratory endpoints. Controlled human exposure studies provide minimal evidence of respiratory effects, specifically decrements in lung function and pulmonary inflammation. Consistent positive associations with respiratory mortality provide evidence of a continuum of effects.	Mean ambient concentrations from epidemiologic studies for: *Hospital Admissions and Emergency Department Visits for Asthma, COPD, Respiratory Infections and Combinations of Respiratory-related Diseases:* U.S. and Canada: 4.7–24. 6 µg/m³ Europe: 8.8–27.7 µg/m³ Asia: 11.8–69.9 µg/m³ *Respiratory mortality:* U.S. and Canada: 7.9–19.9 µg/m³ Europe: 8.0–27.7 µg/m³ Asia: 11.8–69.9 µg/m³ Concentrations from animal toxicological studies for: *Allergic airway disease:* 442–596 µg/m³

Table 1-2 (Continued): Key Evidence contributing to "causal" and "likely to be causal" causality determinations for $PM_{2.5}$ exposure and health effects evaluated in the current draft Integrated Science Assessment for Particulate Matter.

Key Evidence	Health Effect Category[a] and Causality Determination	$PM_{2.5}$ Concentrations Associated with Effects
Section 5.1.12 Table 5-18 (continued)		*COPD:* 171–1,200 µg/m³ *Altered host defense:* 100–350 µg/m³
Respiratory Effects and Long-Term $PM_{2.5}$ Exposure (Section 5.2.13): Likely to be Causal Relationship *No change in causality determination from the 2009 PM ISA; new evidence further supports the previous determination.*		
Section 5.2.13 Table 5-28	Epidemiologic evidence strongly supports a relationship with decrements in lung function growth in children. Additional epidemiologic evidence supports a relationship with asthma development in children, with increased bronchitic symptoms in children with asthma, with an acceleration of lung function decline in adults, and with respiratory mortality and cause-specific respiratory mortality for COPD and respiratory infection. Some epidemiologic studies examined copollutant confounding and reported that results are robust in models with O_3, NO_2, and CO, especially for respiratory mortality. There is limited experimental evidence for these respiratory effects due to long-term $PM_{2.5}$ exposure. However, animal toxicological studies provide biological plausibility for decrements in lung function and asthma development in children, and reduce uncertainty regarding the independent effect of $PM_{2.5}$ for these endpoints. Animal toxicological studies also provide evidence for a wide variety of other biological effects, such as oxidative stress, inflammation and morphologic changes. Epidemiologic studies examining the effects of declining $PM_{2.5}$ concentrations, strengthen the relationship between long-term $PM_{2.5}$ exposure and respiratory health by demonstrating improvements in lung function growth and reduced bronchitic symptoms in children and improved lung function in adults as a result of lower $PM_{2.5}$ concentrations. However, within these studies there is limited examination of copollutant confounding, which is a notable uncertainty due to the corresponding decline in concentrations of other pollutants.	Mean ambient concentrations from epidemiologic studies for: *Decrement in lung function growth:* 6–28 µg/m³ *Asthma development in children:* 5.2–16.5 µg/m³ *Bronchitic symptoms in children with asthma:* 9.9–13.8 µg/m³ *Accelerated lung function decline in adults:* 9.5–17.8 µg/m³ *Respiratory mortality:* 6.3–23.6 µg/m³ Concentrations from animal toxicological studies for: *Impaired lung development:* 16.8 µg/m³ *Development of allergic airway disease:* 100 µg/m³

Table 1-2 (Continued): Key Evidence contributing to "causal" and "likely to be causal" causality determinations for $PM_{2.5}$ exposure and health effects evaluated in the current draft Integrated Science Assessment for Particulate Matter.

Key Evidence	Health Effect Category[a] and Causality Determination	$PM_{2.5}$ Concentrations Associated with Effects
Cardiovascular Effects and Short-Term $PM_{2.5}$ Exposure (Section 6.1.16): Causal Relationship *No change in causality determination from the 2009 PM ISA; new evidence further supports the previous determination.*		
Section 6.1.16 Table 6-33	There is strong evidence for coherence of effects across scientific disciplines and biological plausibility for a range of cardiovascular effects in response to short-term $PM_{2.5}$ exposure. Consistent epidemiologic evidence from multiple, high-quality studies at relevant $PM_{2.5}$ concentrations provide evidence of increases in emergency department visits and hospital admissions for IHD and HF, as well as cardiovascular mortality in multi-city studies conducted in the U.S., Canada, Europe, and Asia. These associations remain positive, but in some cases are reduced with larger uncertainty estimates, in copollutant models with gaseous pollutants. Evidence from controlled human exposure studies provide coherent and consistent evidence for changes in various measures of endothelial dysfunction and generally consistent evidence of changes in blood pressure. These controlled human exposure studies are in agreement with animal toxicological studies also demonstrating endothelial dysfunction and changes in blood pressure or the renin angiotensin system. In addition, animal toxicological studies demonstrating that short-term $PM_{2.5}$ exposure results in decreased cardiac contractility and left ventricular pressure are coherent with epidemiologic studies reporting associations between short-term $PM_{2.5}$ exposure and HF.	Mean ambient concentrations from epidemiologic studies for: *IHD:* 5.8–18.6 $\mu g/m^3$ *HF:* 5.8–18.0 $\mu g/m^3$ Concentrations from controlled human exposure studies: 24–325 $\mu g/m^3$ for 2 h Concentrations from animal toxicological studies: 178–190 $\mu g/m^3$

Table 1-2 (Continued): Key Evidence contributing to "causal" and "likely to be causal" causality determinations for $PM_{2.5}$ exposure and health effects evaluated in the current draft Integrated Science Assessment for Particulate Matter.

Key Evidence	Health Effect Category[a] and Causality Determination	$PM_{2.5}$ Concentrations Associated with Effects
Cardiovascular Effects and Long-Term $PM_{2.5}$ Exposure (Section 6.2.18): Causal Relationship *No change in causality determination from the 2009 PM ISA; new evidence further supports the previous determination.*		
Section 6.2.18 Table 6-52	Multiple high-quality epidemiologic studies continue to provide evidence of consistent, positive associations between long-term $PM_{2.5}$ exposure and cardiovascular mortality at lower ambient concentrations. The cardiovascular mortality associations were observed across different exposure assignment and statistical methods, and were relatively unchanged in copollutant models with both gaseous (i.e., O_3, NO_2, SO_2) and particle (i.e., $PM_{10-2.5}$) pollutants. The evidence for cardiovascular mortality, is supported by a smaller body of epidemiologic studies that further explored associations between long-term $PM_{2.5}$ exposure and cardiovascular morbidity, and reported some evidence for increased risk of $PM_{2.5}$-related MI and stroke, specifically in individuals with a pre-existing cardiovascular disease or diabetes. Recent epidemiologic studies also present evidence for an effect of long-term $PM_{2.5}$ exposure on subclinical features of cardiovascular morbidity, particularly progression of atherosclerosis as reflected by associations with coronary artery calcification (CAC), with more limited evidence for other measures, such as carotid intima-media thickness (CIMT). Key evidence from long-term animal toxicological studies includes consistent evidence for changes in BP, as well as some evidence for decreases in measures of heart function (e.g., contractility and cardiac output) and cardiac remodeling. Moreover, as in the previous review, there is also some additional evidence for atherosclerotic plaque progression in a genetically susceptible mouse model.	Mean ambient concentrations from epidemiologic studies for: *Cardiovascular mortality*: 4.1–17.9 $\mu g/m^3$ *Coronary events*: 13.4 $\mu g/m^3$ *CAC*: 14.2 $\mu g/m^3$ *CHD and Stroke (in those with pre-existing disease)*: 13.4–23.9 $\mu g/m^3$ Concentrations from animal toxicological studies for: *Blood pressure*: 85–375 $\mu g/m^3$ (up to 15 weeks)
Nervous System Effects and Long-Term $PM_{2.5}$ Exposure (Section 8.2.9): Likely to be Causal Relationship *Not evaluated in the 2009 PM ISA; new evidence showing brain inflammation and oxidative stress, neurodegeneration, cognitive effects, and neurodevelopmental effects.*		
Section 8.2.9 Table 8-20	There is evidence that long-term exposure to $PM_{2.5}$ can modulate the autonomic nervous system leading to downstream consequences including cardiovascular effects (Section 6.2.1). A second pathway involving neuroinflammation and morphologic changes in the brain indicative of neurodegeneration, is well substantiated and coherent across experimental animal and epidemiologic studies. The evidence relating to Parkinson disease, and neurodevelopmental effects was more limited. Consideration of copollutant confounding was generally lacking in the epidemiologic studies but the uncertainty in the interpretation of study findings was addressed, in part, by the direct evidence of effects provided by experimental animal studies.	Mean annual concentrations from epidemiologic studies for: *Brain volume:* 11.1–12.2 $\mu g/m^3$ *Cognition:* 8.5 (5-yr avg)–14.9 $\mu g/m^3$ *Autism:* 14.0–19.6 $\mu g/m^3$

Table 1-2 (Continued): Key Evidence contributing to "causal" and "likely to be causal" causality determinations for $PM_{2.5}$ exposure and health effects evaluated in the current draft Integrated Science Assessment for Particulate Matter.

Key Evidence	Health Effect Category[a] and Causality Determination	$PM_{2.5}$ Concentrations Associated with Effects
Section 8.2.9 Table 8-20 (continued)		Concentrations from animal toxicological studies for: *Brain inflammation/Oxidative stress:* 65.7–441.7 μg/m^3 *Neurodegenerative changes:* 94.4 μg/m^3 *Neurodevelopment:* 92.7 μg/m^3
Cancer and Long-Term $PM_{2.5}$ Exposure (Section 10.2): Likely to be Causal Relationship *Change in causality determination from the 2009 PM ISA (suggestive of a causal relationship) due to increased evidence of genotoxicity, carcinogenicity, and epigenetic effects for $PM_{2.5}$ and lung cancer incidence and mortality.*		
Section 10.2.6 Table 10-8	Primarily positive associations from multiple, high-quality studies for increases in lung cancer incidence and mortality. This evidence is supported by analyses focusing on never smokers and limited evidence of associations with histological subtypes of lung cancer found in never smokers. Across studies that examined lung cancer incidence and mortality potential confounding by smoking status and exposure to SHS was adequately controlled. A limited number of studies examined potential copollutant confounding, but associations were relatively unchanged in models with O_3 with more limited assessment of other gaseous pollutants and particle size fractions. Experimental and epidemiologic studies provide evidence for a relationship between $PM_{2.5}$ exposure and genotoxicity, epigenetic effects, and carcinogenic potential. Uncertainties exist due to the lack of consistency in specific cancer-related biomarkers associated with $PM_{2.5}$ exposure across both experimental and epidemiologic studies; however, $PM_{2.5}$ exhibits several characteristics of carcinogens. This provides biological plausibility for $PM_{2.5}$ exposure contributing to cancer development. Additionally, there is limited evidence of cancer occurring in other organ systems, but there is some evidence that $PM_{2.5}$ exposure may detrimentally impact survival from any type of cancer.	Mean annual concentrations from epidemiologic studies for: *Lung cancer incidence and mortality:* U.S. and Canada: 6.3–23.6 μg/m^3 Europe: 6.6–31.0 μg/m^3 Asia: 33.7 μg/m^3 Concentrations from animal toxicological studies for: *Carcinogenic potential:* 17.66 μg/m^3

Table 1-2 (Continued): Key Evidence contributing to "causal" and "likely to be causal" causality determinations for $PM_{2.5}$ exposure and health effects evaluated in the current draft Integrated Science Assessment for Particulate Matter.

Key Evidence	Health Effect Category[a] and Causality Determination	$PM_{2.5}$ Concentrations Associated with Effects
Total Mortality and Short-Term $PM_{2.5}$ Exposure (Section 11.1.12): Causal Relationship *No change in causality determination from the 2009 PM ISA; new evidence further supports the previous determination.*		
Section 11.1.12 Table 11-4	There is consistent epidemiologic evidence from multiple, high quality studies of increases in total (nonaccidental) mortality in multi-city studies conducted in the U.S., Canada, Europe, and Asia at ambient concentrations often below 20 $\mu g/m^3$. The associations observed were relatively unchanged in copollutant models with gaseous pollutants and $PM_{10-2.5}$, which is consistent with copollutant analyses for cardiovascular and respiratory mortality, but copollutant analyses were limited to studies conducted in Europe and Asia. Biological plausibility for the epidemiologic evidence for total mortality is provided by the strong cardiovascular morbidity evidence, particularly for ischemic events and heart failure, while support for biological plausibility is more limited from the respiratory morbidity evidence, with the strongest evidence for exacerbations of COPD and asthma. Although alternatives to linearity have not been systematically evaluated, recent mortality studies continue to support a log-linear, no-threshold C-R relationship.	Mean 24-h avg concentrations from epidemiologic studies for: *Total Mortality*: U.S. and Canada: 4.37–17.97 $\mu g/m^3$ Europe: 13–27.7 $\mu g/m^3$ Asia: 11.8–69.9 $\mu g/m^3$

Table 1-2 (Continued): Key Evidence contributing to "causal" and "likely to be causal" causality determinations for $PM_{2.5}$ exposure and health effects evaluated in the current draft Integrated Science Assessment for Particulate Matter.

Key Evidence	Health Effect Category[a] and Causality Determination	$PM_{2.5}$ Concentrations Associated with Effects
Total Mortality and Long-Term $PM_{2.5}$ Exposure (Section 11.2.7): Causal Relationship *No change in causality determination from the 2009 PM ISA; new evidence further supports the previous determination.*		
Section 11.2.7 Table 11-8	There is consistent epidemiologic evidence from multiple, high-quality studies of increases in total (nonaccidental) mortality from extended follow-ups of the American Cancer Society (ACS) cohort and Harvard Six Cities (HSC) cohort, as well as multiple studies focusing on a Medicare cohort, Canadian cohorts, and North American employment cohorts. The consistent increases in total mortality are observed across different exposure metrics based on ambient measurements, models, remote sensing, or hybrid methods that combine two or more of these methods, providing additional support for the mortality associations due to long-term $PM_{2.5}$ exposure reported in the 2009 PM ISA that relied on exposure metrics from ambient monitors. The consistent epidemiologic evidence for total mortality is supported by positive associations for cardiovascular, respiratory, and lung cancer mortality. Biological plausibility for total mortality is provided by the strong cardiovascular morbidity evidence, particularly for CHD, stroke, and atherosclerosis, while there is more limited evidence for biological plausibility from the respiratory morbidity evidence, with some evidence for development of COPD. Extensive epidemiologic evidence provides additional support for a log-linear, no-threshold concentration-response (C-R) relationship. A recent series of studies demonstrates that decreases in long-term $PM_{2.5}$ concentrations were associated with an increase in life expectancy across the U.S. for multiple time periods examined.	Mean annual concentrations from epidemiologic studies for: *Total mortality*: ACS/HSC Cohorts: 11.4–23.6 $\mu g/m^3$ Medicare Cohort: 8.12–12.0 $\mu g/m^3$ Canadian Cohorts: 8.7–9.1 $\mu g/m^3$ Employment Cohorts: 12.7–17.0 $\mu g/m^3$

CHD = coronary heart disease; COPD = chronic obstructive pulmonary disease; SHS = second hand smoke.

[a]A large spectrum of outcomes is evaluated as part of a broad health effect category including physiological measures (e.g., airway responsiveness, lung function), clinical outcomes (e.g., respiratory symptoms, hospital admissions), and cause-specific mortality. Total mortality includes all nonaccidental causes of mortality and is informed by the nature of the evidence for the spectrum of morbidity effects (e.g., respiratory, cardiovascular) that can lead to mortality. The sections and tables referenced include a detailed discussion of the available evidence that informed the causality determinations.

1.4.2 Health Effects of $PM_{10-2.5}$

At the completion of the 2009 PM ISA, substantial uncertainties remained in the evaluation of the health effects due to short- and long-term $PM_{10-2.5}$ exposures (U.S. EPA, 2009). This was due to a variety of factors including the inability of particles within the $PM_{10-2.5}$ size range to reach the lower respiratory tract of rodents due to nasal deposition (see Figure 4-4) and instead relying on intra-tracheal instillation to assess health effects, and epidemiologic studies relying on multiple methods of varying quality to estimate $PM_{10-2.5}$ concentrations (e.g., direct measurement through dichotomous samplers, difference between collocated PM_{10} and $PM_{2.5}$ monitors,, difference between county-wide average PM_{10} and $PM_{2.5}$ when monitors were not collocated), which had not been systematically compared and potentially contributed to different degrees of exposure measurement error. Limited availability of data and higher spatial variability of $PM_{10-2.5}$ compared with $PM_{2.5}$ also contributed to uncertainty about the representativeness of the $PM_{10-2.5}$ concentrations as a surrogate for exposure.

Recent epidemiologic and experimental studies continue to examine the relationship between short- and long-term $PM_{10-2.5}$ exposure and health effects; however, the uncertainties in the evidence identified in the 2009 PM ISA have, to date, still not been addressed. Specifically, within the epidemiologic studies, there is evidence of positive associations across the various health effects evaluated, but the methods used to estimate $PM_{10-2.5}$ concentrations and subsequently assign exposures to $PM_{10-2.5}$ have not been systematically evaluated in the peer-reviewed literature (see Section 3.3.1.1). Overall, this contributes to uncertainty with respect to the spatial and temporal correlations in $PM_{10-2.5}$ concentrations across methods, which may add to uncertainties in $PM_{10-2.5}$ exposure surrogates given the larger spatial and temporal variability in $PM_{10-2.5}$ concentrations compared to $PM_{2.5}$ (see Section 2.5.1.2.3). Evidence from experimental studies in humans combined with evidence from epidemiologic panel studies and limited evidence from animal toxicological studies continues to provide some evidence to support biologically plausible pathways by which $PM_{10-2.5}$ could impart a variety of health effects. Overall, the uncertainties surrounding the evidence providing biological plausibility for health effects related to $PM_{10-2.5}$ exposure and the methods used to assign $PM_{10-2.5}$ exposure in epidemiologic studies collectively contributed to causality determinations across health effects categories of "*suggestive of, but not sufficient to infer, a causal relationship*" or "*inadequate to infer the presence or absence of a causal relationship*" (Table 1-5).

1.4.3 Health Effects of UFPs

At the completion of the 2009 PM ISA, relatively few studies examined the health effects attributed to short- and long-term UFP exposures. Across broad health categories there was limited and often inconsistent evidence of effects. There was some evidence of cardiovascular and respiratory effects due to UFP CAPs from controlled human exposure and animal toxicological studies with more evidence

from studies of diesel exhaust, but in the diesel exhaust studies it was not possible to determine if the effect observed was due to UFPs, gaseous components, or a combination of the two. Additionally, there were broader uncertainties that spanned atmospheric chemistry, exposure assessment, and epidemiology due to limited information on the spatial and temporal variability in UFP concentrations; the lack of a UFP monitoring network in the U.S.; and insufficient data on the composition of UFPs. These uncertainties were further reflected in epidemiologic studies as a result of most studies relying on a single monitor to estimate UFP exposure.

Recent studies have further explored the relationship between short- and long-term UFP exposure and health effects; however, the assessment of study results across experimental and epidemiologic studies is complicated by the size distribution examined in each discipline and the nonuniformity in the exposure metric examined (i.e., the particle size range and indicators [e.g., particle number concentration (NC), surface area concentration (SC), and mass concentration (MC)]) (see Preface). Specifically, experimental studies include size ranges up to 200 nm or higher. Epidemiologic studies often focus on various size ranges below 100 nm. However, if an epidemiologic study is focusing on NC it can include larger particle sizes, but it has been shown that 67−90% of NC represents particles <100 nm (Section 2.4.3.1).

Although there is some evidence of positive but imprecise associations across epidemiologic studies examining a range of health effects (e.g., cardiovascular and respiratory effects, and mortality), study results are difficult to interpret. This is due to most studies' reliance on a single monitor, which is inadequate as has been reflected in some monitoring campaigns that demonstrate a high degree of spatial variability in UFP concentrations and that the size distribution of UFPs changes with distance from source (Section 2.5.1). As noted above, examining coherence and biological plausibility of UFP-related health effects is complicated by the larger size distribution of UFPs examined in experimental studies compared with the size distribution examined in epidemiologic studies. Based on these overarching uncertainties and inconsistency across studies in the characterization of UFP with respect to size distribution and exposure metric, across most health effects categories the evidence collectively contributed to causality determinations that did not exceed "*suggestive of, but not sufficient to infer, a causal relationship*" (Table 1-5).

1.4.3.1 Nervous System Effects Associated with Long-Term UFP Exposure

The limited findings reported in the 2009 PM ISA indicated that subchronic exposure to UFP CAPs resulted in pro-inflammatory changes in the cortical region of the brains of mice and it was hypothesized that ambient UFP may reach the brain via olfactory transport based on studies demonstrating this mechanism using laboratory generated UFPs. The recent literature has greatly expanded, demonstrating overt neurological changes and providing some evidence suggesting potential translocation of UFPs via olfactory transport. Animal toxicological studies provide evidence for several

nervous system effects due to long-term UFP exposure including brain inflammation and oxidative stress, morphologic changes, and behavioral effects. Epidemiologic evidence is limited to a single study providing initial evidence of effects on attention and memory, but more broadly uncertainties remain with respect to effects due to long-term UFP exposure, specifically due to the uncharacterized temporal and spatial variability in UFP concentrations. Overall, the strong animal toxicological evidence of neurotoxicity and altered neurodevelopment supports a "*likely to be causal relationship*" between long-term UFP exposure and nervous system effects, which represents the first time a causality determination has been made for long-term UFP exposure and nervous system effects (Table 1-3).

Multiple toxicological studies of long-term UFP exposure conducted in adult animals provide consistent evidence of brain inflammation and oxidative stress in the whole brain, hippocampus, and cerebral cortex (Section 8.6.3). Studies also found morphologic changes, specifically neurodegeneration in specific regions of the hippocampus and pathologic changes characteristic of Alzheimer's disease, and initial evidence of behavioral effects in adult mice (Section 8.6.4 and Section 8.6.5). Toxicological studies examining pre- and post-natal UFP exposures provide extensive evidence for behavioral effects, altered neurotransmitters, neuroinflammation, and morphologic changes (Section 8.6.6.2). Persistent ventriculomegaly was observed in male, but not female mice, exposed postnatally to UFP (Section 8.6.6). Epidemiologic evidence is limited to a study of school children that provides support for the experimental results. This study, which did not consider copollutant confounding, reported an association between long-term exposure to UFP, which was measured at the school, and decrements on tests of attention and memory. In general, epidemiologic studies of long term exposure to UFP are sparse because there are challenges in capturing the spatial variation in long-term UFP concentrations that can result in substantial exposure measurement error (Section 8.6.7).

Table 1-3 Key Evidence contributing to a "likely to be causal" causality determination for UFP exposure and health effects evaluated in the current draft Integrated Science Assessment for Particulate Matter.

Key Evidence	Health Effect Category[a] and Causality Determination	UFP Concentrations Associated with Effects
Nervous System Effects and Long-Term UFP Exposure (Section 8.6.7): Likely to be Causal Relationship *Not evaluated in the 2009 PM ISA; new evidence showing brain inflammation and oxidative stress, neurodegeneration, cognitive effects, and neurodevelopmental effects.*		
Section 8.6.7 Table 8-34	Animal toxicological studies provide strong evidence for nervous system effects due to long-term UFP exposure including neuroinflammation, neurodegeneration, and altered neurodevelopment. Multiple toxicological studies conducted in adult animals provided consistent evidence of inflammation and oxidative stress in the whole brain, hippocampus, and cerebral cortex, as well as more limited evidence for neurodegeneration, Alzheimer's disease-related pathology, and behavioral effects. Experimental animal studies examining pre- and post-natal UFP exposures provide evidence for behavioral effects, altered neurotransmitters, neuroinflammation, and morphologic changes, including persistent ventriculomegaly. The epidemiologic evidence was limited to a study, that did not consider copollutant confounding, that provides initial evidence of that UFP may affect attention and memory in school children.	Concentrations from animal toxicological studies for: *Brain inflammation/Oxidative stress:* MC: 342–468 μg/m^3 NC: 140,000–254,000 particles/cm^3 *Neurodegenerative changes:* MC: 342–468 μg/m^3 NC: 140,000–254,000 particles/cm^3 *Cognitive and behavioral effects in adults:* MC: 342 μg/m^3 NC: 140,000 particles/cm^3 *Neurodevelopment:* 96.4–350 μg/m^3 NC: 180,000–200,000 particles/cm^3

MC = mass concentration; NC = number concentration.

[a]A large spectrum of outcomes is evaluated as part of a broad health effect category including physiological measures (e.g., airway responsiveness, lung function), clinical outcomes (e.g., respiratory symptoms, hospital admissions), and cause-specific mortality. The sections and tables referenced include a detailed discussion of the available evidence that informed the causality determinations.

1.5 Policy-Relevant Considerations

In the process of evaluating the current state of the science with respect to the effect of short- and long-term PM exposure on health, studies were identified that conducted analyses focused on addressing some of the main policy-relevant questions of this review, as detailed in the PM IRP (U.S. EPA, 2016), such as:

- Is there new evidence aimed at disentangling the effect of PM from the complex air pollution mixture to inform a direct effect of PM on health, specifically the assessment of potential copollutant confounding?
- Is there new evidence to inform the current indicators (i.e., $PM_{2.5}$ for fine particles and PM_{10} for thoracic coarse particles), averaging times (i.e., 24-hour average, annual average), and levels of the PM NAAQS?
- Is there new evidence on the shape of the concentration-response relationship and whether a threshold hold exists between PM exposure and various health outcomes (e.g., mortality, hospital admissions, etc.), especially for concentrations near or below the levels of the current PM NAAQS?
- Is there new evidence that individual PM component(s) or source(s) (e.g., industrial facilities, roads, atmospheric formation), are more strongly associated with health effects than PM mass, particularly for health effects for which there is sufficient evidence of a strong relationship (e.g., cardiovascular effects, mortality) with PM exposure?
- Is there new evidence indicating that specific populations or lifestages are at increased risk of a PM-related health effect compared to a referent population?

The following sections summarize the evidence that can inform consideration of these policy-relevant questions, specifically: potential copollutant confounding (Section 1.5.1), timing of effects (Section 1.5.2), concentration-response (C-R) relationship (1.5.3), PM components and sources (Section 1.5.4), and populations potentially at increased risk of a PM-related health effect (Section 1.5.5).

1.5.1 Potential Copollutant Confounding

Recent studies further evaluated the potential confounding effects of copollutants, both gaseous and particulate, on the relationship between short- and long-term $PM_{2.5}$ exposure and health effects. These studies build upon the evidence detailed in the 2009 PM ISA and continue to provide evidence indicating that associations with $PM_{2.5}$ are relatively unchanged in copollutant models. Evidence from epidemiologic studies, in combination with experimental studies detailed in previous chapters (i.e., Respiratory Effects-CHAPTER 5 and Cardiovascular Effects-CHAPTER 6) that examined exposure to PM (e.g., CAPs, resuspended PM, and whole mixtures in the presence and absence of a particle trap), demonstrate a direct effect of PM on health.

1.5.1.1 Short-term $PM_{2.5}$ Exposure

Building upon the studies evaluated in the 2009 PM ISA, recent epidemiologic studies have further examined whether copollutants confound associations between short-term $PM_{2.5}$ exposure and respiratory and cardiovascular effects and mortality. These studies continue to demonstrate $PM_{2.5}$-associations are relatively unchanged in copollutant models with both gaseous (i.e., O_3, NO_2, SO_2, and CO) and particulate (i.e., $PM_{10-2.5}$) pollutants.

The examination of potential copollutant confounding on the relationship between short-term $PM_{2.5}$ exposure and respiratory effects has been assessed most extensively through studies examining respiratory-related emergency department visits and hospital admissions, particularly for asthma, with more limited assessments of COPD and respiratory infection, and studies examining respiratory mortality (Section 5.1.10.1). Correlations between $PM_{2.5}$ and gaseous and particulate pollutants varied across studies, with low-to-moderate correlations (i.e., <0.7) observed for NO_2, SO_2, CO, and $PM_{10-2.5}$, and correlations spanning low-to-high for O_3. O_3 was most commonly examined, followed by NO_2, across the studies that assessed copollutant confounding, and $PM_{2.5}$ results were relatively unchanged in copollutant models. Although fewer studies focused on SO_2 and CO, the results from copollutant analyses were consistent with studies evaluated in the 2009 PM ISA, indicating that results are relatively unchanged in copollutant models. Recent studies that examined $PM_{10-2.5}$ further expand upon the initial results detailed in the 2009 PM ISA, and although results are consistent with observations from analyses of gaseous pollutants, there is greater uncertainty in these results due to the various methods employed across studies to estimate $PM_{10-2.5}$ concentrations.

While studies of respiratory-related emergency department visits and hospital admissions and respiratory mortality reported the strongest correlations between $PM_{2.5}$ and O_3, for cardiovascular effects moderate-to-strong correlations were reported for NO_2 and CO, with low to moderate correlations for O_3, SO_2, and $PM_{10-2.5}$. Across studies of various cardiovascular-related emergency department visits and hospital admissions and cardiovascular mortality, results were relatively unchanged in copollutant models, but there were some instances of attenuation of the $PM_{2.5}$ association in models with NO_2 and CO (Section 6.1.14.1). Overall, there was not an observed difference in the trend or pattern of copollutant model results across cardiovascular endpoints (e.g., aggregate CVD endpoints, IHD, heart failure, cardiovascular mortality). However, the few instances of attenuation were with traffic-related pollutants (i.e., NO_2, CO), which generally had higher correlations with $PM_{2.5}$ than the other copollutants. As a result, it is difficult to distinguish if the instances of observed attenuation in $PM_{2.5}$ associations are due to confounding or collinearity between pollutants.

Compared to epidemiologic studies that examined the potential confounding effects of copollutants on respiratory and cardiovascular effects, a more limited number of studies focused on mortality (Section 11.1.4). Recent multi-city studies conducted in Europe and Asia support the single- and multi-city studies examined in the 2004 PM AQCD and 2009 PM ISA that reported limited evidence of confounding by copollutants. Across studies examining both gaseous and particulate (i.e., $PM_{10-2.5}$)

pollutants, low-to-moderate correlations were reported with $PM_{2.5}$. Associations with $PM_{2.5}$ were relatively unchanged in copollutant models across the various study locations examined.

In addition to conducting traditional copollutant analyses, epidemiologic studies of respiratory (Section 5.1.10.1.1) and cardiovascular (Section 6.1.14.1.1) effects have also examined the role of PM within the broader air pollution mixture. These studies do not inform whether PM is independently associated with a respiratory effect, but they can assess whether days with higher $PM_{2.5}$ concentrations are more closely related to health effects. Studies of respiratory effects demonstrate that days where the air pollution mixture has high $PM_{2.5}$ concentrations often represent the days with the largest associations (in terms of magnitude) with a respiratory effect. Additionally, results indicate that risk estimates for a mixture are often similar, but in some cases larger, than those reported for $PM_{2.5}$ alone. However, for cardiovascular effects, generally, the evidence neither consistently or coherently indicated a stronger or weaker effect of combined exposure to $PM_{2.5}$ and another pollutant compared to exposure to $PM_{2.5}$ and other pollutants alone.

1.5.1.2 Long-term $PM_{2.5}$ Exposure

Epidemiologic studies focusing on long-term $PM_{2.5}$ exposure and health effects have traditionally provided a more limited assessment of the potential confounding effects of copollutants on $PM_{2.5}$ associations. Recent studies provide the initial evidence to inform copollutant confounding for some health outcomes, while in other instances (e.g., mortality) an assessment of copollutant confounding directly addresses a previously identified uncertainty in the scientific evidence.

Across the health effects evaluated within this ISA, relatively few studies examined the potential confounding effects of copollutants on the relationship between long-term $PM_{2.5}$ exposure and respiratory (Section 5.2.13), cardiovascular (Section 6.2.18), and cancer (Section 10.2.7), with a general lack of studies of assessing the role of copollutant confounding on observed associations with nervous system effects (Section 8.2.9). These studies often did not examine the full suite of gaseous pollutants, but tended to focus on traffic-related pollutants (i.e., NO_2, NO_X, and CO) and O_3, with some studies also examining $PM_{10-2.5}$. Across studies low-to-moderate correlations (i.e., $r < 0.7$) were often observed between copollutants and $PM_{2.5}$. Collectively, studies that examined the potential confounding effects of copollutants on the $PM_{2.5}$ association with respiratory (i.e., lung function and asthma development) and cardiovascular effects (i.e., cardiovascular mortality), along with lung cancer incidence and mortality, reported associations that were relatively unchanged in copollutant models, but these assessments were conducted in a limited number of studies.

Compared to other health effects, several studies of long-term $PM_{2.5}$ exposure and mortality examine potential copollutant confounding. Within studies that examined the potential confounding effects of copollutants on the relationship between long-term $PM_{2.5}$ exposure and mortality, the most extensive analyses occurred for O_3, with a limited number of studies examining NO_2, SO_2, $PM_{10-2.5}$, and

the air toxic, benzene. Studies that examined O_3 reported correlations that were generally moderate (ranging from $r = 0.49–0.73$), with a few studies reporting weak correlations ($r < 0.4$). Overall, associations remained relatively unchanged in copollutant models for total (nonaccidental) mortality, cardiovascular, and respiratory mortality (Figure 11-18). Studies focusing on copollutant models with NO_2, $PM_{10-2.5}$, SO_2 and benzene were examined in individual studies, and across these studies the $PM_{2.5}$-mortality association was relatively unchanged (Figure 11-19).

1.5.2 Timing of Effects

An important question to address when evaluating the scientific evidence demonstrating health effects due to short-term $PM_{2.5}$ exposure is the timing of observed effects. Studies have attempted to address this question through two primary avenues: (1) examining various averaging times of the exposure metric used to represent short-term exposure to $PM_{2.5}$ to determine whether PM averaged over time periods other than 24-hours are more closely associated with health effects; and (2) assessing whether the relationship between exposure and effect is biologically plausible by examining the lag days over which associations are observed.

1.5.2.1 Averaging Time

Most epidemiologic studies that examine the relationship between short-term $PM_{2.5}$ exposures and health effects rely primarily on an exposure metric that is averaged over 24-hours. Some recent studies, focusing on respiratory and cardiovascular effects and mortality, have examined whether there is evidence that subdaily exposure metrics are more closely related to health effects than the traditional 24-hour average metric.

Epidemiologic studies that examined both respiratory-related emergency department visits and hospital admissions as well as subclinical markers of respiratory effects explored associations with subdaily exposure metrics (Section 5.1.10.5). In studies of respiratory-related emergency department visits and hospital admissions, positive associations were not consistently observed with subdaily exposure metrics, and often there was no information on spatiotemporal variability of the subdaily metrics. Additionally, in a study that examined multiple subdaily averaging times and compared them to the 24-hour average exposure metric there was no difference in associations across metrics, but this was limited to a single study location. Panel studies also examined subdaily exposure metrics through personal monitoring, but associations were not consistently observed at these shorter averaging times for markers of pulmonary inflammation and changes in lung function.

A more limited number of studies examined subdaily exposure metrics and cardiovascular effects (Section 6.1.14.3). Studies of ST-elevation, myocardial infarction, out-of-hospital cardiac arrest, and cerebrovascular disease emergency department visits and hospital admissions reported positive

associations with subdaily exposure metrics, but the magnitude of the association tended to be larger when averaging over multiple hours up to one day (i.e., 24-hour average). These studies provide evidence that continues to support the use of a 24-hour average exposure metric.

A few studies examined subdaily $PM_{2.5}$ exposure metrics and associations with mortality, focusing on comparisons between the 24-hour average and an hourly peak exposure metric (Section 11.1.8.2). In these studies, positive associations were reported for both the 24-hour average and hourly peak exposure metric with the association often slightly larger in magnitude for the 24-hour average metric. Collectively, the available evidence does not indicate that subdaily averaging periods for $PM_{2.5}$ are more closely associated with health effects than the 24-hour average exposure metric.

1.5.2.2 Lag Structure of Associations

Often epidemiologic studies have examined associations between short-term $PM_{2.5}$ exposure and health effects over a series of single-day lags, multi-day lags, or by selecting lags *a priori*. Recent studies have expanded the assessment of examining the timing of effects by systematically examining lag days by focusing on whether there is evidence of an immediate (e.g., lag 0−1 days), delayed (e.g., lag 2−5 days), or prolonged (e.g., lag 0−5 days) effect of PM on health.

Epidemiologic studies of respiratory effects have primarily focused on examining the lag structure of associations for respiratory-related emergency department visits and hospital admissions, with most studies examining asthma with a more limited assessment for COPD and respiratory infection (Section 5.1.10.3). Across the studies that examined asthma, COPD, respiratory infections and combinations of respiratory-related diseases, the strongest association reported, in terms of magnitude and precision, is generally within a few days after exposure, but there is some evidence demonstrating the potential for a prolonged effect of $PM_{2.5}$ (i.e., lags ranging from 0−5 days). Recent studies of respiratory mortality provide additional insight on the lag structure of associations for respiratory-related effects due to short-term $PM_{2.5}$ exposure. Studies of respiratory mortality tend to support more immediate $PM_{2.5}$ effects (i.e., lags of 0 to 2 days), but initial evidence of stronger associations, in terms of magnitude and precision, at lags of 0−5 days. Collectively, the studies of respiratory morbidity and mortality that conducted systematic evaluations of $PM_{2.5}$ associations across a range of lags, provide evidence of effects within the range of 0–5 days after exposure.

Similar to respiratory effects, the majority of epidemiologic studies examining the lag structure of associations for cardiovascular effects focus on cardiovascular-related emergency department visits and hospital admissions. Studies of IHD, MI and cardiovascular-related outcomes emergency department visits and hospital admissions reported stronger associations for multi-day lags, but these effects tended to be in the range of 0−1 or 0−2 days. When examining cerebrovascular disease there was no evidence of an association at any of the lag days examined; however, when focusing on specific stroke types, particularly ischemic stroke there was evidence of immediate effects at lags of 0 and 1 day, which is consistent with

other cardiovascular outcomes. The immediate effects of $PM_{2.5}$ on cardiovascular morbidity outcomes, specifically those related to ischemic events, are consistent with the lag structure of associations observed in studies of cardiovascular mortality that report immediate effects (i.e., lag 0−1 day). There is some evidence indicating $PM_{2.5}$-cardviovascular mortality associations with exposures over longer durations, but this is not supported by studies examining single-day lags that encompass the same number of days.

An evaluation of recent epidemiologic studies of short-term $PM_{2.5}$ exposure and mortality found that studies either conducted analyses of single-day lags over many days or various iterations of multi-day lags (e.g., 0−1, 0−2, 0−3, etc.) (Section 11.1.8.1). Across studies, associations were largest in terms of magnitude and precision for total (nonaccidental) mortality at lags of 0 to 1 day, but there is some evidence that associations remain positive at multi-day lags up to 0−4 days. The combination of the multi- and single-day lag analyses provides further support of an immediate effect of short-term $PM_{2.5}$ exposure on mortality.

1.5.3 Concentration-Response (C-R) Relationship

In assessing the relationship-between short- and long-term PM exposure and health effects, an important consideration is whether the relationship is linear across the full range of ambient concentrations and whether there is a threshold concentration below which there is no evidence of an effect. As detailed in the 2004 AQCD and 2009 PM ISA, conducting C-R and threshold analyses is challenging due to the "(1) limited range of available concentration levels (i.e., sparse data at the low and high end); (2) heterogeneity of (at-risk) populations (between cities); and (3) influence of measurement error" (U.S. EPA, 2004). Recent studies that focus on the shape of the C-R curve expand upon the health effects evaluated in previous reviews and continue to provide evidence of a linear, no threshold, relationship between both short- and long-term $PM_{2.5}$ exposure and several respiratory and cardiovascular effects, and mortality, with some recent evidence indicating a steeper slope (i.e., supralinear curve) at lower concentrations for some outcomes (i.e., long-term $PM_{2.5}$ exposure and mortality). However, cut-point analyses that focus on whether risk changes at different concentration ranges provide some evidence of nonlinearity, specifically in the relationship between short-term $PM_{2.5}$ exposure and respiratory-related emergency department visits and hospital admissions. It is important to note that although recent studies have used many different statistical methods to examine the shape of the C-R relationship and generally provide evidence for a linear, no-threshold relationship, many of these studies have not systematically evaluated alternatives to a linear relationship.

1.5.3.1 Short-Term Exposure

Recent epidemiologic studies that examined the C-R relationship between short-term $PM_{2.5}$ exposure and health are limited to studies of respiratory-related emergency department visits and hospital

admissions (Section 5.1.10.6), and mortality (Section 11.1.10). Across studies that examined respiratory effects, different analytical methods have been employed to examine the C-R relationship, either explicitly examining the shape of the C-R curve and whether there is evidence of linearity across the full range of $PM_{2.5}$ concentrations, or through cut-point analyses that examine whether the risk of a $PM_{2.5}$-related respiratory effect changes within specified ranges of $PM_{2.5}$ concentrations. These studies primarily focused on asthma emergency department visits and hospital admissions, with some studies examining combinations of respiratory emergency department visits and hospital admissions. Studies that focused on the shape of the C-R curve provide initial evidence of a log-linear relationship for short-term $PM_{2.5}$ exposure and both respiratory disease and asthma hospital admissions and emergency department visits, with less certainty at concentrations below 10 $\mu g/m^3$. However, cut-point analyses provide some initial evidence indicating nonlinearity in the relationship (i.e., larger risk estimates at various quintiles when compared to the lowest quintile) between short-term $PM_{2.5}$ exposure and asthma emergency department visits and hospital admissions.

The examination of the C-R relationship for short-term PM exposure and mortality was initially limited to studies of PM_{10}. Recent epidemiologic studies focus on $PM_{2.5}$ and specifically the shape of the C-R curve at the low end of the $PM_{2.5}$ concentration distribution. Evidence from U.S. studies, which can examine the shape of the C-R curve at lower $PM_{2.5}$ concentrations compared to other countries, provide evidence indicating a log-linear relationship at concentrations as low as 5 $\mu g/m^3$. The observations from C-R analyses are further supported by cut-point analyses examining associations at different $PM_{2.5}$ concentrations as well as analyses that reported no evidence of a threshold. Overall, recent studies focusing on short-term $PM_{2.5}$ exposure and mortality support a log-linear, no threshold relationship at ambient $PM_{2.5}$ concentrations lower than those evaluated in the 2009 PM ISA.

1.5.3.2 Long-Term Exposure

The most extensive analyses of the C-R relationship between long-term PM exposure and a health outcome traditionally has been for $PM_{2.5}$ and mortality. Recent studies further expand and provide new insights on the relationship between long-term $PM_{2.5}$ exposure and mortality, and provide initial examinations of the C-R relationship for respiratory and cardiovascular effects, as well as lung cancer mortality and incidence.

While the assessment of the C-R relationship for long-term $PM_{2.5}$ exposure is more limited for most health outcomes, it has been extensively examined in studies of mortality (Section 11.2.4). Across studies a variety of statistical methods have been examined to assess whether there is evidence of deviations in linearity as well as cut point analysis that focus on examining risk at specific ambient concentrations (Table 11-7). These studies report results that generally support a linear, no-threshold relationship for total (nonaccidental) mortality, especially at lower ambient $PM_{2.5}$ concentrations, with confidence in some studies in the range of 5−8 $\mu g/m^3$. Additionally, there is initial evidence indicating

that the slope of the C-R curve may be steeper (supralinear) at lower concentrations for cardiovascular mortality.

Epidemiologic studies examining the C-R relationship for long-term $PM_{2.5}$ exposure and respiratory effects (Section 5.3.2.1.1) are limited in number and focus on asthma incidence and childhood wheeze. Studies of asthma incidence that examine the shape of the C-R curve and whether risk changes at different quartiles of $PM_{2.5}$ concentrations do not find any evidence for deviations in linearity and evidence of monotonically increasing risk, respectively. In an initial study of childhood wheeze, specifically repeated wheeze events, there is evidence of a linear C-R relationship with the greatest confidence at long-term $PM_{2.5}$ concentrations ranging from 10 to 12 $\mu g/m^3$.

A limited number of studies report initial assessments of the C-R relationship for long-term $PM_{2.5}$ concentrations and cardiovascular effects, specifically IHD incidence, coronary artery calcification (CAC), and hypertension (Section 6.2.16). For IHD incidence, there was evidence of a linear C-R relationship at concentrations below 15 $\mu g/m^3$, which is consistent with the shape of the curve when compared to the full range of $PM_{2.5}$ concentrations. Analyses of the relationship between long-term $PM_{2.5}$ exposure and CAC indicated both linear and nonlinear relationships, while there is initial evidence of a linear relationship between long-term $PM_{2.5}$ exposure and incidence of hypertension. A few studies that examined the relationship between long-term $PM_{2.5}$ exposure and lung cancer incidence and mortality also examined the shape of the C-R curve through assessments of linearity, and cut-point and threshold analyses (Section 10.2.5.1.4). These collective assessments provide initial evidence supporting a no-threshold, log-linear relationship across the range of $PM_{2.5}$ concentrations observed in the U.S., with confidence in some studies in the range of 5−10 $\mu g/m^3$.

1.5.4 PM Components and Sources

Building upon the initial evaluation conducted in the 2004 PM AQCD, the 2009 PM ISA conducted a formal evaluation of the relationship between exposures to PM components and sources and health effects. Through the evaluation of experimental and epidemiologic studies that focused on individual PM components as well as studies that used quantitative approaches aimed at reducing the correlation between components it was identified that many components and sources representative of combustion-related activities (e.g., motor vehicle emissions, coal combustion, oil burning, vegetative burning) are associated with a range of health effects. This assessment led to the 2009 PM ISA concluding that "many [components] of PM can be linked with differing health effects and the evidence is not yet sufficient to allow differentiation of those components or sources that are more closely related to specific health outcomes".

Building upon the evaluation of PM sources and components in the 2009 PM ISA, and as detailed in the Preface, this PM ISA systematically evaluated whether there was evidence that specific PM components or sources are more strongly associated with health effects than PM mass by focusing on

those studies that: (1) included a composite metric of PM (e.g., mass of $PM_{2.5}$ and/or $PM_{10-2.5}$, or in the case of ultrafine particles [UFP] mass, particle number, etc.) and PM components; (2) applied some approach to assess the particle effect (e.g., particle trap) of a mixture; or (3) conducted formal statistical analyses using source-based exposures that were not defined a priori (see Preface). Overall, these criteria allow for a thorough evaluation of whether there is evidence that an individual component(s) and/or source(s) is more closely related to health effects than PM mass. Across the health effects categories evaluated in this ISA, most studies that examine PM sources and components focus on $PM_{2.5}$. As such, the following sections summarize the current state of the science on $PM_{2.5}$ components and sources for those health effects categories where it was concluded that a "causal" or "likely to be causal" relationship exists, with details on the $PM_{2.5}$ components and sources evidence for the other health effects categories (e.g., Reproductive and Developmental Effects) in subsequent health chapters of this ISA.

Overall, recent studies continue to demonstrate that many $PM_{2.5}$ components and sources are associated with health effects ranging from subclinical (e.g., changes in heart function, such as HRV, or circulating biomarkers) to the more overt (i.e., emergency department visits, hospital admissions, and mortality). The results of these studies confirm and further support the conclusion of the 2009 PM ISA, i.e., that many $PM_{2.5}$ components and sources are associated with many health effects, and the evidence does not indicate that any one source or component is consistently more strongly related with health effects than $PM_{2.5}$ mass.

1.5.4.1 Respiratory Effects

The examination of $PM_{2.5}$ components and sources and respiratory effects was limited to epidemiologic studies (Section 5.1.11). Epidemiologic studies that examined associations between short-term $PM_{2.5}$ components and respiratory health effects and examined associations with $PM_{2.5}$ mass (n = 113), primarily focus on the components nitrate (n = 29), sulfate (n = 40), OC (n = 50), and EC/BC (n = 95). Across these studies the health effects examined range from inflammation and changes in lung function to respiratory-related emergency department visits and hospital admissions. When examining the pattern of associations for individual $PM_{2.5}$ components with those observed for $PM_{2.5}$ mass, all the components examined (i.e., evaluated in at least three studies) were positively associated with a respiratory effect in at least a few studies (Section 5.1.11.7). For EC/BC, the most extensively examined $PM_{2.5}$ component, many studies reported positive associations, but some studies also reported results indicating no association, which is consistent with the pattern of associations for $PM_{2.5}$ mass.

A more limited number of studies examined associations between long-term $PM_{2.5}$ components and respiratory effects (Section 5.2.12). Similar to short-term exposure studies, the majority of studies focus on EC/BC, and did not observe a different pattern of associations with respiratory effects than what was observed for $PM_{2.5}$ mass. Collectively, positive associations were observed in studies examining

short- and long-term $PM_{2.5}$ component exposure and respiratory effects, but there is no evidence that any one component is more strongly associated with respiratory effects than $PM_{2.5}$ mass.

Few studies examined the relationship between $PM_{2.5}$ sources and respiratory health effects. Through analyses where $PM_{2.5}$ components were apportioned into source factors, positive associations were reported for several respiratory effects, particularly asthma exacerbation, and sources representative of combustion-related activities, such as traffic and biomass burning. There were no recent studies that examined long-term exposure to $PM_{2.5}$ sources and respiratory effects.

1.5.4.2 Cardiovascular Effects

Both epidemiologic and experimental studies examined the relationship between $PM_{2.5}$ component and sources exposures and cardiovascular effects (Section 6.1.15). In short-term exposure studies, the epidemiologic evidence focuses on studies examining cardiovascular-related emergency department visits and hospital admissions with only a few studies examining other cardiovascular effects. Similar to studies examining respiratory effects and $PM_{2.5}$ components, of the studies that examined both $PM_{2.5}$ mass and components (n = 14), the most extensively examined components include EC (n = 12), OC (n = 10), sulfate (N = 9), and nitrate (n = 9). Across all components examined, most were positively associated with cardiovascular-related emergency department visits and hospital admissions in at least one study (Section 6.1.15). Although EC was positively associated with cardiovascular-related emergency department visits and hospital admissions in many of the studies evaluated, it was not possible to decipher if EC was independently associated or a marker of exposure to $PM_{2.5}$ mass.

Studies examining long-term exposure to $PM_{2.5}$ components and cardiovascular effects were few, and consistent with the long-term exposure and respiratory effects studies primarily focus on EC/BC (Section 6.2.17). These studies did not provide evidence that any one component is more strongly associated with a cardiovascular effect. Collectively, studies examining short- and long-term $PM_{2.5}$ components exposure continue to support there is not one component that is more strongly associated with a cardiovascular effect than $PM_{2.5}$ mass.

Epidemiologic and animal toxicological studies conducted source based analyses using mathematical methods to apportion $PM_{2.5}$ components into source factors (Section 6.1.15.6 and Section 6.1.15.8). Epidemiologic studies focused on cardiovascular-related emergency department visits and hospital admissions and reported positive associations with sources representative of combustion-related activities (e.g., industrial combustion, traffic), with more limited evidence for wildfires. Animal toxicological studies, which focused on markers of heart function (e.g., HR, HRV), reported associations with a variety of source categories, but the associations were dependent on the location of the study (i.e., where the $PM_{2.5}$ CAPS were collected). Additional studies focusing on long-term exposures to $PM_{2.5}$ sources were fewer in number, with epidemiologic studies only examining traffic

sources and animal toxicological studies reporting associations with a number of sources and various cardiovascular effects.

1.5.4.3 Mortality

Epidemiologic studies that examined associations with $PM_{2.5}$ components and sources and mortality have primarily focused on examining short- and long-term exposures to components (Section 11.1.11 and Section 11.2.6). Both short- and long-term exposure studies reported consistent, positive associations with $PM_{2.5}$ mass across all studies that also examined a component. While for respiratory and cardiovascular effects most studies focused on EC/BC, for studies of mortality no one component was disproportionally examined compared to the rest. Of the $PM_{2.5}$ components examined, each were found to be positively associated with mortality in at least a few studies, but overall one component was not found to be as consistently associated with mortality as $PM_{2.5}$ mass.

Compared to the 2009 PM ISA, where most epidemiologic studies of mortality conducted formal source apportionment analyses, recent studies focus more exclusively on $PM_{2.5}$ components. Of the limited number of studies that examined associations between short- and long-term source exposures and mortality, positive associations were observed for those sources representative of combustion-related activities including traffic, coal, and vegetative fires.

1.5.5 Populations and Lifestages at Potentially Increased Risk of a PM-related Health Effect

An important consideration in the evaluation of the scientific evidence for PM, and in the consideration of the extent to which the NAAQS provides public health protection with an adequate margin of safety, is whether specific populations or lifestages are at increased risk of a PM-related health effect. As detailed in the preceding sections of this chapter and subsequent chapters of this ISA, a large body of evidence demonstrates health effects related to PM exposure, particularly $PM_{2.5}$ exposure, across populations with diverse characteristics (e.g., children, older adults, people with pre-existing cardiovascular diseases, etc.). While this larger body of evidence informs the causal nature of the relationship between PM exposure and health effects, this section focuses on answering the question:

Are there specific populations and lifestages at increased risk of a PM-related health effect, compared to a reference population? That is, is the magnitude of effect or exposure greater for some populations or lifestages compared to a reference population, where applicable, or are health effects observed at lower PM concentrations for some populations or lifestages compared to others?

The evaluation of populations and lifestages potentially at increased risk builds off the approach used in the 2009 PM ISA and includes the application of a framework to characterize the evidence

informing increased risk detailed in the 2013 O_3 ISA (U.S. EPA, 2013). The focus of this evaluation is on determining the extent to which specific factors may increase the risk of a PM-related health effect in a population or lifestage relative to a reference population, where applicable. Importantly, this builds on the conclusions drawn elsewhere in the ISA, taking into consideration the relationship between exposure to PM and health effects. As detailed in the Preamble to the ISAs (U.S. EPA, 2015), the evaluation of the evidence includes (1) epidemiologic studies that conducted stratified analyses, (2) evidence from animal toxicological studies using animal models of disease and epidemiologic or controlled human exposure studies conducted in specific populations (e.g., lung function growth in children, people with mild asthma), (3) information on the dosimetry of PM within the body, and (4) consideration of information on differential exposure to PM within a population or lifestage. Overall, the framework allows for a transparent characterization of the collective body of evidence in order to draw conclusions on the degree to which the scientific evidence indicates that a specific population or lifestage is at increased risk of a PM-related health effect (Table 12-1).

Based on the causality determinations briefly summarized within this chapter, and more fully detailed in subsequent chapters, the strongest evidence indicating an effect of short- and long-term PM exposure on health is for $PM_{2.5}$ and the broad health categories of respiratory and cardiovascular effects, cancer, and mortality. As a result, the assessment of populations and lifestages potentially at increased risk of a $PM_{2.5}$-related health effect primarily focuses on studies that form the basis of these causality determinations that also conducted analyses to inform whether there is differential risk in a specific population or lifestage. It is important to note that in the evaluation of studies a number of factors can influence the ability to observe an association including, but not limited to, publication bias (i.e., not reporting null findings when examining evidence of differential risk), variability in how indicators or metrics are defined across studies (e.g., socioeconomic status, obesity, age), and variability in the population as a whole, particularly with respect to behavioral differences, biological differences (e.g., obese vs. nonobese), and adherence to treatment for pre-existing diseases.

Of the factors evaluated (see Table 12-18 for a full list), children and race were the only factors for which it was concluded that "*adequate evidence*" was available indicating that people of a specific lifestage and race are at increased risk of $PM_{2.5}$-related health effects (Section 12.5.1.1 and Section 12.5.4). For children, although stratified analyses do not indicate a difference in the risk of PM-related health effects between children and adults, there is strong evidence from studies focusing on children demonstrating health effects that are only observable in growing children, attributed to $PM_{2.5}$ exposure. Particularly recent epidemiologic studies of long-term $PM_{2.5}$ exposure have provided strong evidence of impaired lung function growth with additional evidence of decrements in lung function and asthma development. These longitudinal epidemiologic studies are consistent with and extend the evidence that was available in the 2009 PM ISA demonstrating health effects in children due to long-term $PM_{2.5}$ exposure. For race, this conclusion was based on studies that examined whether there was evidence of increased risk for $PM_{2.5}$-related health effects as well as studies focusing on whether there was evidence of differential exposure by race. Multiple studies reported that nonwhite populations across

different geographical regions are exposed to higher $PM_{2.5}$ concentrations and at increased risk for $PM_{2.5}$-related mortality, particularly due to long-term exposure. Collectively, the combination of evidence demonstrated that nonwhite populations are at increased risk for both $PM_{2.5}$-related health effects and $PM_{2.5}$ exposure compared to whites.

It was concluded that there is "*suggestive evidence*" that populations with pre-existing cardiovascular (Section 12.3.1) or respiratory (Section 12.3.5) disease, that are overweight or obese (Section 12.3.3), with particular genetic variants (Section 12.4), or that are of low SES (Section 12.5.3) are at increased risk for $PM_{2.5}$-related health effects. Epidemiologic studies that conducted analyses stratified by pre-existing cardiovascular disease tended to focus on hypertension, one of the most easily measurable cardiovascular conditions, and did not consistently indicate increased risk for several outcomes examined (e.g., mortality, stroke, blood pressure). However, the strong evidence supporting a "*causal relationship*" between short- and long-term $PM_{2.5}$ exposure cardiovascular-related mortality and ischemic heart disease (Section 6.1.16 and Section 6.2.18) indicates that individuals with underlying cardiovascular conditions related to these serious outcomes may be at increased risk of a $PM_{2.5}$-related health effect. Similarly, when evaluating pre-existing respiratory diseases, including asthma (Section 12.3.5) and COPD (Section 12.3.5), there are a limited number of studies evaluating whether there is evidence of increased risk between people with pre-existing asthma and COPD and those that do not have a pre-existing respiratory disease. However, it is important to note that epidemiologic studies, particularly those studies examining short-term $PM_{2.5}$ exposure and asthma or COPD emergency department visits and hospital admissions report generally consistent positive associations (Section 5.1.2.1 and Section 5.1.4.1), which represent exacerbations that are only possible in people with asthma or COPD. Therefore, there is limited evidence to support that people with pre-existing respiratory diseases, specifically asthma or COPD, are at increased risk for a $PM_{2.5}$-related health effect, but there is generally consistent evidence demonstrating these populations experience health effects due to a $PM_{2.5}$ exposure. Studies that examined the role of being obese or overweight on the risk of a $PM_{2.5}$-related health effect, reported evidence of increased risk for mortality associated with long-term exposures to $PM_{2.5}$, but inconsistent evidence for subclinical cardiovascular outcomes, when comparing obese or overweight individuals to normal weight individuals. However, the evaluation of studies focusing on differences in risk by weight were complicated by the different definitions of obesity used across studies. The examination of whether specific genetic characteristics dictate increased risk of a $PM_{2.5}$-related health effect is based on studies of a variety of genetic variants. Across the large number of genetic variants examined there is a consistent trend for increased risk of respiratory and cardiovascular effects associated with $PM_{2.5}$ exposure across gene variants involved in the glutathione pathway. These results are consistent with underlying mechanisms that provide biological plausibility for $PM_{2.5}$-related health effects and have shown that oxidative stress is an early response to $PM_{2.5}$ exposure. Lastly, epidemiologic studies have examined several measures of SES (e.g., income level, educational attainment, etc.) in assessing whether populations are at increased risk of a $PM_{2.5}$-related health effect. In studies examining both differential exposure as well as increased risk of health effects, there is some evidence that low SES populations are more likely to have higher $PM_{2.5}$ exposures and that low SES populations, as measured by metrics for

income, are at increased risk of $PM_{2.5}$-related mortality when compared to populations defined as higher SES.

For the remaining factors evaluated, "*inadequate evidence*" exists to determine whether having diabetes (Section 12.3.2), being in an older lifestage (i.e. older adults) (Section 12.5.1.2), residential location (including proximity to source and urban residence; Section 12.5.5), sex (Section 12.5.2), or diet (Section 12.6.2) increase the risk of $PM_{2.5}$-related health effects. Across these factors there is either limited assessment of differential risk or exposure (i.e., residential location, diet), or inconsistency in results across studies to support evidence of increased risk of a $PM_{2.5}$-related health effect (i.e., diabetes and sex). However, as stated previously this does not indicate there is no evidence of a $PM_{2.5}$-related health effect for these populations and lifestages, but limits the assessment of determining whether a specific population is at disproportionately increased risk of a health effect. For example, for older adults (Section 12.5.1.2) there is a relatively small number of studies that examined whether there is evidence of differential risk between age groups. In the evaluation of these studies there is limited evidence indicating that older adults are at increased risk of $PM_{2.5}$-related health effects when compared to other age ranges; however, epidemiologic studies focusing only on older adults demonstrate associations with respiratory-related emergency department visits and hospital admissions with additional, but more limited, evidence from epidemiologic panel studies and controlled human exposure studies that observed associations between $PM_{2.5}$ exposure and subclinical cardiovascular effects.

1.6 Welfare Effects of PM

Whereas the evaluation of the evidence for PM exposures and health effects are specific to exposure duration (i.e., short- and long-term) and PM size fraction (i.e., $PM_{2.5}$, $PM_{10-2.5}$, and UFP), the evaluation of the evidence for welfare effects focuses generally on whether there is a causal relationship between PM and visibility impairment, climate effects, and effects on materials. As detailed below, the evidence continues to support a "*causal relationship*" between PM and visibility impairment (Section 1.6.1), climate effects (Section 1.6.2), and materials effects (Section 1.6.3).

1.6.1 Visibility Impairment

It has been well characterized that light extinction from pollution is primarily due to $PM_{2.5}$, resulting in the conclusion that there is a "*causal relationship*" between PM and visibility impairment, which is consistent with the conclusions of the 2009 PM ISA (Table 1-4). This conclusion is based on additional characterization of the impact of PM size and composition on light extinction.

The relationship between PM and light extinction has been well documented (Section 13.2.2). Although reconstruction of light extinction is best achieved with detailed information on the size and

composition of PM measurements, empirical relationships between light extinction of PM components are more practical and have been successfully evaluated and widely used (Section 13.2.3). Light extinction has been found to vary depending on the available PM species monitoring data, with light extinction efficiencies varying by a factor of 10 between species. Additionally, the variation in PM species by region and season as well as urban and rural location can impact light extinction. The steep decline in $PM_{2.5}$ sulfate of −4.6% per year in rural areas and −6.2% per year in urban areas from 2002–2012 (Section 1.2.1) has impacted the apportionment of light extinction among $PM_{2.5}$ species. Although $PM_{2.5}$ sulfate is still responsible for more light extinction than any other single species, visibility in many areas has improved, and a smaller and less seasonally variable fraction of light extinction can be attributed to $PM_{2.5}$ sulfate, and an increasing share is due to nitrate and organic matter (Section 13.2.4).

1.6.2 Climate Effects

Substantial evidence indicates that PM affects the radiative forcing of the climate system, both through direct scattering and absorption of radiation, and indirectly, by altering cloud properties, resulting in the conclusion that there is a "*causal relationship*" between PM and climate effects, which is consistent with the conclusions of the 2009 PM ISA (Table 1-4). This conclusion is based on multiple recent studies that have strengthened the evidence for the effects of PM on radiative forcing and have improved the characterization of major sources of uncertainty in estimating PM climate effects, including the indirect radiative forcing effects associated with PM-cloud interactions, and the additional climate impacts and feedbacks involving atmospheric circulation and the hydrologic cycle resulting from PM effects on radiative forcing.

Due to these radiative effects, the net effect of PM has been to cool the planet over the last century, masking some of the effects of greenhouse gases on warming (Section 13.3.3). The decrease in PM concentrations in many developed countries over the last few decades has likely contributed to the recent shift toward "global brightening," which may in turn have helped drive rapid warming in North American and Europe as this greenhouse-gas warming was unmasked (Section 13.3.6). In developing countries in Asia, by contrast, there has been an increase in PM concentrations over the last several decades, but the associated radiative forcing effects are highly uncertain, due to uncertainties in emissions estimates and the lack of accurate information on the proportion of reflecting versus absorbing species. Although uncertainties in the relationship between PM and climate effects have been further elucidated since the 2009 PM ISA, there are still substantial uncertainties with respect to key processes linking PM and climate, specifically clouds and aerosols. This is because of the small scale of PM-relevant cloud microphysical processes compared to the resolution of state-of-the-art models, and because of the complex cascade of indirect impacts and feedbacks in the climate system that result from a given initial radiative perturbation caused by PM.

1.6.3 Materials Effects

Multiple recent studies further characterize soiling and corrosion processes associated with PM and add to the body of evidence of PM damage to materials. Approaches to quantify pollutant exposure corresponding to perceived soiling and damage continue to indicate that deposition can result in increased cleaning and maintenance costs and reduced usefulness of soiled material. The combination of this evidence results in the conclusion that there is a "*causal relationship*" between PM and effects on materials, which is consistent with the conclusions of the 2009 PM ISA (Table 1-4).

Assessments of the relationship between PM and effects on materials have often focused on quantitative assessments including the development of dose-response relationships and application of damage functions to stone used for historic monuments and buildings. Recent studies provide additional information on understanding soiling and corrosion process for glass and metals, and allowed for the development of new dose-response curves (Section 13.4.3), particularly for glass as well as new damage functions for materials (Section 13.4.4). Additional evidence demonstrates that atmospheric soiling can impact energy costs and climate control, energy consumption of large buildings, and efficiency of photovoltaic systems (Section 13.4.2).

Table 1-4 Key Evidence contributing to a "causal" causality determination for PM exposure and welfare effects evaluated in the current draft Integrated Science Assessment for Particulate Matter.

Key Evidence	Welfare Effect Category[a] and Causality Determination
Visibility Impairment and PM Exposure (Section 13.2): Causal Relationship	
No change in causality determination from the 2009 PM ISA; new evidence further supports the previous determination.	
Section 13.2.6	Visibility impairment by atmospheric PM with the strongest effects in the size range from 0.1 to 1.0 μm, is supported by numerous studies summarized in the 1969 PM AQCD (NAPCA, 1969), although the relationship between PM and atmospheric visibility impairment was well-established decades earlier. Additional studies supporting the relationship have been described in subsequent documents, and additional new evidence is based on extensive simultaneous network measurements of $PM_{2.5}$ and light extinction.
Climate Effects and PM Exposure (Section 13.3): Causal Relationship	
No change in causality determination from the 2009 PM ISA; new evidence further supports the previous determination.	
Section 13.3.9	Effects of PM on radiative forcing of the climate system through both absorption and scattering of radiation directly, as well as through indirect effects involving interactions between PM and cloud droplets, with corresponding impacts on temperature, precipitation, and atmospheric circulation, is supported by numerous observational and modeling studies. Research since the 2009 ISA (U.S. EPA, 2009) has improved understanding of climate-relevant aerosol properties and processes, as well as characterization of key sources of uncertainty in estimating PM climate effects, particularly with respect to PM-cloud interactions.
Materials Effects and PM Exposure (Section 13.4): Causal Relationship	
No change in causality determination from the 2009 PM ISA; new evidence further supports the previous determination.	
Section 13.4.5	Both soiling and corrosion associated with PM contribute to materials damage (U.S. EPA, 2009, 2004, 1982). Deposition of PM can physically affect materials by promoting or accelerating the corrosion of metals, by degrading paints and by deteriorating building materials such as stone, concrete and marble. Further characterization of PM effects on glass and metals along with quantitative dose-response relationships and damage functions for stone and other materials lend additional support to the causal relationship in the 2009 ISA. Recent evidence shows that deposition of PM reduces energy efficiency of photovoltaic systems.

[a]The sections referenced include a detailed discussion of the available evidence that informed the causality determinations.

1.7 Summary of Causality Determinations for All Health and Welfare Effects

The preceding sections of this chapter focused on summarizing the key evidence that formed the basis for causality determinations within this ISA of a "*causal relationship*" and "*likely to be causal relationship*". Table 1-5 details the causality determinations for each of the exposure duration and health or welfare effects categories evaluated in this ISA along with the conclusions from the 2009 PM ISA. The following chapters provide extensive evaluations of the evidence that forms the basis of these causality determinations.

Table 1-5 Causality determinations from the 2009 PM ISA and the current PM ISA for the health and welfare effects categories evaluated.

Summary of Causality Determinations		
Chapter 5. Respiratory Effects		
Short-term Exposure		
Size Fraction	2009 PM ISA	Current PM ISA
$PM_{2.5}$	Likely to be causal	Likely to be causal
$PM_{10-2.5}$	Suggestive of, but not sufficient to infer	Suggestive of, but not sufficient to infer
UFP	Suggestive of, but not sufficient to infer	Suggestive of, but not sufficient to infer
Long-term Exposure		
Size Fraction	2009 PM ISA	Current PM ISA
$PM_{2.5}$	Likely to be causal	Likely to be causal
$PM_{10-2.5}$	Inadequate	Inadequate
UFP	Inadequate	Inadequate

Table 1-5 (Continued): Causality determinations from the 2009 PM ISA and the current PM ISA for the health and welfare effects categories evaluated.

Summary of Causality Determinations		
Chapter 6. Cardiovascular Effects		
Short-term Exposure		
Size Fraction	2009 PM ISA	Current PM ISA
$PM_{2.5}$	Causal	Causal
$PM_{10-2.5}$	Suggestive of, but not sufficient to infer	Suggestive of, but not sufficient to infer
UFP	Suggestive of, but not sufficient to infer	Suggestive of, but not sufficient to infer
Long-term Exposure		
Size Fraction	2009 PM ISA	Current PM ISA
$PM_{2.5}$	Causal	Causal
$PM_{10-2.5}$	Inadequate	Suggestive of, but not sufficient to infer
UFP	Inadequate	Inadequate
Chapter 7. Metabolic Effects		
Short-term Exposure		
Size Fraction	2009 PM ISA	Current PM ISA
$PM_{2.5}$	---	Suggestive of, but not sufficient to infer
$PM_{10-2.5}$	---	Inadequate
UFP	---	Inadequate
Long-term Exposure		
Size Fraction	2009 PM ISA	Current PM ISA
$PM_{2.5}$	---	Suggestive of, but not sufficient to infer
$PM_{10-2.5}$	---	Suggestive of, but not sufficient to infer
UFP	---	Inadequate

Table 1-5 (Continued): Causality determinations from the 2009 PM ISA and the current PM ISA for the health and welfare effects categories evaluated.

Summary of Causality Determinations		
Chapter 8. Nervous System Effects		
Short-term Exposure		
Size Fraction	2009 PM ISA	Current PM ISA
$PM_{2.5}$	Inadequate	Suggestive of, but not sufficient to infer
$PM_{10-2.5}$	Inadequate	Inadequate
UFP	Inadequate	Suggestive of, but not sufficient to infer
Long-term Exposure		
Size Fraction	2009 PM ISA	Current PM ISA
$PM_{2.5}$	---	Likely to be causal
$PM_{10-2.5}$	---	Suggestive of, but not sufficient to infer
UFP	---	Likely to be causal
Chapter 9. Reproductive and Developmental Effects		
Male and Female Reproduction and Fertility		
Size Fraction	2009 PM ISA	Current PM ISA
$PM_{2.5}$	Suggestive of, but not sufficient to infer	Suggestive of, but not sufficient to infer
$PM_{10-2.5}$	Inadequate	Inadequate
UFP	Inadequate	Inadequate
Pregnancy and Birth Outcomes		
Size Fraction	2009 PM ISA	Current PM ISA
$PM_{2.5}$	Suggestive of, but not sufficient to infer	Suggestive of, but not sufficient to infer
$PM_{10-2.5}$	Inadequate	Inadequate
UFP	Inadequate	Inadequate

Table 1-5 (Continued): Causality determinations from the 2009 PM ISA and the current PM ISA for the health and welfare effects categories evaluated.

Summary of Causality Determinations		
Chapter 10. Cancer		
Size Fraction	2009 PM ISA	Current PM ISA
$PM_{2.5}$	Suggestive of, but not sufficient to infer	Likely to be causal
$PM_{10-2.5}$	Inadequate	Suggestive of, but not sufficient to infer
UFP	Inadequate	Inadequate
Chapter 11. Mortality		
Short-term Exposure		
Size Fraction	2009 PM ISA	Current PM ISA
$PM_{2.5}$	Causal	Causal
$PM_{10-2.5}$	Suggestive of, but not sufficient to infer	Suggestive of, but not sufficient to infer
UFP	Inadequate	Inadequate
Long-term Exposure		
Size Fraction	2009 PM ISA	Current PM ISA
$PM_{2.5}$	Causal	Causal
$PM_{10-2.5}$	Inadequate	Suggestive of, but not sufficient to infer
UFP	Inadequate	Inadequate
Chapter 13. Welfare Effects		
	2009 PM ISA	Current PM ISA
Climate	Causal	Causal
Visibility	Causal	Causal
Materials Damage	Causal	Causal

The 2009 PM ISA made causality determinations for the broad category of "Reproductive and Developmental Effects". Causality determinations for 2009 represent this broad category and not specifically for "Male and Female Reproduction and Fertility" and "Pregnancy and Birth Outcomes".

1.8 References

NAPCA (National Air Pollution Control Administration). (1969). Air quality criteria for particulate matter. Washington, DC.

NHLBI (National Institutes of Health, National Heart Lung and Blood Institute). (2017). NHLBI fact book, fiscal year 2012: Disease statistics. Available online at https://www.nhlbi.nih.gov/about/documents/factbook/2012/chapter4 (accessed August 23, 2017).

U.S. EPA (U.S. Environmental Protection Agency). (1982). Air quality criteria for particulate matter and sulfur oxides (final, 1982) [EPA Report]. (EPA 600/8-82/029a). Washington, DC: Environmental Criteria and Assessment Office. http://cfpub.epa.gov/ncea/cfm/recordisplay.cfm?deid=46205

U.S. EPA (U.S. Environmental Protection Agency). (1996). Air quality criteria for particulate matter [EPA Report]. (EPA/600/P-95/001aF-cF. 3v). Research Triangle Park, National Center for Environmental Assessment-RTP Office NC.

U.S. EPA (U.S. Environmental Protection Agency). (2004). Air quality criteria for particulate matter [EPA Report]. (EPA/600/P-99/002aF-bF). Research Triangle Park, NC: U.S. Environmental Protection Agency, Office of Research and Development, National Center for Environemntal Assessment- RTP Office. http://cfpub.epa.gov/ncea/cfm/recordisplay.cfm?deid=87903

U.S. EPA (U.S. Environmental Protection Agency). (2009). Integrated science assessment for particulate matter [EPA Report]. (EPA/600/R-08/139F). Research Triangle Park, NC: U.S. Environmental Protection Agency, Office of Research and Development, National Center for Environmental Assessment- RTP Division. http://cfpub.epa.gov/ncea/cfm/recordisplay.cfm?deid=216546

U.S. EPA (U.S. Environmental Protection Agency). (2013). Integrated science assessment for ozone and related photochemical oxidants [EPA Report]. (EPA/600/R-10/076F). Research Triangle Park, NC: U.S. Environmental Protection Agency, Office of Research and Development, National Center for Environmental Assessment-RTP Division. http://cfpub.epa.gov/ncea/isa/recordisplay.cfm?deid=247492

U.S. EPA (U.S. Environmental Protection Agency). (2015). Preamble to the integrated science assessments [EPA Report]. (EPA/600/R-15/067). Research Triangle Park, NC: U.S. Environmental Protection Agency, Office of Research and Development, National Center for Environmental Assessment, RTP Division. https://cfpub.epa.gov/ncea/isa/recordisplay.cfm?deid=310244

U.S. EPA (U.S. Environmental Protection Agency). (2016). Integrated review plan for the national ambient air quality standards for particulate matter [EPA Report]. (EPA-452/R-16-005). Research Triangle Park, NC. https://yosemite.epa.gov/sab/sabproduct.nsf/0/eb862b233fbd0cde85257dda004fcb8c!OpenDocument&TableRow=2.0

U.S. EPA (U.S. Environmental Protection Agency). (2017). EPA's report on the environment (ROE). Available online at https://cfpub.epa.gov/roe/index.cfm (accessed January 29, 2018).

U.S. EPA (U.S. Environmental Protection Agency). (2018). Integrated science assessment for oxides of nitrogen, oxides of sulfur and particulate matter -Ecological criteria (2nd external review draft). (EPA/600/R-18/097). Research Triangle Park, NC: U.S. Environmental Protection Agency, Office of Research and Development, National Center for Environmental Assessment. http://cfint.rtpnc.epa.gov/ncea/prod/recordisplay.cfm?deid=340671

CHAPTER 2 SOURCES, ATMOSPHERIC CHEMISTRY, AND AMBIENT CONCENTRATIONS

Summary of Sources, Atmospheric Chemistry, and Ambient Concentrations of Particulate Matter (PM)

- National 3-year average $PM_{2.5}$ concentrations decreased from 12 μg/m^3 to 8.6 μg/m^3 between the 3-year periods 2005–2007 and 2013–2015.
- SO_2 emissions decreased from 13.9 million metric tons in 2006 to 4.8 million metric tons in 2014. This decrease led to large decreases in the sulfate contribution to $PM_{2.5}$ and contributed to the decrease in $PM_{2.5}$ concentration. Emissions of NO_X and primary $PM_{2.5}$ have also decreased, but not NH_3.
- Seasonal patterns of $PM_{2.5}$ concentrations have changed from summer as the season with highest national average $PM_{2.5}$ concentration to rough equivalence in national average concentration between summer and winter. Sulfate concentrations have been historically highest in summer.
- The relative $PM_{2.5}$ contribution to PM_{10} has decreased and the relative $PM_{10-2.5}$ contribution to PM_{10} has increased since 2004.
- Extensive research has led to advances in understanding the formation of secondary organic aerosols, in particular with regard to biogenic precursor reactions, heterogeneous reactions, and production of organonitrates and organosulfates.
- For the first time, a national multipollutant monitoring network was implemented, and it includes simultaneous measurements for $PM_{2.5}$ and $PM_{10-2.5}$ using a Federal Reference Method at 78 monitoring sites.
- For the first time, a national near road $PM_{2.5}$ monitoring method was implemented, and it includes 36 monitoring sites.
- For the first time, routine monitoring of particle number count was implemented at 23 monitoring sites.

2.1 Summary Overview

This chapter presents basic concepts and new research in atmospheric sciences relevant for understanding exposure, health effects, and welfare effects discussed throughout this document. It builds on information presented in the 2009 Integrated Science Assessment for Particulate Matter (hereafter referred to as the 2009 PM ISA) (U.S. EPA, 2009) and earlier PM Air Quality Criteria Documents (AQCDs) by reviewing recent research on PM sources, chemistry, composition, measurement, monitoring, modeling, and atmospheric concentrations. Among the new results and observations are some fundamental changes in PM in the Eastern U.S. over the past decade, including a sharp decrease in the contribution of sulfate to PM, a shift in particle size distribution toward particles in 2.5 to 10 μm diameter size range, and a shift in seasonal maximum concentrations from summer to winter. These changes likely resulted from a recent sharp decline in SO_2 emissions due to stronger emission controls, as well as fuel switching and closures of coal-fired power plants. The highest $PM_{2.5}$ and PM_{10} concentrations continue to

persist in some areas in the Western U.S. Recent progress in PM measurement includes network implementation of improved methodologies for accurate measurement of particulate mass in the size range between 2.5 and 10 μm diameter, initiation of near road monitoring of $PM_{2.5}$, initiation of routine monitoring of particle number counts at a small number of near road and remote locations, and advancement of methods for retrieval and application of satellite data for estimating $PM_{2.5}$.

This chapter is organized into sections by major topic (sources, measurements, etc.) and where appropriate, content in each section is divided into subsections by size range and other subtopics such as PM composition. Section 2.2 contains a basic description of ambient PM size distributions and typical particle size characteristics to set the stage for this organization. Section 2.3 discusses sources and emissions of PM and its major precursors as well as atmospheric chemistry of PM. Section 2.4 addresses advances in measurement and modeling of PM and describes PM monitoring networks. Section 2.5 summarizes recent concentration trends, including spatial and temporal variability on national and local scales. Section 2.6 provides an overall synthesis of the chapter highlighting major new findings.

2.2 Atmospheric Size Distributions

Airborne particulate matter is a mixture of substances suspended in air as small liquid and/or solid particles. These individual particles range in size from less than 0.01 μm to more than 10 μm. Particle size is an important characteristic for health effects because different size particles penetrate into different regions of the human respiratory tract, potentially leading to distinctive health consequences for various particle size ranges (U.S. EPA, 2009). The effect of particle size on particle behavior in the respiratory system is described in Section 4.1.6. Particle size also plays an important role in welfare effects covered in CHAPTER 13, particularly for effects on radiative forcing and visibility. Properties and effects of various particle size ranges are considered separately in this document, and particle size is used as an important organizing framework for the various sections both in this chapter and in the entire document.

PM subscripts refer to the aerodynamic diameter in micrometers (μm) of 50% cut points of sampling devices. For example, U.S. EPA defines $PM_{2.5}$ as particles collected by a sampler with an upper 50% cut point of 2.5 μm aerodynamic diameter and a specific, sharp penetration curve as defined in the Code of Federal Regulations (40 CFR Part 58) (U.S. EPA, 2009). Similarly, $PM_{10-2.5}$ is the PM mass collected with an upper 50% cut point of 10 μm and a lower 50% cut point of 2.5 μm. Ultrafine particles (UFP) are often defined as particles with a diameter of <0.1 μm based on physical size, thermal diffusivity or electrical mobility (U.S. EPA, 2009). By definition, UFP encompass all particles smaller than the defined upper diameter limit. However, in practice UFP measurement methods (Section 2.4.3) have varying lower and upper size limits and measured concentration is instrument-dependent (see Preface).

Material presented in this and following chapters will focus on particles in the fine ($PM_{2.5}$), coarse ($PM_{10-2.5}$), and ultrafine particle (UFP) size ranges as shown in Figure 2-1. There is also some limited discussion of PM_{10}. This is because longer term monitoring data exist for PM_{10} than for either $PM_{2.5}$ or $PM_{10-2.5}$, and occasionally PM_{10} data are available when $PM_{2.5}$ or $PM_{10-2.5}$ data are lacking. Each of these size ranges were described in detail in the 2009 PM ISA (U.S. EPA, 2009).

Atmospheric particle size distributions usually exhibit distinct size modes which roughly align with the above PM size ranges. An example particle size distribution, showing a nucleation mode, accumulation mode, and coarse mode, is illustrated in Figure 2-1 (Kittelson and Kraft, 2015; Kittelson, 1998). Both number of particles and particulate mass are unevenly distributed in a typical atmospheric particle size distribution, forming distinct lognormal size modes in the atmospheric particle size distribution, each with different local maxima and measurable variance (Whitby, 1978). The nucleation mode is generally made up of freshly generated particles, formed either during combustion or by atmospheric reactions of precursor gases. The nucleation mode is especially prominent near sources like heavy traffic, industrial emissions, biomass burning, or cooking (Vu et al., 2015). Particle size is not static and nucleation mode particles grow rapidly through coagulation of particles or uptake of gases by particle surfaces, giving rise to the accumulation mode. Particle size in the accumulation mode is limited by removal from the atmosphere (Friedlander, 1977) through wet and dry deposition. Coarse mode particles are formed by mechanical generation, and through processes like dust resuspension and sea spray formation (Whitby et al., 1972). Usually, the accumulation mode is the predominant contributor to PM mass and surface area, but only a minor contributor to particle number. Conversely, nucleation mode particles are only a minor contributor to PM mass and surface area, but the main contributor to particle number.

In principle, PM measurement methods are designed to correspond to one or more of the PM size modes in Figure 2-1. In practice, they are restricted to fixed particle size ranges while PM size modes are dynamic and continually changing. As a result, the subscripted PM size ranges (i.e., $PM_{2.5}$, $PM_{10-2.5}$) may not exactly match up with distinct PM size modes. However, there is a rough correspondence that can be useful for interpreting PM measurements. By number, most nucleation mode particles usually fall into the UFP range, but it is possible some fraction of the nucleation mode number distribution extends beyond above 0.1 μm in diameter. By surface area or mass, the peak of the nucleation mode corresponds to a greater diameter than for particle number, and it is more likely that a substantial fraction of particle surface area or mass is due to nucleation mode particles larger than the UFP upper limit. Most of the nucleation and accumulation mode mass is captured by $PM_{2.5}$ sampling, although a small fraction of particles that make up the accumulation mode are greater than 2.5 μm in diameter. Most coarse mode mass is captured by $PM_{10-2.5}$ sampling, but small fractions of coarse mode mass are usually smaller than 2.5 μm or greater than 10 μm in diameter.

Particles of different sizes differ in their sources, composition, chemical properties, atmospheric lifetimes, transport distances, and removal processes (U.S. EPA, 2009). Typical differences in particle

characteristics for different particle size ranges are described in Table 2-1. Although atmospheric lifetime depends on atmospheric conditions, usually UFP are transformed into the accumulation mode and $PM_{10-2.5}$ are removed from the atmosphere more rapidly than accumulation mode particles are transformed or removed, leading to shorter average atmospheric lifetimes and transport distances for particles in the UFP and $PM_{10-2.5}$ size ranges than for particles in the $PM_{2.5}$ size range (U.S. EPA, 2009). Differences in transport and atmospheric wet and dry deposition processes between different size particles were discussed in detail in the 2009 PM ISA (U.S. EPA, 2009).

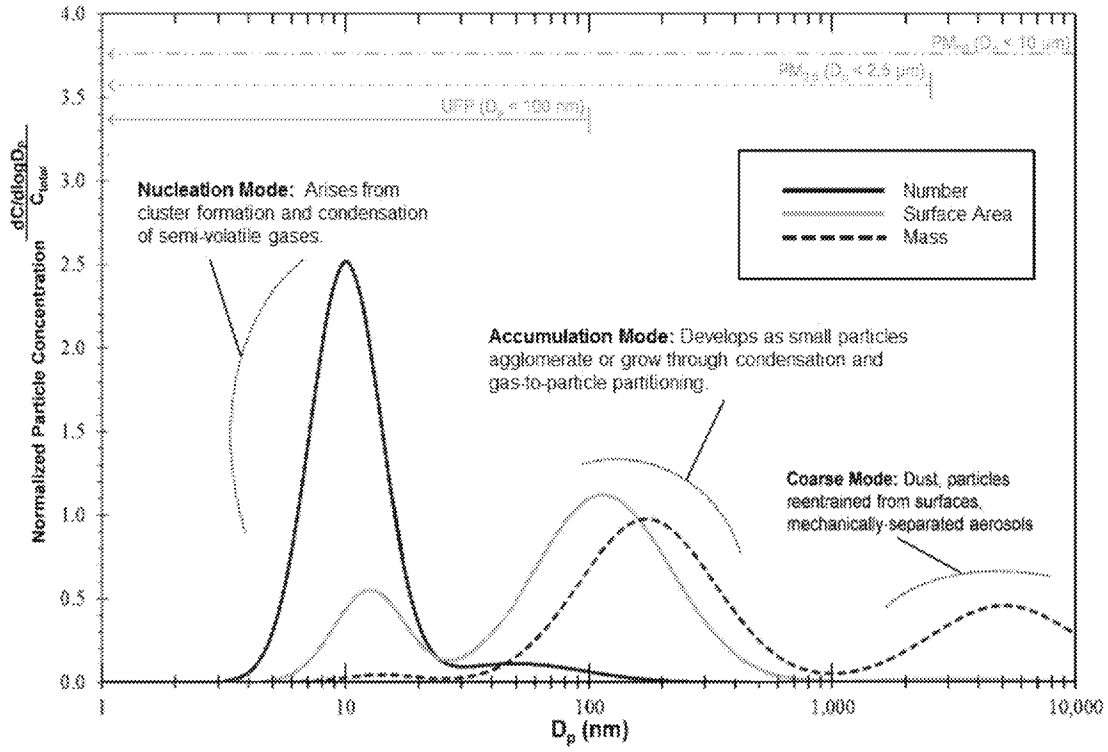

Source: Adapted from Kittelson and Kraft (2015); Kittelson (1998).

Figure 2-1 Comparison of particle size distribution by particle number, surface area, and mass. The integrated area under the number, mass, and area size-distributions are proportional to the total number, surface area, and mass concentrations.

Table 2-1 Particle transport and removal by size.

	UFP	$PM_{2.5}$	$PM_{10-2.5}$
Atmospheric residence time	Hours	Days to weeks	Hours
Transport range (km, in orders of magnitude)	<1–10	10–100	<1–1,000
Removal processes	Evaporation Atmospheric reactions Growth into larger particles Diffusion to raindrops and other surfaces	Formation of cloud droplets and rain out Dry deposition Diffusion to surfaces	Dry deposition by fallout Scavenging by falling rain drops

Adapted from Kittelson and Kraft (2015); Solomon (2012); U.S. EPA (2004).

2.3 Primary Sources and Atmospheric Formation

Particulate matter is composed of both primary and secondary chemical components. Primary PM is derived from particle emissions from a specific source. Secondary PM originates from gas-phase chemical compounds present in the ambient atmosphere that have participated in new particle formation or condensed onto existing particles. Primary particles, and the gas-phase compounds that ultimately contribute to PM, are emitted by both natural and anthropogenic sources. Earlier assessments have described, in detail, the important sources of primary and secondary atmospheric particles (U.S. EPA, 2009, 2004). Table 2-2 summarizes the anthropogenic and natural sources for the major primary and secondary constituents of $PM_{2.5}$ and $PM_{10-2.5}$.

Anthropogenic sources can be divided into stationary and mobile sources. Stationary sources include fuel combustion for electricity production and other purposes, industrial processes, agricultural activities, road and building construction and demolition, and biomass combustion. Mobile sources include diesel- and gasoline-powered highway vehicles and other engine-driven sources such as locomotives, ships, aircraft, and construction and agricultural equipment. These sources directly emit combustion-derived primary PM, as well as secondary PM precursors (discussed below), and generate particles during vehicle braking, as well as fugitive dust from paved and unpaved roads.

Table 2-2 Particle formation, composition and sources.

	UFP	$PM_{2.5}$	$PM_{10-2.5}$
Formation processes	Combustion Pyrogenesis Homogeneous and/or heterogeneous nucleation Condensation and adsorption (gas-particle partitioning)	Gas-particle partitioning Particle agglomeration Reactions of gases in or on particles Cloud droplet evaporation	Mechanical degradation of solid materials (crushing, grinding, abrasion of surfaces) Evaporation of sea spray Suspension of dust
Typical chemical/material components	Sulfate Elemental carbon Metal compounds Low volatility organic compounds	Sulfate, nitrate, ammonium, and hydrogen ions Elemental carbon Low and moderate volatility organic compounds Metals: compounds of Pb, Cd, V, Ni, Cu, Zn, Mn, Fe, etc. Water	Suspended soil or street dust Fly ash from coal, oil, and wood combustion Nitrates/chlorides/sulfates from HNO^3/HCl/SO_2 reactions with coarse particles Oxides of crustal elements (Si, Al, Ti, Fe) Sea salt (Na, K, Ca, carbonate, sulfate and chloride) Pollen, mold, fungal spores Plant and animal detritus Tire, brake pad, and road wear debris
Dominant[1] primary particle sources	Combustion of fossil fuels and biomass High temperature processes (i.e., smelters, steel mills, etc.)	Combustion of fossil fuels and biomass High temperature processes	Resuspension of industrial dust and soil tracked on to roads and streets Suspension from disturbed soil (e.g., farming, mining, unpaved roads) Construction and demolition Coal and oil combustion Sea spray Biological sources
Secondary particle formation processes	Particle formation and growth due to oxidation of gas-phase anthropogenic, biogenic and geogenic precursors (NO_X, SO_2, and organic compounds)	Partitioning of gas phase products of precursor oxidation; aqueous oxidation of dissolved precursors with evaporation and growth cycling	

[1]All source-specific particles are produced in a distribution of sizes, with usually one major mode. This means that all sources will generate small quantities of particles that are both much larger and much smaller than the main size mode. For example, particles generated by construction activities generally fall into the $PM_{10-2.5}$ size fraction. However, the distribution extends into the UFP size range.

Ambient PM also forms in the atmosphere from photochemical oxidation of precursor gases. This material is referred to as secondary PM. The large, semi- and nonvolatile reaction products of these oxidation reactions may condense to form new particles or onto existing particles. Table 2-2 includes sources for several PM precursor gases. Discussion of the photochemical reactions that transform these precursor gases into secondary PM can also be found in earlier assessments (U.S. EPA, 2009, 2004). An overview of estimates of emissions of primary PM and precursors to secondary PM from major sources is given in this section.

In general, the sources of $PM_{2.5}$ are very different from those of $PM_{10-2.5}$. $PM_{10-2.5}$ is almost entirely primary in origin, as described in Section 2.2, and is produced by surface abrasion or by suspension of sea spray or biological material (e.g., microorganisms, pollen, plant and insect debris).

2.3.1 Primary $PM_{2.5}$ Emissions

2.3.1.1 National Scale Emissions

The relative contributions of specific sources to national emissions of primary $PM_{2.5}$ are similar to those reported in the 2009 PM ISA (U.S. EPA, 2009). Figure 2-2 shows the U.S. national average emissions of primary $PM_{2.5}$ from the 2002 National Emissions Inventory (NEI) described in the 2009 PM ISA (U.S. EPA, 2009), and the 2014 NEI, Version 2 (U.S. EPA, 2018). The NEI is a national compilation of emissions information provided by state, local, and tribal air agencies as well as source sector emission estimates developed by the U.S. Environmental Protection Agency (U.S. EPA). It focuses largely on anthropogenic sources, with information about natural sources where available. Emissions composition and mass estimates undergo continual revision as better information becomes available but are subject to varying degrees of uncertainty. For these and other reasons, ambient PM mass and composition can be quite different from what might be inferred by examining emission inventories alone (U.S. EPA, 2009).

Dust and fire each account for approximately 36% of total $PM_{2.5}$ emissions included in the 2014 NEI. Dust includes agricultural, construction, and road dust. Of these, agricultural dust and road dust make the greatest contributions to $PM_{2.5}$ mass on a national scale. Fires include wildfires, prescribed fires, and agricultural fires, with wildfires and prescribed fires accounting for most of the $PM_{2.5}$ fire emissions on a national scale.

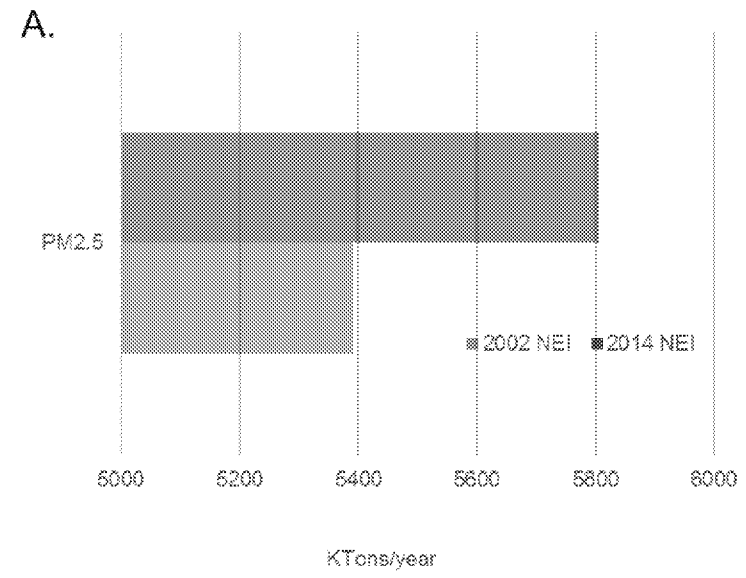

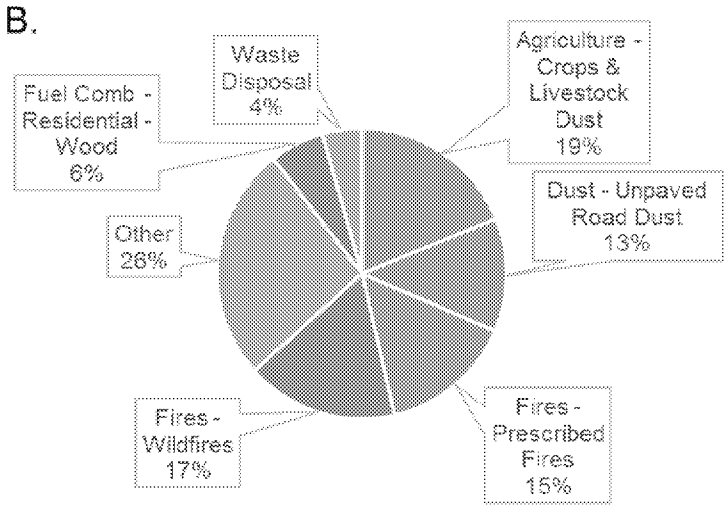

Source Permission pending: U.S. EPA (2018) and U.S. EPA (2009).

Figure 2-2 **Primary $PM_{2.5}$ emissions at the U.S. national scale. (A) $PM_{2.5}$ emissions from the 2002 U.S. EPA National Emissions Inventory versus the 2014 U.S. EPA National Emissions Inventory. (B) Largest, national-scale sources of $PM_{2.5}$. "Other" includes all remaining source sectors, all of which are emitting 2% or less of the national $PM_{2.5}$ emissions total.**

2.3.1.2 Urban Scale Emissions

The sources and relative annual average emissions of primary $PM_{2.5}$ at the urban scale can vary substantially from city to city. Figure 2-3 shows five U.S. counties containing large cities that were selected from the 2014 NEI to illustrate the variation in primary $PM_{2.5}$ source composition. In urban settings, the majority of primary $PM_{2.5}$ emissions estimated in the NEI include some combination of industrial activities, motor vehicles, cooking, and fuel combustion, and often include wood smoke. Dust accounts for a large fraction of primary $PM_{2.5}$ emissions in several of the counties, due to construction and entrainment of paved road dust, in contrast to the national scale where the largest emissions are attributed to agricultural processes and vehicular traffic on unpaved roads. While fire emissions comprise a large fraction of annual average emissions at the national scale, they represent a much smaller fraction with respect to other sources for the urban counties shown.

A. Queens County, NY

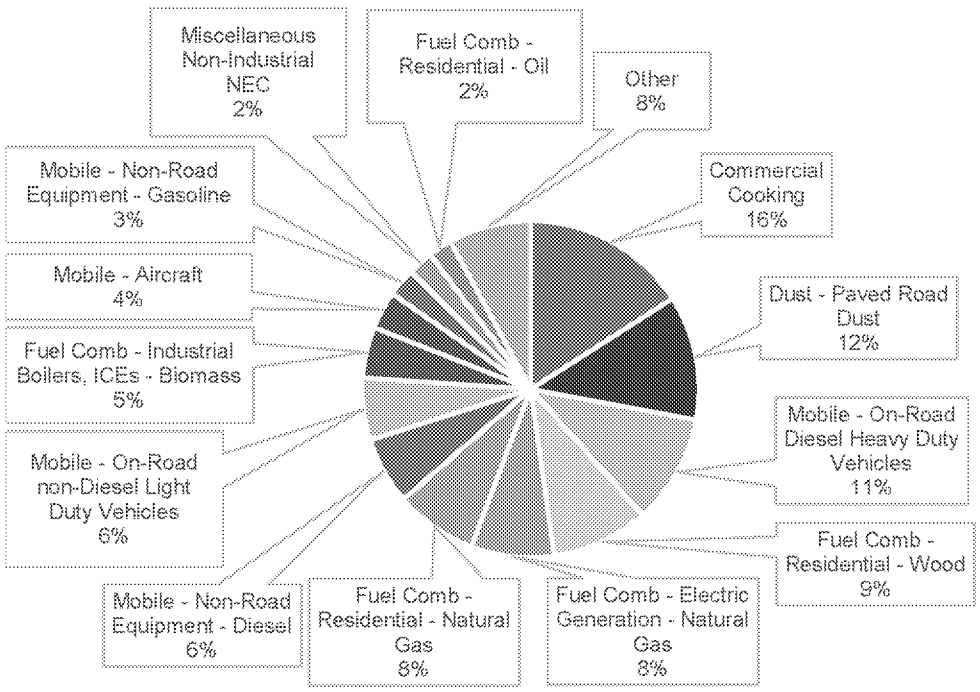

B. Philadelphia County, PA

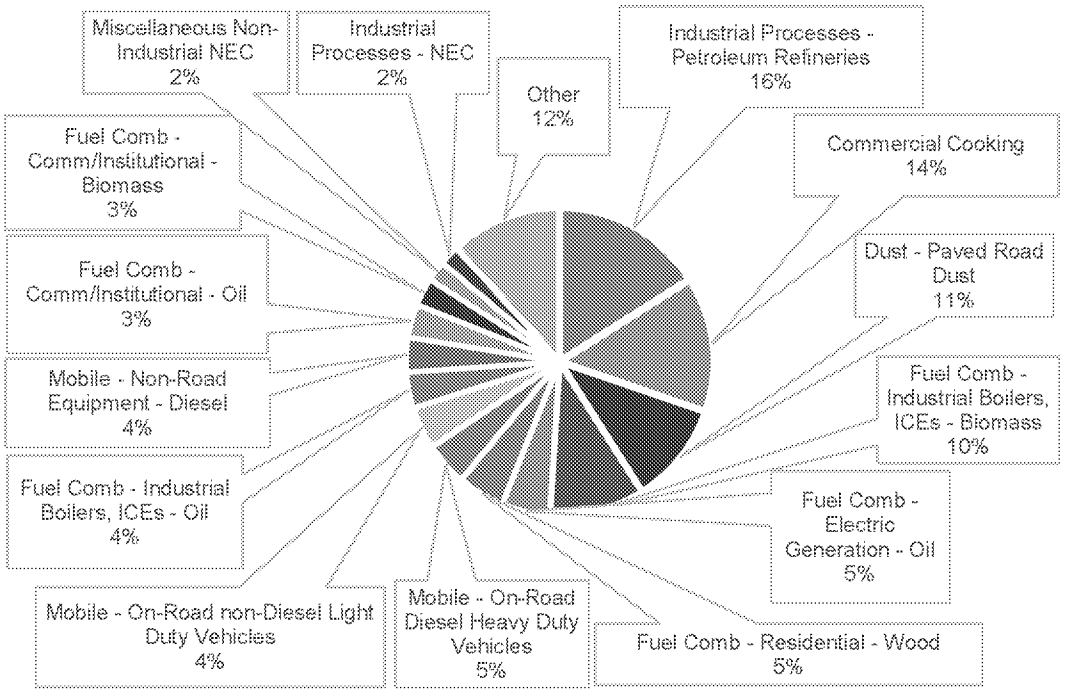

C. Los Angeles County, CA

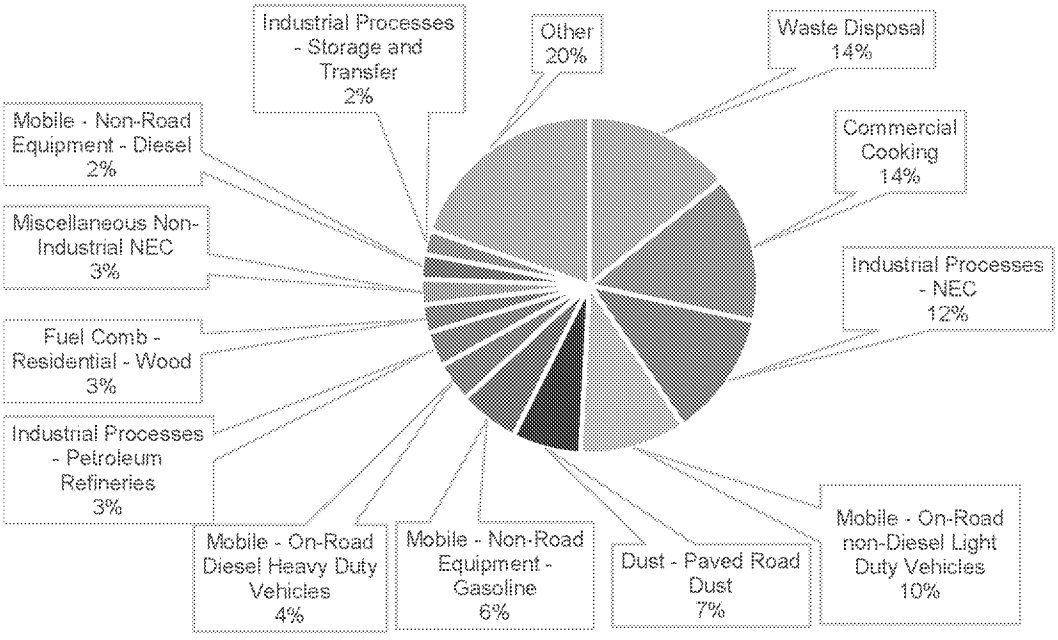

D. Sacramento County, CA

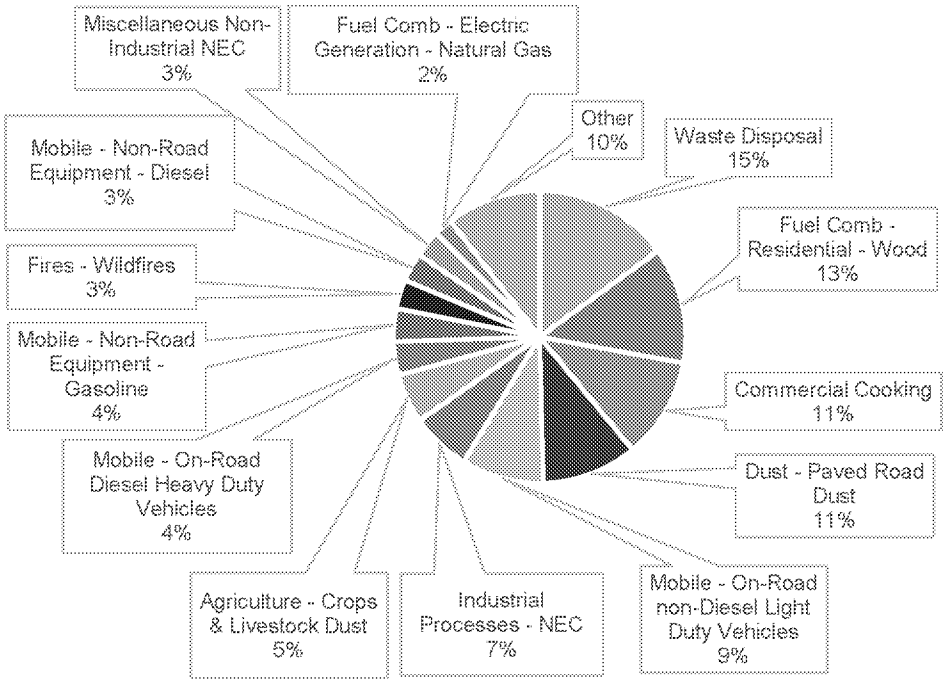

E. Maricopa County (Phoenix), AZ

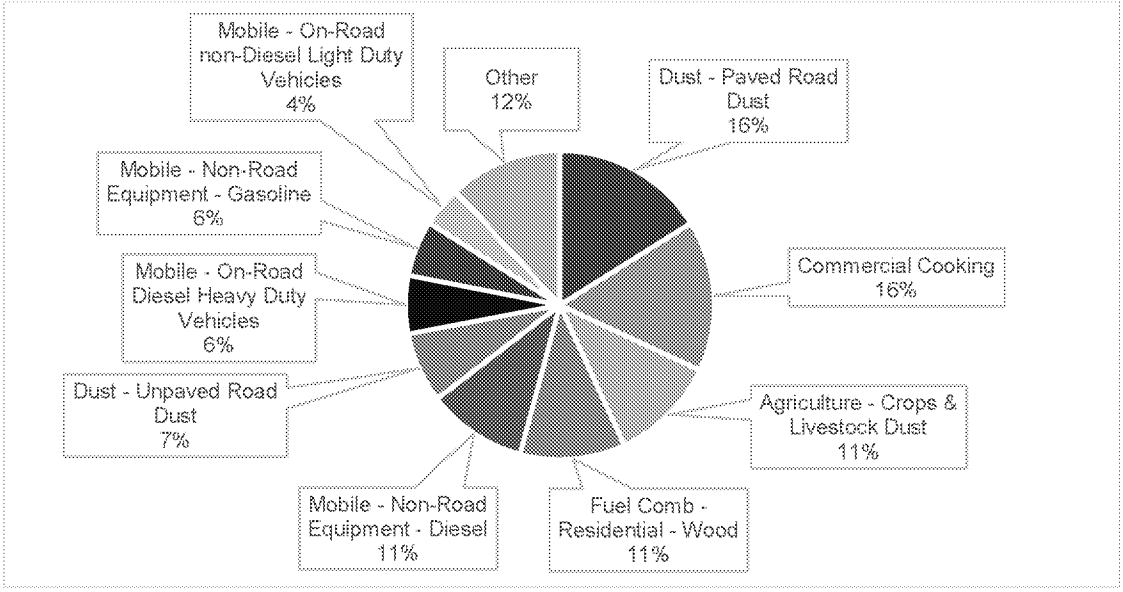

Source Permission pending: 2014 U.S. EPA National Emissions Inventory, Version 1. (U.S. EPA, 2016a).

Figure 2-3 Primary $PM_{2.5}$ emissions for (A) Queens County, NY; (B) Philadelphia County, PA; (C) Los Angeles County, CA; (D) Sacramento County, CA; (E) Maricopa County, AZ (Phoenix).

Mobile sources, as noted in the 2009 PM ISA, are a major source of primary PM at urban scales, especially light-duty gasoline and heavy duty diesel vehicles (U.S. EPA, 2009). They are discussed in further detail here because they represent a consistently large fraction of total $PM_{2.5}$ emissions in all urban areas (Section 2.3.1.2), and several important advances in engine and pollution control technology have occurred in recent years. For the example counties shown in Figure 2-3, mobile sources account for an estimated 13–23% of the NEI's total primary $PM_{2.5}$ emissions. Primary $PM_{2.5}$ emitted by mobile sources is due to direct tailpipe emissions, brake, clutch and tire wear. Significant changes in both gasoline and diesel emissions controls have led to reductions in primary $PM_{2.5}$ emitted from newer vehicles. Light-duty vehicles in the U.S. (i.e., passenger cars and light-trucks under 8,500 lbs. gross vehicle weight rating) are rapidly transitioning from port fuel injection (PFI) with fuel injected upstream of the exhaust valve to direct, in-cylinder fuel injection systems, also known as gasoline direct injection (GDI). In 2007, a new U.S. EPA PM emissions standard required reduction of diesel PM emissions by 90% to 0.01 g/bhp-hour (U.S. EPA, 2009). Their impact on UFP are discussed in Section 2.3.4. Mobile sources are also responsible for $PM_{2.5}$ dust suspension on and off-road. (Note: dust is also present in the coarse mode and is discussed further in Section 2.3.3 as it pertains to primary $PM_{10-2.5}$ emissions).

2.3.2 Secondary $PM_{2.5}$ Formation

After emission, primary particles transform in size and chemical composition due to coagulation with other particles, gas-to-particle condensation of semivolatile gases, and photochemical aging processes that oxidize particle components or generate oligomers. Particle dynamics, gas-particle partitioning, aging and other heterogeneous chemical processes have been discussed in earlier PM assessments (U.S. EPA, 2009, 2004). Much is understood about the physical processes that lead to the growth of particles in the atmosphere, but the reaction mechanisms that contribute to these processes as well as to the formation and chemical transformation of particles with time remains an area of active research.

Secondary $PM_{2.5}$ accounts for a substantial fraction of the $PM_{2.5}$ mass with both natural and anthropogenic sources (U.S. EPA, 2009). It forms by way of atmospheric photochemical oxidation reactions of both inorganic and organic gas-phase precursors. Reactions leading to sulfate production from SO_2, nitrate production from NO_X (i.e., NO + NO_2) and the gas-to-particle equilibrium between NH_3 and NH_4^+ are relatively well understood. As noted, above, formation of secondary PM, often referred to as secondary organic aerosol (SOA) in the atmospheric chemistry literature, is less well resolved. Considerable recent research on mechanisms, kinetic details, and secondary organic component identification has been reported in the literature since the 2009 PM ISA. The following sections will briefly summarize the important developments in new secondary organic PM formation, including the identification of previously unknown precursors, interactions among biogenic and anthropogenic reactants, and the role of aqueous-phase chemistry.

2.3.2.1 Precursor Emissions

Secondary PM is derived from the oxidation of a range of organic and inorganic gases of anthropogenic and natural origin. Figure 2-4 shows relative source contributions to emissions of major $PM_{2.5}$ precursors from the 2014 NEI. Anthropogenic SO_2 and NO_X are the predominant precursor gases in the formation of secondary $PM_{2.5}$. Ammonia plays an important role in the formation of sulfate and nitrate PM by neutralizing sulfuric and nitric acid, leading to more stable PM with lower volatility (i.e., ammonium nitrate). The oxidation of volatile organic compounds (VOCs) may also yield semi- and nonvolatile compounds that contribute to PM and the formation of new particles.

The relative proportions of the various anthropogenic source categories (i.e., as fractions of the total emissions inventory) are very similar to those presented in the 2009 PM ISA (U.S. EPA, 2009). Sulfur dioxide emissions are mainly from electricity generating units (fuel combustion used in electricity generation (66%). NO_X is emitted by a range of combustion sources, including various mobile sources (54%). Ammonia emissions are primarily emitted by livestock waste from animal husbandry operations (55%) and fertilizer application (22%). Estimates of biogenic emissions were provided in the 2014 NEI and appear as the predominant organic precursor on the national scale (71%).

The greatest change in precursor emissions since the publication of the 2009 PM ISA (U.S. EPA, 2009) is the reduction in SO_2 emissions.

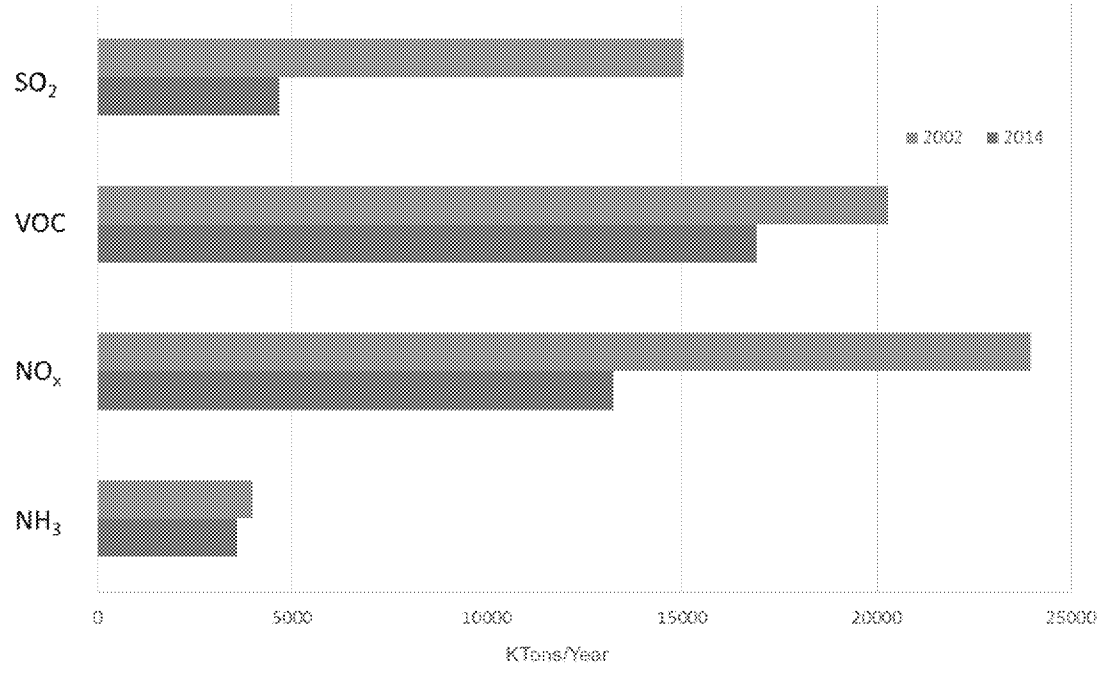

SO2 = sulfur dioxide; VOC = volatile organic compounds; NO_X = nitrogen oxides; NH_3 = ammonia; KTons = kilotons.

Source Permission pending: U.S. EPA (2018) and U.S. EPA (2009).

Figure 2-5 shows the difference in NEI national emission estimates for SO_2, NO_X, and NH_3 between the 2006 NEI and the 2014 NEI, showing SO_2 decreasing from 13.9 million metric tons (MMT) in 2006 to 4.8 MMT in 2014, a 65% decrease. NO_X also exhibited a substantial decrease over this period while NH_3 emissions are similar. VOC's cannot be compared because biogenics were not included in the 2006 NEI.

Anthropogenic emissions of SO_2 in the U.S. have shown dramatic declines since the implementation of the 1990 amendments to the Clean Air Act (USC Title 42 Chapter 85). Annual SO_2 emissions from electric utilities declined by 79% in the 2004−2016 time frame (U.S. EPA, 2017). In the same period, SO_2 emissions by highway and nonhighway vehicles declined by 84% and 90%, respectively. Hand et al. (2012b) studied reductions in EGU-related annual SO_2 emissions during the 2001−2010 period. They found that emissions decreased throughout the U.S. by 6.2% per year, with the largest reductions in the western U.S. at 20.1% per year. The smallest reduction (1.3% per year) occurred in the Great Plains states. These trends, and emissions of sulfide gases that serve as precursors to ambient SO_2, are discussed in detail in the 2017 Integrated Science Assessment for the Sulfur Oxides (U.S. EPA, 2017).

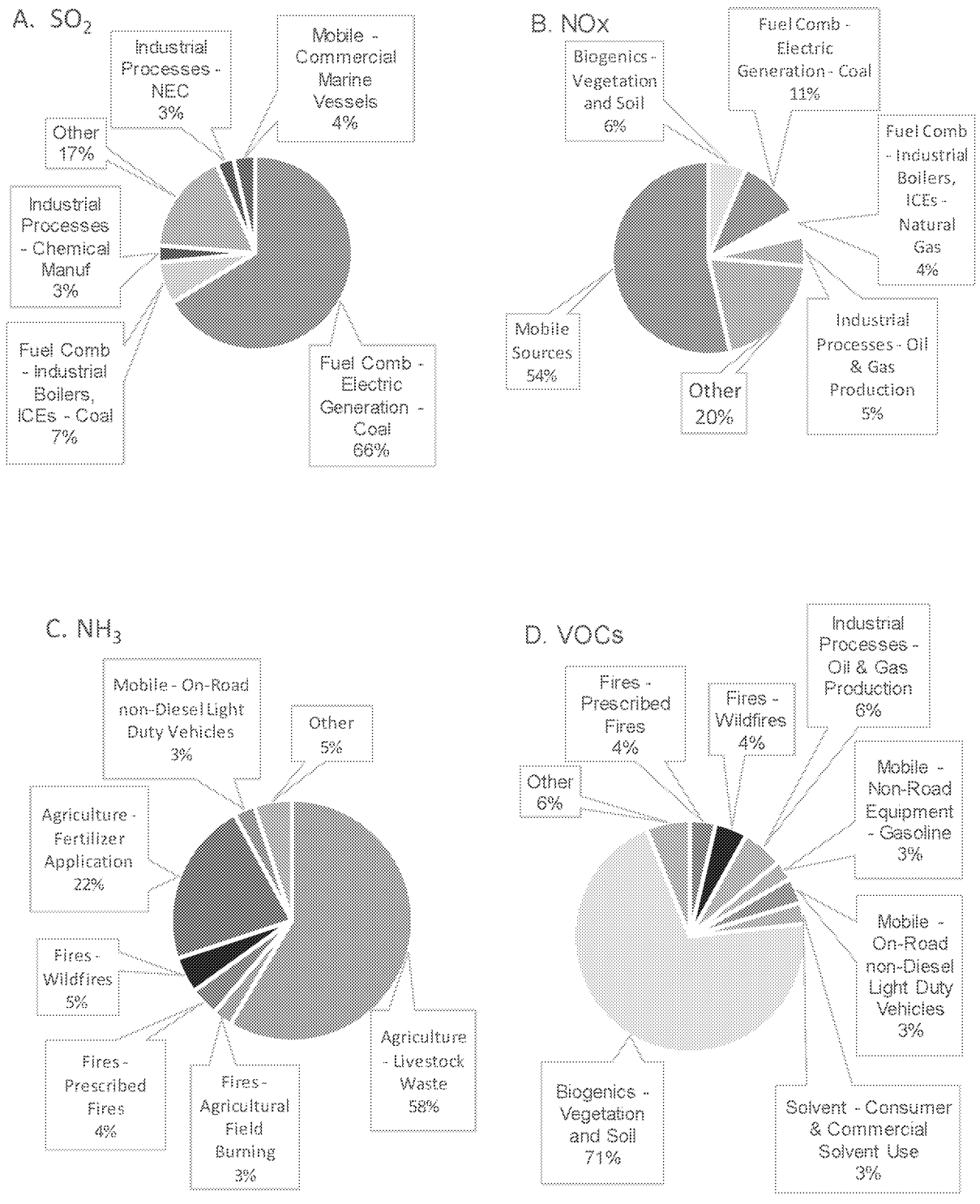

Source Permission pending: 2014 U.S. EPA National Emissions Inventory, Version 2 (U.S. EPA, 2018).

Figure 2-4 Relative $PM_{2.5}$ precursor emissions by U.S. sector: (A) sulfur dioxide (SO_2), (B) nitrogen oxide; (NO_X), (C) ammonia (NH_3), (D) volatile organic compounds (VOCs).

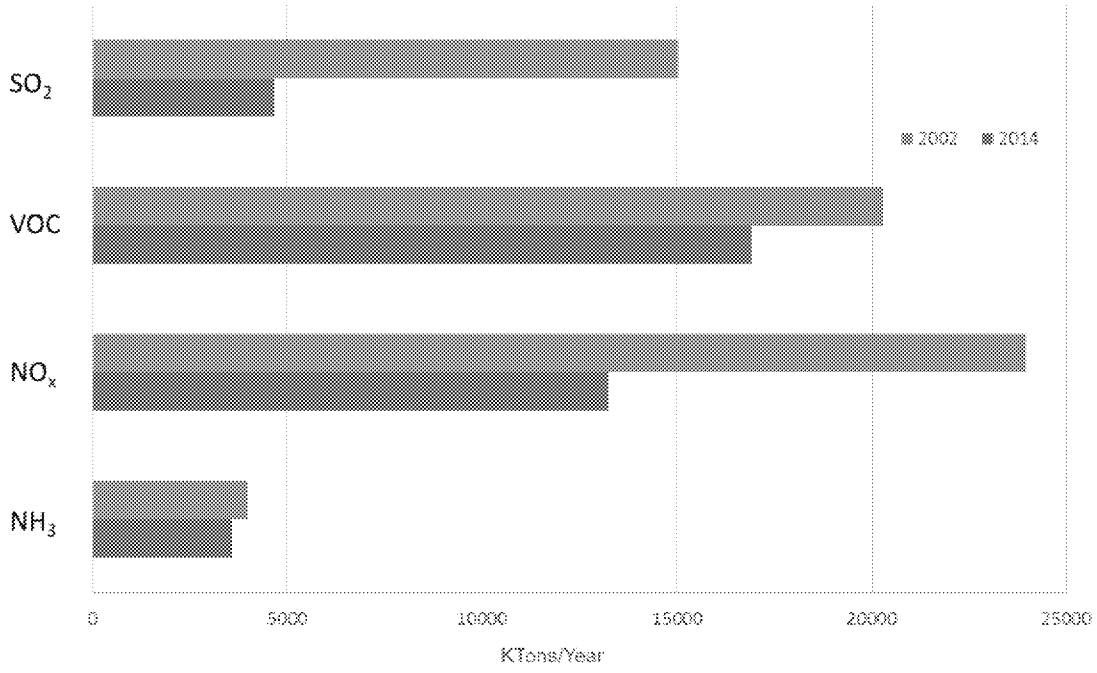

SO_2 = sulfur dioxide; VOC = volatile organic compounds; NO_X = nitrogen oxides; NH_3 = ammonia; KTons = kilotons.
Source Permission pending: U.S. EPA (2018) and U.S. EPA (2009).

Figure 2-5 Difference in select $PM_{2.5}$ precursor emissions from the 2002 and 2014 National Emission Inventories.

2.3.2.2 Secondary Inorganic Aerosols

Particulate sulfate, nitrate, and ammonium formation processes were summarized in the 2009 PM ISA (U.S. EPA, 2009) and presented in more detail in the 2004 PM AQCD (U.S. EPA, 2004) and ISAs for oxides of sulfur and nitrogen (U.S. EPA, 2008b). Together, these $PM_{2.5}$ components produced by secondary formation often account for the majority of $PM_{2.5}$ mass (see Section 2.5.2.1.4).

SO_2 reacts in both the gas phase and in aqueous solution in clouds and particles to form sulfate. Dissolved SO_2 rapidly partitions into four forms with the same oxidation state, with their relative concentrations dependent on pH:

$$S(IV) = SO_2(aq) + H_2SO_3(aq) + HSO_3^-(aq) + SO_3^{2-}(aq)$$

Equation 2-1

S(IV) is then oxidized to sulfuric acid in cloud water by H_2O_2, O_3, or O_2 in the presence of Fe(III). Reaction with H_2O_2 dominates at pH values below 5.3. Reaction with either dissolved O_3 or O_2 catalyzed by Fe(III) becomes most important at pH values greater than about 5.3 (U.S. EPA, 2008a). SO_2

is also oxidized to H_2SO_4 in the gas phase by hydroxyl radical or organic radicals formed in atmospheric photochemical processes (Berndt et al., 2012; Mauldin et al., 2012; Welz et al., 2012) with a characteristic time scale of about 10 days (Sander et al., 2011).

NO_2 can be converted to gaseous HNO_3 by reaction with OH radicals during the day. At night, NO_2 is also oxidized to HNO_3 by a sequence of reactions initiated by O_3 that produce nitrate radicals and dinitrogen pentoxide as intermediates. Both processes are important in the atmosphere.

Both H_2SO_4 and HNO_3 react with atmospheric ammonia (NH_3). Atmospheric particulate NH_4NO_3 is in equilibrium with gas-phase NH_3 and HNO_3. Lower temperature and higher relative humidity shifts the equilibrium towards particulate NH_4NO_3 because of the large sensitivity of the equilibrium constant to temperature. This results in a strong seasonal dependence in particulate nitrate concentrations, with much higher winter than summer concentrations in many locations (see Section 2.5.2.2.4). In aqueous aerosols, sulfuric acid can be partly or totally neutralized by NH_3. At low atmospheric NH_3 concentrations, equilibrium formation of ammonium sulfate is favored over ammonium nitrate; any nitrate remains in the gas phase as nitric acid. When NH_3 concentration exceeds SO_4^{2-} concentration, excess NH_3 can react with HNO_3 to form NH_4NO_3. (U.S. EPA, 2008a).

Ambient particle acidity is a difficult property to measure and is usually estimated by models. Recent measurement attempts in the U.S. Southeast have led to questions concerning the predictability of particle acidity on the basis of relative atmospheric NH_3, H_2SO_4 and HNO_3 concentrations—species which would otherwise be expected to quickly react and achieve thermodynamic equilibrium. For example, Weber et al. (2016), after evaluating the observational record, suggested that pH buffering by partitioning of ammonia between the gas and particle phases produced a relatively constant particle pH of 0–2 throughout the 15 years of decreasing atmospheric sulfate concentrations. They saw little change in particle ammonium nitrate concentrations that would have been expected, had particle pH values increased with decreasing sulfuric acid concentrations. They concluded that fairly constant emissions of semivolatile NH_3 related to agriculture ensures that the acid/base gas-particle system in the southeastern U.S. remains insensitive to changing SO_2 concentrations. Other observations indicated that the extent of neutralization of sulfuric acid and bisulfate by ammonium can be incomplete even in the presence of excess atmospheric NH_3 and proposed that uptake of NH_3 is inhibited by organic compounds coating particle surfaces (Kim et al., 2015), in accord with laboratory studies (Liggio et al., 2011). Pye et al. (2018), in their combined modeling study and evaluation of available measurements, suggest that the inconsistencies among the different measurements of particle composition, especially concerning to the fraction of condensed-phase organosulfate, must be resolved before conclusions can be drawn concerning the validity of current approaches to modeling particle acidity.

2.3.2.3 Secondary Organic Aerosols

As discussed in the 2004 PM AQCD (U.S. EPA, 2004) the study of the chemical mechanisms responsible for the formation of secondary PM related to VOC precursor oxidation has been the subject of active research. Oxygenated organic compounds appeared, based on observations, to be the dominant form of organic PM in Northern Hemisphere midlatitudes (Zhang et al., 2007). However, the mechanism(s) responsible for their formation were not well resolved, as evidenced by the persistent underprediction of observed OC concentrations by chemical transport models. This underprediction was significant for summertime PM (Wyat Appel et al., 2008; Morris et al., 2006), when biogenic precursor concentrations and photochemical reaction conditions are most favorable for SOA formation.

Substantial research on isoprene, aromatic hydrocarbons and further reaction of gas phase secondary products has been reported. Studies of isoprene as a major precursor led to identification of a number of previously unknown products as well as advances in understanding yields and mechanisms (Carlton et al., 2009). Modeling studies that included oxidation of aromatic precursors indicated that a large fraction of SOA could be derived from aromatic precursors. SOA production not only from simple aromatic compounds, but also from less volatile polycyclic aromatic compounds like naphthalene and substituted naphthalenes were reported (Kleindienst et al., 2012; Chan et al., 2009), and polycyclic aromatic hydrocarbons could account for up to 54% of total SOA from oxidation of diesel emissions (Zhao et al., 2014). Additional precursors remain possible, and the products of aromatic and biogenic compound oxidation that appear in particles may have not been fully identified.

As reported in the 2009 PM ISA (U.S. EPA, 2009), in the presence of high NO_X concentrations, the oxidation of biogenic hydrocarbons is observed to produce larger quantities of SOA. High ambient NO_X concentrations in the atmosphere are typically due to anthropogenic emissions. Mixtures, as a rule, of both biogenic and anthropogenic precursors produce greater SOA yields than mixtures dominated by just one class of precursors (Shilling et al., 2013). The presence of anthropogenic particles also enhances the formation of SOA, by providing additional volume and surface area to which semivolatile VOC oxidation products can partition or adsorb (Hoyle et al., 2011). Carlton et al. (2010) predicted that more than 50% of biogenic SOA in the Eastern U.S. could be controlled by reducing anthropogenic NO_X emissions. These findings are consistent with the satellite observations of (Goldstein et al., 2009) of a cooling haze of secondary particles over the Southeastern U.S. associated with a mixture of biogenic VOCs with anthropogenic NO_X.

Recent insight into the role of anthropogenic NO_X and SO_X in enhancing the production secondary PM include the identification of organosulfates and organonitrates among particle-phase organic compounds. The 2009 PM ISA discussed the early indications that SOA chemistry with anthropogenic SO_X yielded compounds with oxidized sulfur functional groups (U.S. EPA, 2009). Organosulfates had been observed as products of isoprene (Surratt et al., 2007), and monoterpenes (Surratt et al., 2008). Subsequently, oxidation of sesquiterpenes (Chan et al., 2011), and glyoxal (Lim et al., 2016) were also found to yield organosulfates under similar conditions. These products have been

estimated to account for 40% of PM sulfate (Vogel et al., 2016), 30% of PM organic matter (Surratt et al., 2008), 6−14% of total atmospheric sulfur concentration (Lukacs et al., 2009), and 5−10% of $PM_{2.5}$ organic mass (Tolocka and Turpin, 2012). The chemical mechanism that may explain the formation of organosulfate compounds is described in the ISA for Sulfur Oxides (U.S. EPA, 2017).

Substantial SOA mass from highly functionalized nitrate products of isoprene and monoterpenes were observed in several studies (Fisher et al., 2016; Lee et al., 2016; Kourtchev et al., 2014; Nguyen et al., 2011), accounting for as much as 10−20% of carbonaceous aerosol mass in urban locations (Day et al., 2010; Holzinger et al., 2010). In flow reactor experiments, organic nitrates accounted for up to 40% of SOA mass (Berkemeier et al., 2016). O'Brien et al. (2013), in their study of SOA collected during the CalNex 2010 field study, found that the identities of nitrogen-containing organics and total proportion of OC varied as a function of time-of-day. These differences could be explained by multiple reaction mechanisms, including one that relies upon the nitrate radical as a reactant. In the presence of both NO_X, SO_X and O_3, Lim et al. (2016) identified organonitrates, organosulfates, and organic compounds containing both nitrogen and sulfur, in their smog chamber study of the photochemistry of glyoxal in the presence of sulfate or sulfuric acid particles at high and low relative humidities.

Aqueous particle reactions and cloud processing as well as repeated cycles of volatilization and condensation of semivolatile reaction products have been shown to be important processes for SOA evolution. Production of OH in cloud water was described by Hallquist et al. (2009) and estimates of the magnitude of in-cloud formation of SOA comparable to that of gas phase formation were reported (Liu et al., 2012). High molecular weight organic compounds appear to increase with decreasing cloud water pH (Cook et al., 2017). Cloud water has been shown to provide a medium for oligomer formation involving methylglyoxal (Cook et al., 2017; Yasmeen et al., 2010), syringol and guaiacol (Cook et al., 2017; Yu et al., 2016; Yu et al., 2014a) when influenced by wildfire emissions (Cook et al., 2017; Yasmeen et al., 2010).

In summary, consistently higher-than-predicted measured OC concentrations, along with the observations of unexpectedly large fractions of secondary-to-total organic $PM_{2.5}$, motivated an intensive research effort to identify additional chemical processes that could explain these differences. This effort has yielded new observations of high SOA yields from isoprene and intermediate volatility organic compounds; identification of new sulfur and nitrogen containing products that account for a substantial fraction of SOA mass; identification of cloud water and aqueous aerosols as reaction media potentially as productive as the gas phase; and enhancement of SOA yields from biogenic precursors when anthropogenic reactants are also present. Given the rapid discovery of new precursors, products, and even reaction media, a high degree of uncertainty remains regarding the contribution of SOA to organic aerosol.

2.3.3 Primary $PM_{10-2.5}$ Emissions

As described in the 2004 PM AQCD (U.S. EPA, 2004), crustal materials dominate the $PM_{10-2.5}$ fraction throughout the U.S. and fugitive dust has been identified as the largest source of measured PM_{10} in many locations in the western U.S. Mineral dust, organic debris, and sea spray have also been identified as mainly in the coarse fraction (U.S. EPA, 2004). Road and construction dust represent a mechanism for suspension of crustal material on paved and unpaved roads. Wildfire plumes are now known to entrain soil representing another potential source of ambient $PM_{10-2.5}$ (Kavouras et al., 2012). Estimates of $PM_{10-2.5}$ sources from the 2014 NEI are summarized in Figure 2-6, and are very similar to those reported in the 2009 PM ISA (U.S. EPA, 2009).

Quantification of dust emissions is highly uncertain. Dust storms, like wildfires, are common but intermittent emissions sources. The suspension and resuspension of dust by any mechanism is difficult to quantify. Current NEI estimates of dust emissions across the U.S. are based on limited emissions profile and activity information. Dust injected into the upper troposphere is also transported from other continents into the U.S. by strong atmospheric currents, notably from the African and Asian deserts. Some of these particles fall into the $PM_{10-2.5}$ size range. These particles are considered to be part of the "background" component of PM, discussed in Section 2.5.4.

As discussed in the 2004 PM AQCD (U.S. EPA, 2004) and the 2009 PM ISA (U.S. EPA, 2009), primary biological aerosol particles (PBAP) contribute to coarse PM. However, estimating emissions is highly problematic. No emission rates have yet been reported, though Despres et al. (2012) described the occurrence, sources and measurement methods for different categories of PBAP. Barberán et al. (2015) characterized the distribution of airborne microbes in settled dust from ~1,200 locations in the continental U.S. They found substantial variability in the composition of microbial communities that could be related largely to climatic factors (mean annual temperature and precipitation) and soil composition (soil pH and net primary productivity). No estimates were given of the rates at which these particles are emitted into the atmosphere.

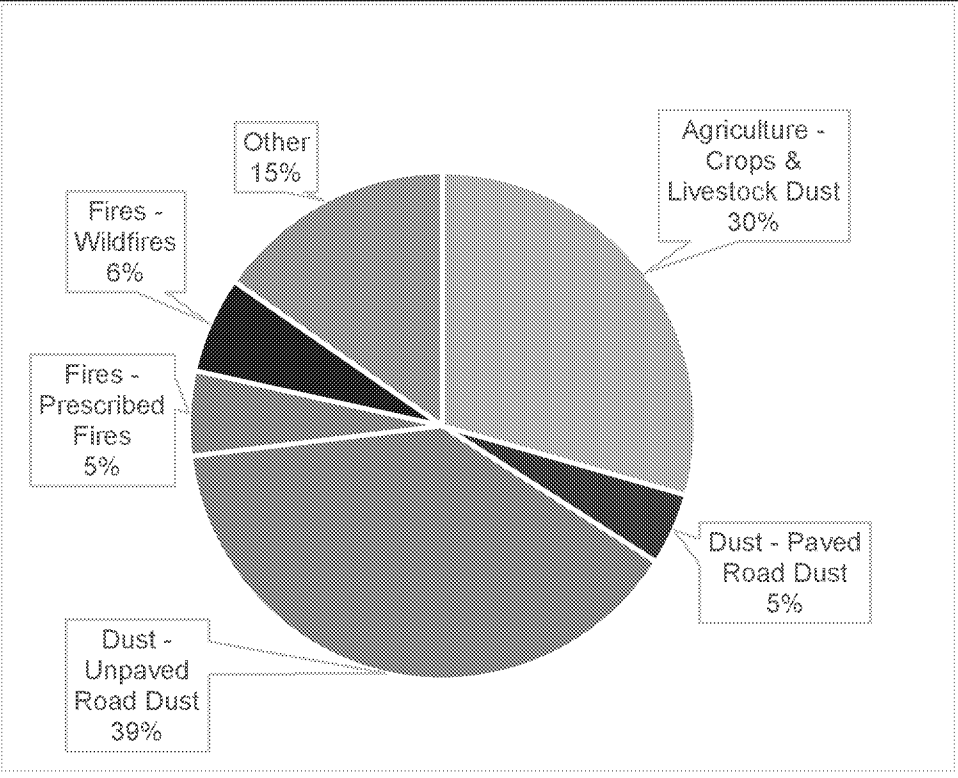

Source Permission pending: 2014 U.S. EPA National Emissions Inventory, Version 2 (U.S. EPA, 2018).

Figure 2-6 National emissions of PM_{10}.

2.3.4 Ultrafine Particles

UFP primary sources were not treated separately in the 2009 PM ISA because there is almost complete overlap between UFP and $PM_{2.5}$ sources. Particles in the $PM_{2.5}$ size range typically begin as primary UFP, or are formed through secondary particle formation, and grow through coagulation or gas-to-particle condensation (see Section 2.2). However, UFP sources are addressed independently in this ISA with a focus on sources for which near-source human exposure is substantial, such as roads and airports, as well as on new particle formation, for which a substantial amount of new research has recently been conducted.

Ambient UFPs originate from two distinct processes: primary emissions and new particle formation (NPF). Primary UFP originate from a large variety of sources, such as transportation (road traffic, ships and aircraft), power plants, municipal waste incineration, construction and demolition, vegetation fires, domestic biomass burning, cooking and cigarette smoke (Kumar et al., 2013; Janhaell et al., 2010; Langmann et al., 2009; Morawska et al., 2008). Primary sources of UFP are largely the same as $PM_{2.5}$, and much of $PM_{2.5}$ mass is initially emitted as UFP before atmospheric coagulation and growth (see Section 2.2). Atmospheric NPF involves the production of very small, molecular clusters and

subsequent growth of these clusters to larger sizes, typically a few tens of nm in particle diameter (Kulmala et al., 2014; Zhang et al., 2012b). As described in Section 2.2, UFP consists mainly of nucleation mode particles, but nucleation mode aerosols often have short atmospheric lifetimes as particles coagulate into the accumulation mode.

As Table 2-3 shows, UFP can be subdivided into a cluster mode, nucleation mode, Aitken mode, and a portion of the accumulation mode in order of increasing size, although a naming convention for primary ultrafine particles has not been established (Giechaskiel et al., 2014; Kumar et al., 2010). The size ranges refer to the particle diameter, encompassing the disparate definitions found in the scientific literature.

Table 2-3 Modes of atmospheric particle populations.

Mode	Size Range	Sources[a]	Main Components
Cluster mode	<3 nm	NPF	Secondary compounds capable of forming extremely low volatility complexes
Nucleation mode	<30 nm	NPF, COM	Secondary compounds of very low volatility, nonvolatile additives in fuels, lubricants
Aitken mode	10–100 nm	NPF, COM	Soot, secondary compounds of very low volatility, semivolatile compounds
Accumulation mode	30–1,000 nm	NPF, COM, OTH	Soot, secondary semi- and low-volatility organic and inorganic compounds

[a]NPF = atmospheric new particle formation and growth, COM = combustion, OTH = other primary sources.

In the atmosphere, the cluster mode is usually well separated from the other modes and has a relatively high number concentration (Figure 2-7 and Figure 2-8), even though only few atmospheric measurements on the character of this mode currently exist. The relative magnitudes and mean diameters of the nucleation, Aitken and accumulation modes vary with the time of day and location depending on the dominant particle sources and aging processes. As a result, these three modes are often not distinguishable in individual particle number distributions. Even when cluster mode or sub-0.01 μm size particles are not considered, ultrafine particles tend to dominate the total particle number concentration. Contrary to this, accumulation mode particles dominate the submicron particulate mass concentration, as explained in Section 2.2.

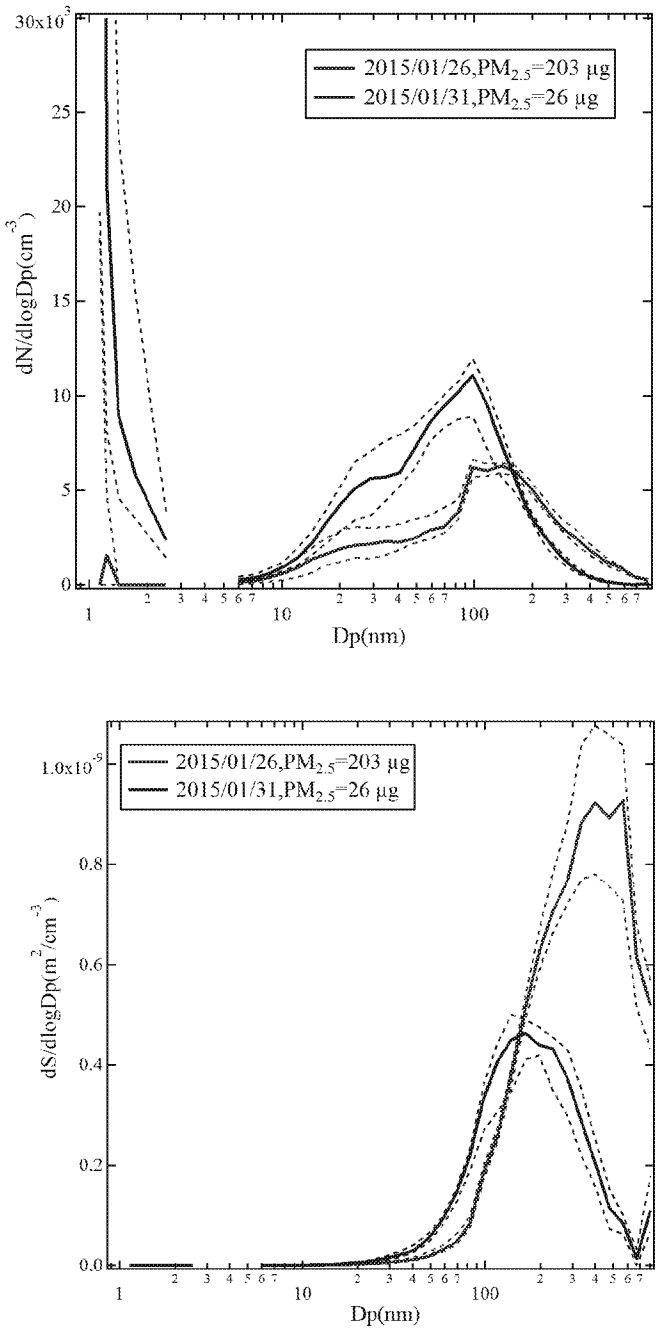

[a]The cluster mode, along with overlapping nucleation, Aitken and accumulation modes can be seen in the particle number distribution.

Source Permission pending: Kulmala et al. (2014).

Figure 2-7 Examples of the particle number distribution (top) and surface-area distribution (bottom) during clean (blue) and polluted (red) conditions in Nanjing, China, during winter.[a]

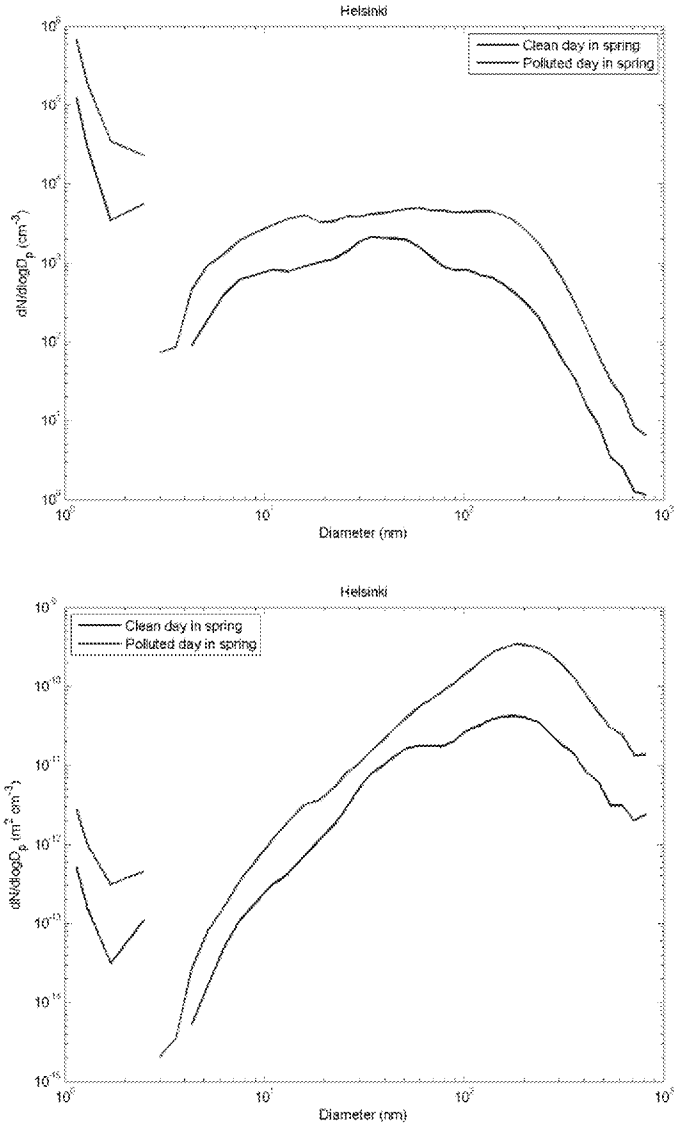

[a]The cluster mode, along with the overlapping nucleation, Aitken and accumulation modes can be seen in both the number and size distributions.

[b]Units on the bottom panel should be dS/dlogDp but are mislabeled in the original figure.

Source Permission pending: Kulmala et al. (2014).

Figure 2-8 Examples of the particle number distribution (top) and surface-area distribution (bottom) during clean (blue) and polluted (red) conditions in Helsinki, Finland, during spring.[a,b]

2.3.4.1 Primary Sources

Motor vehicles are a major, if not the most important, source of UFP in urban environments (Morawska et al., 2008). Their role as a major source of $PM_{2.5}$ mass and impacts of new engines and control technologies were discussed in Section 2.3.1.2. Here, these new engine and control technology advances are discussed with a focus on their impact on UFP emissions.

The number concentration, size distribution, morphology and chemical composition of mobile source-derived primary UFP are determined by the composition of the fuel used and lubricating oil, driving conditions, engine after-treatment system, as well as environmental conditions (Karjalainen et al., 2014; Rönkkö et al., 2014; Fushimi et al., 2011; Gidney et al., 2010; Heikkilä et al., 2009; Johnson, 2009). As discussed in Section 2.3.2.1, recent changes in engine and emissions control technology have influenced PM emissions from both gasoline and diesel vehicles, with light duty vehicles rapidly transitioning from port fuel injection (PFI) to gasoline direct injection (GDI), and heavy-duty diesel vehicles complying with a new U.S. EPA PM emission standard requiring reduction of diesel PM emissions by 90% to 0.01 g/bhp-hour (U.S. EPA, 2009).

The number of particles emitted by GDI vehicles can be one to two orders of magnitude higher than for PFI vehicles (Fushimi et al., 2016; Mamakos et al., 2012). For both GDI and PFI vehicles, the largest number of particles are sub-200 nm, with a more distinctly bimodal distribution characterized by a larger contribution to particle number from a sub-30 nm nucleation-mode particles for PFI (Karavalakis et al., 2013; Kittelson et al., 2006), and somewhat larger particles generally observed for GDI (Fushimi et al., 2016; Myung et al., 2015; Choi et al., 2014; Myung et al., 2014).

The new heavy-duty diesel PM emissions requirements as well as additional required reductions in NO_X emissions phased in by 2010 led to UFP emissions reduction of more than 90% compared to earlier diesels. However, CDPF regeneration resulted in approximately one order of magnitude increase in particle number. As a result, in spite of much lower average UFP emissions, there can still be discrete periods of extremely high UFP formation that do not reflect the overall reduction in UFP emissions. These UFP releases may have been due to thermal desorption of adsorbed sulfates stored within the exhaust catalyst system (Khalek et al., 2015; Ruehl et al., 2015).

Most of the particles emitted by marine and aircraft engines are in the ultrafine size range (Moldanova et al., 2013; Jonsson et al., 2011; Lack et al., 2009; Whitefield et al., 2008). Emissions of UFPs appears to be a strong function of fuel sulfur content, with reduced emissions for lower sulfur fuels (Lack et al., 2009). The size distribution of UFP produced by marine ships is usually bimodal with a nucleation mode below 30 nm and another mode between about 30 and 100 nm (Pirjola et al., 2014; Hallquist et al., 2013; Petzold et al., 2010).

Biomass burning is also a major source of UFP. The mean particle number diameter produced by burning fresh vegetation varies usually from a few tens of nm up to about 150–200 nm (Maruf Hossain et al., 2012; Zhang et al., 2011a; Janhaell et al., 2010).

2.3.4.2 New Particle Formation

New particle formation (NPF) was described in the 2009 PM ISA (U.S. EPA, 2009) as an important atmospheric process responsible for the formation of UFP, especially in remote continental areas but also in urban environments under certain conditions. Particle nucleation rates are observed to be higher in summer than in winter, and during daytime as compared to nighttime, consistent with photochemical processes. While sulfuric acid and water vapor had been identified as the major nucleating species, research was proceeding on nucleation mechanisms involving other chemical species. Numerous subsequent advances in our understanding of these mechanisms have occurred since the 2009 PM ISA (U.S. EPA, 2009).

Atmospheric NPF starts with the formation of molecular clusters. Subsequent growth via the uptake (condensation) of low volatility gas molecules occurs for some of these clusters, while others dissociate (Vehkamaki and Riipinen, 2012; Zhang et al., 2012b). If growing clusters reach the size threshold of 1.5−2 nm in diameter, they are more likely to grow further by additional vapor uptake (Kulmala et al., 2014). The processes involved in the initial steps of atmospheric NPF are collectively referred to as nucleation (Kulmala et al., 2013).

Key constituents in the initial steps of atmospheric NPF are (1) gaseous compounds of very low volatility, mainly sulfuric acid and highly oxidized organic compounds, (2) compounds which can facilitate the formation of low volatility complexes, such as gaseous ammonia or amines that form acid-base complexes with inorganic or organic acids, (3) water molecules which cluster through hydrogen-bonding, and (4) possibly ions that can form clusters through electrostatic interactions. Low-volatility compounds capable of initiating NPF primarily originate from photochemical oxidation reactions in the gas phase. As noted, above, the most important compound in this respect is sulfuric acid (Kulmala et al., 2014; Kerminen et al., 2010; Sipila et al., 2010). Other low-volatility compounds that play important roles in the early steps of NPF, at least in continental boundary layers, are extremely low volatility organic compounds (ELVOC) (Krechmer et al., 2015; Ehn et al., 2014; Riccobono et al., 2014; Donahue et al., 2013; Kulmala et al., 2013). Gas-phase ammonia and amines form acid-base complexes with inorganic or organic acids, facilitating cluster formation and subsequent NPF (Kürten et al., 2014; Almeida et al., 2013). Ions originating from radon decay and external radiation (cosmic rays and gamma radiation from soils) participate actively in the formation of clusters in the atmosphere, having the potential to affect nucleation rates (Kirkby et al., 2011) and ion-induced, or ion-mediated, particle formation mechanisms are expected to be important in locations with low temperatures and pre-existing aerosol surface areas, and high ion and sulfuric acid concentrations (Yu, 2010). Measurements conducted at a few continental locations suggest that ion-mediated pathways typically contribute a few percent to the total new particle formation rate, with slightly higher contributions estimated for some elevated sites and in Antarctica (Hirsikko et al., 2011; Manninen et al., 2010).

Averaged over a large-scale (~100 mile^2) NPF event, observed particle formation rates varied mostly in the range 0.01−10 cm^{-3} s^{-1} (Kulmala and Kerminen, 2008). Higher formation rates, up to about

100 cm^{-3} s^{-1} have been reported in some urban areas, and especially in heavily-polluted environments (Salma et al., 2011; Shen et al., 2011; Yue et al., 2009; Iida et al., 2008). The vast majority of particle growth rates associated with large-scale NPF events lie in the range 1−10 nm/hour (Kulmala and Kerminen, 2008) and increase with particle size (Hakkinen et al., 2013; Kuang et al., 2012b; Yli-Juuti et al., 2011). These findings indicate that it typically takes a few hours for newly-formed particles to grow into the 25−100 nm size range and between about half a day and 3 days before newly-formed particles grow larger than 100 nm in diameter. The main sink for molecular clusters and new particles is their coagulation with larger pre-existing particles and, in cases where their number concentration is very large, also by their coagulation with each other (Westervelt et al., 2014).

Direct observations show that secondary particles (i.e., those originating from NPF) are usually composed primarily of organic compounds, especially in forests (Han et al., 2014; Pennington et al., 2013; Pierce et al., 2012; Pierce et al., 2011), but also in many rural or urban environments (Bzdek et al., 2014; Setyan et al., 2014; Bzdek et al., 2013; Ahlm et al., 2012; Smith et al., 2008). Exceptions for this pattern are areas near large sulfur emissions sources, in which sulfate may comprise up to about half of the ultrafine particle (Crilley et al., 2014; Bzdek et al., 2012; Zhang et al., 2011b; Wiedensohler et al., 2009).

Pre-existing particles serve as an important sink for low-volatility vapors, clusters, and growing UFPs. Therefore, primary ultrafine particles tend to decrease both new particle formation and growth rates (Kulmala et al., 2014). It is because of this competition that particle number concentrations are expected to be governed by primary particle emissions in highly polluted settings and by nucleation in remote continental sites, although nucleation still occurs in urban environments and can still be the major source (U.S. EPA, 2009).

2.4 Measurement, Monitoring and Modeling

2.4.1 $PM_{2.5}$ and PM_{10}

PM Federal Reference Method (FRM) samplers and Federal Equivalence Method (FEM) monitors are designed to measure the mass concentrations of ambient particulate matter. An FRM is a method that has been approved (40 CFR Part53) for use by states and other monitoring organizations to assess NAAQS compliance and implementation. The FRMs for $PM_{2.5}$, $PM_{10-2.5}$, and PM_{10} measurement are specified in CFR 40 Part 50, Appendices L, O, and J, respectively. A FEM is based on different sampling or analytical technology from the FRM but provides the same decision-making quality for making NAAQS attainment determinations. In practice, a large fraction of the FEM monitors in operation for PM are automated and designed to provide hourly data, while the FRMs for $PM_{2.5}$, PM_{10}, and $PM_{10-2.5}$ require sampling for 24-hours and provide a daily average $PM_{2.5}$ concentration, including pre- and

post-sampling gravimetric laboratory analysis. $PM_{2.5}$ FEMs, their performance criteria, and evaluation of their performance were described in detail in the 2009 PM ISA (U.S. EPA, 2009).

Operating principles and performance of FRMs and FEMs for PM were discussed in detail in the 2004 PM AQCD (U.S. EPA, 2004) and 2009 PM ISA (U.S. EPA, 2009). The FRMs for PM are based on gravimetric measurement of mass concentration after collection on filters. There are two broad categories of FEMs for PM measurement, those that are filter-based and designed for collection of 24-hour samples, of which very few are in use, and automated monitors designed for quantification of PM on hourly or shorter time scales, of which there are several hundred in operation. Filter-based FEMs include virtual impactor/dichotomous sampler techniques, in which a sampler is designed to separate particles by their inertia into separate flow streams, in this case $PM_{2.5}$ and $PM_{10-2.5}$. There are three widely used short time resolution automated FEMs: (1) beta attenuation monitors which measures absorption of beta radiation by PM, which is proportional to PM mass; (2) Tapered Element Oscillating Microbalance (TEOM), monitors, which continuously records the mass of particles collected on a filter substrate and are typically configured with the Filter Dynamics Measurement System (FDMS), which is designed to ensure the sample is appropriately conditioned and that volatile aerosols are measured; and (3) optical methods that utilize a spectrometer, which allow calculation of aerosol mass concentrations over a wide range of cut points.

At the time of completion of both the 2004 AQCD (U.S. EPA, 2004) and 2009 PM ISA (U.S. EPA, 2009), considerable effort was still focused on improvement of measurement methods for PM mass. Examples are the development of the $PM_{10-2.5}$ FRM and the Filter Dynamics Measurement System-TEOM (FDMS-TEOM) (Grover et al., 2006), both of which are described in detail in the 2009 PM ISA (U.S. EPA, 2009). More recently, there has been little new emphasis on method development research for PM mass measurement.

2.4.2 $PM_{10-2.5}$

Although the $PM_{10-2.5}$ FRM and FEMs were already discussed in the 2009 PM ISA (U.S. EPA, 2009), the state of technology for $PM_{10-2.5}$ measurement is reviewed here because the large data set of nationwide $PM_{10-2.5}$ network measurements is reported for the first time in Section 2.5. $PM_{10-2.5}$ FRM and FEMs now used for routine network monitoring are considerably improved compared to methods used in the previous key analyses of $PM_{10-2.5}$ sampling issues (U.S. EPA, 2004; Vanderpool et al., 2004). New results reveal changing trends in $PM_{2.5}/PM_{10}$ ratios (see Section 2.5.1.1.4).

There are three categories of methods widely used for ambient sampling of $PM_{10-2.5}$. The first is the $PM_{10-2.5}$ FRM (40 CFR Part 50, Appendix O), which determines $PM_{10-2.5}$ mass as the arithmetic difference between separate, collocated, concurrent 24-hour PM_{10} and $PM_{2.5}$ measurements at local conditions of temperature and pressure. This is sometimes referred to as the difference method for $PM_{10-2.5}$ sampling. The difference method was selected as the FRM to preserve the particle size limits for

$PM_{2.5}$ and PM_{10}, which are defined by fractionation curves with characteristic shapes and cut-off sharpnesses established for the $PM_{2.5}$ and PM_{10} FRMs as well as to preserve integrated sample filter collection and gravimetric measurement technology used for all previous FRMs for PM indicators to maximize comparability between $PM_{2.5}$, PM_{10}, and $PM_{10-2.5}$ measurements. $PM_{10-2.5}$ FRMs are largely deployed as part of a multipollutant monitoring network (see Section 2.4.6).

A second category of $PM_{10-2.5}$ methods are the automated FEM monitors that utilize either a difference method or dichotomous separator in the design of the method. Automated difference method FEMs use two measurement devices similar to the FRM difference method. Automated dichotomous FEMs also rely on two measurement devices, but instead of having separate inlets, use one flow stream, that splits the particles into larger and smaller PM mass fractions to be analyzed separately. Automated $PM_{10-2.5}$ FEMs are also largely deployed at NCore stations.

The third category of $PM_{10-2.5}$ methods deployed are for the IMPROVE program. In the IMPROVE sampling methods, two of the four sampling modules operated provide data that are used to calculate a $PM_{10-2.5}$ concentration similar to how the FRM difference method is calculated. Although not an FRM or FEM, the IMPROVE program $PM_{10-2.5}$ data are included as they represent a consistent national network at over 150 locations. IMPROVE program sites are typically located in class one areas and national parks to support the Regional haze program.

There were early observations of poor precision for $PM_{10-2.5}$ mass measurements for both the difference method (Allen et al., 1999; Wilson and Suh, 1997), and dichotomous samplers (Camp, 1980), as well as discussion of the inherently lower precision of both the old difference method and dichotomous sampling compared to $PM_{2.5}$ and PM_{10} FRMs (Allen et al., 1999). The early observations of poor precision were not based on the performance of $PM_{10-2.5}$ samplers in current use in the NCore and other sampling networks, as a number of improvements have facilitated greater precision of the difference method (Allen et al., 1999) and the development of a FRM for $PM_{10-2.5}$ (40 CFR Part 50 Appendix O). Precision better than 5% was demonstrated by using identical instrumentation for both $PM_{2.5}$ and PM_{10} except for the sampler cut-point; using the same filter type, filter material, filter face velocity, and ambient-to-filter temperature difference, lowering blank variability, and increasing gravimetric analytical precision (Allen et al., 1999). These are provisions that are now specified in the FRM and used for measurements of $PM_{10-2.5}$ in national sampling networks that use the $PM_{10-2.5}$ FRM or FEM to obtain differences in PM_{10} and $PM_{2.5}$ mass. Because of these improvements, high uncertainties reported for previous measurements described in U.S. EPA (2004) no longer apply to the difference methods in use as FRMs and FEMs on which current $PM_{10-2.5}$ network measurements are based.

2.4.3 Ultrafine Particles: Number, Surface Area, Mass

In this section measurement methods for UFP are reviewed. In Section 2.4.3.1 methods for counting particle number and measuring particle number distribution are described. Because UFP mass is

usually so small, the number rather than the mass of UFP are usually reported. As this can be instrument-dependent, differences in particle number measurement methods in common use are discussed. Section 2.4.3.2 reviews surface area measurements and Section 2.4.3.3 reviews mass measurements. There are a number of reasons why measurements in the UFP size range are more challenging than mass measurements of $PM_{2.5}$ or $PM_{10-2.5}$, and these can result in differences in the upper size limit for sampling UFP mass and number. These challenges and differences are explained in Section 2.4.3.3.

2.4.3.1 Particle Number and Number Distribution

Particle number measurement is a rapidly advancing area of research, and large uncertainties and biases are likely associated with UFP measurement. The U.S. EPA has not yet established reference methods for ambient or source UFP number measurement. However, use of particle number measurements for regulatory and certification purposes has driven technological development of particle number measurements in the European Union (EU), where a network of UFP monitoring stations that uses PM electrical properties for both counting and sizing particles to measure particle number distributions are classified into six size classes every 10 minutes has been developed (Wiedensohler et al., 2012).

Condensation particle counters (CPC) are one of the most common means of determining total number concentration (the majority which is usually in the UFP range) for both ambient and source particle measurements. Particles enter a water or alcohol saturated vapor chamber and grow by condensation to a size that allows measurement using an optical particle counter (OPC). In some cases CPC instrumentation is used to measure UFP number without size classification under the assumption that particles with Dp > 0.1 μm do not significantly contribute to particle number measurements. The 2009 PM ISA (U.S. EPA, 2009) reported the development of a water-based CPC more suitable for long-term field studies. Before the development of this technology particle number measurements were mainly restricted to short-term, intensive field studies. Water-based CPC instruments have since found limited use in network monitoring applications (see Section 2.4.5 and Section 2.5.1.1.5).

The 2009 PM ISA also reported a reduction in detection size down to <0.002 μm in diameter with mobility particle sizers (U.S. EPA, 2009). More recently, substantial progress has been made in measuring sub-0.003 μm particles and clusters, as well as gaseous compounds involved in the initial steps of atmospheric NPF. Advances include development of particle counters (CPCs) capable of measuring particle number counts and number distributions down to about 0.001 μm in particle mobility diameter (Kangasluoma et al., 2015; Lehtipalo et al., 2014; Kuang et al., 2012a; Jiang et al., 2011; Vanhanen et al., 2011; Iida et al., 2008). These advances are especially useful for investigating atmospheric nucleation of particles (see Section 2.3.4).

Other recent advances include current efforts to develop a miniaturized CPC for use in personal monitoring applications (He et al., 2013). CPCs can be used as stand-alone instruments to measure total particle number but are often used downstream of other particle classifiers to determine UFP number or particle-number size distributions. Classification of UFP size may be via the inertial, diffusional, or electric mobility properties of the aerosol and sometimes more than one means of classification may be used. Faraday cup electrometers (FCE) can also be used downstream of other particle classifiers to determine UFP number or particle-number size distributions (Dhaniyala et al., 2011; McMurry et al., 2011; Fletcher et al., 2009). Size classification of UFP was reviewed in the 2009 PM ISA (U.S. EPA, 2009) and methods based on inertial, gravitational, centrifugal, and thermal techniques were reviewed (Marple and Olson, 2011). Advances in the development of size classification methods have mainly concerned classification by electrical mobility. A unique particle mobility within an electric field can be established relative to particle size (Hinds, 1999) and aerosols can be charged with radioactive sources such as Kr-85, Am-241, or Po-210 or using a soft-X-ray source (Jiang et al., 2014). Other instruments that classify by size using electrical mobility were described in the 2009 PM ISA (U.S. EPA, 2009).

The size ranges measured by instruments widely used in field research are superimposed on a typical particle number size distribution (Whitby et al., 1972) illustrated in Figure 2-9. The vertical lines in Figure 2-9 show the lower and upper size limits of various UFP sampling methods. In earlier literature, CPCs used for particle number measurement variable lower limit particle size detection levels were reported, but they were often near 0.01 μm (Liu and Kim, 1977), shown as Line A. In several field studies described in this ISA, particles are sized by diffusive or electrical methods before counting to limit measurements to particle number count to below 0.1 μm (Evans et al., 2014; Liu et al., 2013; Rosenthal et al., 2013), shown as Line B. In these cases, resulting particle number measurements are the number of particles between Line A and Line B in Figure 2-9. Since the number distribution continues below 0.01 μm (Line A), it is possible that some fraction of the total number of particles smaller than 0.01 μm are too small to be detected, except without specialized research methods for counting clusters, as described above.

Moreover, the peak of the number distribution can change considerably over time or over short distances. At less than 50 meters from a major highway there were more particles in the 0.006 to 0.025 μm size range than in the 0.025 to 0.05 μm size range, but at 100 meters from the highway there were more particles in the 0.025 to 0.05 μm size range than in the 0.006 to 0.025 μm size range (Zhu and Hinds, 2002). It is possible that actual particle number could decrease with distance from a busy road at the same time that the fraction of the particles is large enough to be detected may increasing, making interpretation of particle number data difficult.

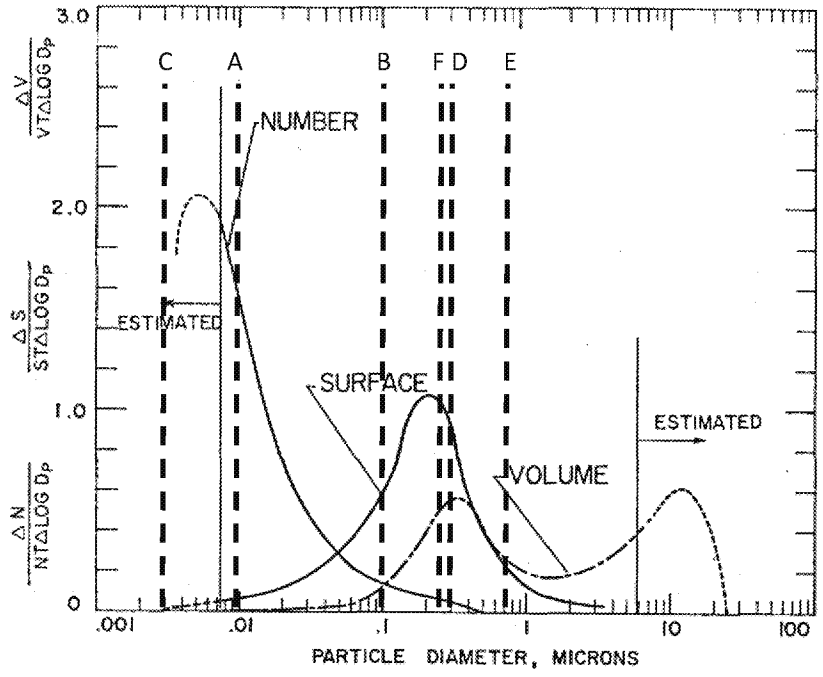

Vertical lines are: (A) lower size limit from a widely used condensation particle counter (CPC) from 1977; (B) upper size limit definition of UFP; (C) lower size limit of a newer CPC; (D) and (E) upper size limits for particle number measurements from different epidemiologic studies. (Line F is not used.)

Source Permission pending: Original figure showing example particle size distribution from Whitby et al. (1972), vertical lines correspond to lower and upper size ranges for sampling procedures reported by Viana et al. (2015); Evans et al. (2014); Meier et al. (2014); Olsen et al. (2014); Liu et al. (2013); Rosenthal et al. (2013); Hampel et al. (2012); Iskandar et al. (2012); Verma et al. (2009); Liu and Kim (1977).

Figure 2-9 Size ranges collected by various UFP sampling procedures.

The development of CPCs that can detect particles as small as 0.003 μm could complicate comparison of particle number concentrations measured with different particle counters. As Figure 2-9 shows there is a difference in number of particles counted between older particle counters with size limits down to 0.010 μm (between Lines A and B) and newer particle counters with size limits down to 0.003 μm (between Lines B and C). In one study where two different particle counters were used, one with a lower size limit of 0.003 μm gave 14−16% higher number counts than one with a lower size limit of 0.007 μm (Hampel et al., 2012). In the Pittsburgh Air Quality Study, the average particle number count in the size range 0.003 to 0.010 μm was 5,600 cm^{-3} (Stanier et al., 2004), while the average particle number count for the entire 0.003 to 2.5 μm size range was 22,100 cm^{-3}. This corresponds to 25% of total particle number count accounted for by particles in the range of 0.003 to 0.010 μm.

In other studies, particle number has been counted without size classifying before counting over size ranges up to 0.3 μm (Meier et al., 2014; Olsen et al., 2014) or 0.7 μm (Iskandar et al., 2012), as shown in Lines D and E of Figure 2-9 as an indicator UFP number. Although 0.3 μm is well above the nominal UFP upper limit of 0.1 μm, the use of a larger upper size limit was more convenient and was

justified by observations that most particles are smaller than 0.1 μm. Figure 2-9 shows that the greatest number of particles are smaller than 0.1 μm, but that a part of the particle number distribution extends beyond it. Recent studies verified that 75% of particles smaller than 0.7 μm (Iskandar et al., 2012) and roughly 5/6 of particles smaller than 0.5 μm by number were smaller than 0.1 μm (Evans et al., 2014).

An additional complication for electrometer based measurements (but not for CPCs) is that the number of particles that can be detected varies with particle size. For example, an electrometer can have a size detection limit of 0.02 μm, this does not indicate that a single particle with a diameter of 0.02 μm can be detected. Instead, lower count detection varies with particle size because the amount of charge required for detection by an electrometer increases with decreasing particle size. For example, a UFP 3031 electrometer has an estimated lower detection limit of 408 cm^{-3} for 0.02–0.03 μm particles but falls off to 120 cm^{-3} for 0.07 to 0.1 μm particles (Vedantham et al., 2015). Detection of particle number using an electrometer is thus limited by a size below which no particles are counted, as well as by a minimum detectable particle number count that varies with size.

To summarize, the variety of instruments and approaches used for measuring particle number present potentially large uncertainties for use in field studies to estimate exposure and health impacts, and complicate comparison of particle number concentrations between field studies using different measurement methods. Not removing particles larger than 0.1 μm before measurement introduces a bias of greater than 10–20%. Differences in the lower size limit of detection between different particle counters could produce an even greater uncertainty that has not been fully characterized. Underlying these uncertainties is the knowledge that because there is a lower size limit for particle detection, there is inherently some unknown fraction of particle number concentration that is accounted for by particles that are too small to be detected. This is an especially important consideration for comparing recent data to older data. As particle number counting technology rapidly advances, the lower size limit of detection is decreasing and the number of particles capable of being detected is correspondingly increasing. In essence, different widely used UFP measurement methods do not measure the same particle size range, and serious biases in particle number measurements are both likely and difficult to assess.

2.4.3.2 Surface Area

Particle surface area is usually measured by radioactive or electrical labeling of particles using an electrical aerosol detector or radiation detector (U.S. EPA, 2009). There have been new advances in measurement of UFP surface area. The epiphaniometer directly measures surface area via surface deposition of Pb-211 onto sampled particles and subsequent measurement of the α-activity of particles deposited on a filter using an annular surface barrier detector (Gini et al., 2013; Gaggeler et al., 1989). Surface area may also be approximately determined via unipolar diffusion charging of particles with active surface area related to the electrical charge transferred to particles under controlled charging conditions (Jung and Kittelson, 2005). Excess ions are removed using an ion trap charge is measured via

electrometer (Geiss et al., 2016). The diffusion charge surface area relationship is only valid within a particle size range of approximately 0.02 to 0.4 μm (Geiss et al., 2016; Kaminski et al., 2012; Asbach et al., 2009). Diffusion charge surface area shows good agreement with TEM projected surface area for particle sizes of primary interest for UFP characterization (i.e., DP < 0.1 μm) but appears to underestimate surface area for larger particles (Ku and Maynard, 2005). Instrumentation and methods used to estimate "lung-deposited surface area" are described in Section 4.1.7.

2.4.3.3 Mass

Inertial classification to the most common UFP size definition (i.e., an inertial 50% cutpoint Dp less than 0.1 μm) can be accomplished for UFP mass sampling by using a low-pressure impactor as an initial scalper stage and using sample filter media in the flow exiting the impactor. In such cases, UFP mass can be designated as $PM_{0.1}$, which makes reference to the 0.1 μm 50% cutpoint in a manner analogous to nomenclature used for other size-classified particle mass measurements (e.g., $PM_{2.5}$).

Measurement of UFP mass gravimetrically can be problematic due to the small amount of collected mass, long sampling periods involved, and the potential loss of semivolatile particles. While inertial classifiers can be used to classify or determine the size distribution of UFP, the pressure drop across the sub-0.1 μm stage required for sampling UFP may present challenges with respect to evaporative loss of particulate matter (Hata et al., 2012; Furuuchi et al., 2010; Singh et al., 2003).

To address this, particles with a larger aerodynamic diameter cutpoint have been sampled using a high volume slit impactor with 50% cutpoints of 0.18 or 0.25 μm to increase the sample collected for mass determination and/or compositional analyses and to reduce the pressure drop across the inertial classification stage to reduce evaporative losses. For example, Misra et al. (2002) designed a sampler with a 0.25 μm inertial 50% cutpoint D_p to quantify $PM_{0.25}$ (Saffari et al., 2015; Misra et al., 2002), and a design by Demokritou et al. (2002) later evolved into a commercial sampler with a 0.18 μm cutpoint for sampling near the UFP range.[38] Sampling of $PM_{0.25}$ or $PM_{0.18}$ increases sampled mass over a time interval and reduces the pressure differential necessary for inertial classification relative to $PM_{0.1}$. In the available studies, the estimated upper limit of the measured PM mass that has been referred to as the ultrafine particle size range usually varies between about 0.1 and 0.3 μm of the particle aerodynamic diameter, depending on the PM sampling device used (Cheung et al., 2016; Borgie et al., 2015; Viana et al., 2015; Daher et al., 2013; Kudo et al., 2012; Mueller et al., 2012; Chen et al., 2010; Bruggemann et al., 2009).

Concentrated ambient particles (CAPs) are frequently used in controlled human exposure and animal toxicology studies. The technology that allows for CAPs is the virtual impactor with a high volume slit design (Sioutas et al., 1994c; Sioutas et al., 1994a, b). Briefly, ambient air is accelerated

[38] BGI 900 High Volume Cascade Impactor Guidance Manual, https://bgi.mesalabs.com/wp-content/uploads/sites/35/2014/10/BGI900_MANUAL_1.0.0.pdf.

through a high-volume nozzle that lets smaller particles pass through in a small fraction of the flow stream, but removes larger particles by impaction in a larger fraction of the flow stream. Classification by size has been achieved by placing two or three virtual impactors in sequence in a Versatile Aerosol Concentration Enrichment System (VACES) (Maciejczyk et al., 2005; Ghio et al., 2000; Sioutas et al., 1995b; Sioutas et al., 1995a). The Ultrafine Particle Concentrator (UPC) was developed by Sioutas et al. (1999) as a laboratory aerosol concentration device and was incorporated into a variation of the VACES by Kim et al. (2001). Ambient air is introduced in the system through three inlets: 0.18 μm impactor, 2.5 μm impactor, and ambient air with no upstream cutpoint (Kim et al., 2001). The VACES was briefly described in the 2004 PM AQCD (U.S. EPA, 2009). Because virtual impaction works best for particles much larger than 0.1 μm, UFP concentration requires supersaturation for particle growth to an optimal size for virtual impactor operation, and a subsequent drying step after separation to return particles to their original size.

The original description of the Harvard Ultrafine Concentrated Ambient Particle System (HUCAPS) includes an outlet impactor with a 0.2 μm cut point (Gupta et al., 2004). A 0.3 μm cut point using the HUCAPS has also been described (Liu et al., 2017) and the VACES, uses 0.18 μm cut point inlet impactor for its nominally ultrafine size range (Kim et al., 2001).

Other approaches to PM delivery in controlled exposure studies can result in particle size ranges up to 0.3 μm. Previously described high volume ambient samplers designed to collect a UFP fraction have also been used in controlled exposure studies with UFP, by collecting PM on a filter substrate, extracting the PM from the filter, and nebulizing and drying the extract to reconstitute the aerosol (Cheng et al., 2016; Morgan et al., 2011), (Zhang et al., 2012a), (Cacciottolo et al., 2017; Woodward et al., 2017). In other controlled clinical exposure studies PM with MMD <0.1 μm was generated by spark discharge (Schaumann et al., 2014) or sampled directly from automobile exhaust (Tyler et al., 2016).

UFP CAPS and other delivery systems for controlled exposure studies are generally not limited to the nominal UFP size limit of less than 0.1 μm. Instead, they usually involve a particle size ranging up to 0.18 to 0.3 μm without exclusion by impaction or other means of removal. Under these circumstances, a large fraction of the mass range targeted for investigation of UFP effects in controlled exposure studies can come from particles larger than the nominal size of 0.1 μm. Consequently, a difference in mass between practical mass sampling methods targeting UFP and what would be measured below 0.1 μm is likely. However, as described in Section 2.4.3.1, the difference in particle number measurements is likely to be much less.

2.4.4 Chemical Components

Measurement of PM components is potentially useful for providing insight into what sources contribute to PM mass as well as for discerning differential toxicity. Sulfate, nitrate, ammonium, organic carbon and elemental carbon as well as a suite of elements are measured in national speciation monitoring

networks (see Section 2.4.5) and intensive field studies mainly by collection on filters, using methods described in detail in the 2004 PM AQCD (U.S. EPA, 2004) and 2009 PM ISA (U.S. EPA, 2009). New advances in PM speciation analysis has included new network applications for OC analysis and better characterization of sampling errors of major PM components. Fourier Transform Infrared Spectroscopy has been applied to OC and organic functional group determination in national networks (see Section 2.4.6) for monitoring $PM_{2.5}$ species (Weakley et al., 2016). Characterization of sampling errors due to loss of ammonium nitrate and semivolatile organic material during sampling, adsorption of organic vapors during sampling, and generation of elemental carbon during analysis of organic carbon have emerged as the main sources of measurement error and considerable effort has been devoted to their minimization or correction (U.S. EPA, 2009, 2004).

New research has focused on seasonal differences in the impacts of these errors, indicating 40−50% loss of $PM_{2.5}$ nitrate from Teflon filters in summer and less than 10% in winter, with summer losses largely balanced out by an increase in retained water (Malm et al., 2011; Nie et al., 2010; Vecchi et al., 2009). The volatilized nitrate is minimized in network nitrate sampling methods (Solomon et al., 2014), but not with most $PM_{2.5}$ mass methods, making a negative bias in the $PM_{2.5}$ FRM possible if the nitrate contribution to $PM_{2.5}$ mass is large enough. Further research has also continued on quantification of positive OC artifacts due to vapor adsorption on filters (Vecchi et al., 2009; Watson et al., 2009), including observation of more vapor adsorption in summer than winter (Cheng et al., 2010; Vecchi et al., 2009). Minimization of sampling error has been investigated by adjusting filter deposit area, flow rate, and passive exposure time (Chow et al., 2010a); using denuders upstream of filters (Chow et al., 2010b); and characterizing backup filter correction and its influence on the split between OC and EC (Cheng et al., 2009) to reduce the positive adsorption artifact. Considerable research has also focused on measurement of particulate organic species, elemental analysis, and single particle mass spectrometric analysis, and some novel sampling and analytical approaches for measurement of PM components, but these are beyond the scope of this review because they have not been used for interpreting health and welfare impacts.

2.4.5 Satellite Remote Sensing

Instruments sensing back-scattered solar radiation on satellites have made it possible to characterize tropospheric aerosol properties on the global scale. Satellite-based measurements used for estimating $PM_{2.5}$ are becoming more widely used and have recently been combined with modeled data and ground-level measurements to extend the spatial coverage over which $PM_{2.5}$ concentrations can be estimated and to improve the spatial resolution of $PM_{2.5}$ estimates used to assign exposure in health studies. The satellite borne instruments vary in their complexity and in the aerosol properties they can measure. Satellite instruments measure radiance (electromagnetic energy flux), that can then be used to provide information on the aerosol column amount, or the aerosol optical depth (AOD). Because $PM_{2.5}$ is not directly measured, computational algorithms involving a range of assumptions must be applied to

obtain estimates of $PM_{2.5}$ concentrations from AOD. These inferred measurements involve potential errors that are not encountered with the FRM or other ground-based $PM_{2.5}$ measurements. This section focuses on the estimation of $PM_{2.5}$ concentration from AOD and its strengths and limitations. Studies involving fusion of AOD with spatiotemporal modeling for prediction of exposure concentration are discussed in Section 3.3.3.

Depending on the wavelengths sampled and the spectral resolution of the instruments, information about the composition of particles of diameter <2 μm and particles of diameter >2 μm can be obtained (Engel-Cox et al., 2004). Satellite AOD observations have extensive spatial coverage, making these data attractive for estimating surface PM concentrations. AOD is a measure of the extinction of light in the atmosphere and is directly related to the presence of particulate matter as the individual particles scatter light. A higher AOD reflects greater scattering, indicating higher PM loadings. However, this relationship is not linear due to multiple factors including atmospheric (e.g., thickness of the boundary layer, cloud presence, humidity) and particle (chemical speciation, size distribution) characteristics, and can be impacted by surface characteristics as well (Martin, 2008). Data cannot be collected when clouds and snow are present, limiting the completeness of satellite datasets (Hoff and Christopher, 2009) or from excessive amounts of smoke being mistaken for clouds when AOD > 4 (van Donkelaar et al., 2011).

Spatial and temporal resolution with which concentration can be estimated by satellite images varies with the satellite data source. Satellite/instrument retrievals, and further analyses, provide AOD at varying spatial resolutions down to 500 meters [e.g., Reid et al. (2015); Hoff and Christopher (2009)]. The Moderate Resolution Imaging Spectroradiometer (MODIS) passes the U.S. twice daily with 10 km or 1 km resolution, while the Geostationary Operational Environmental Satellite (GOES) Aerosol/Smoke Product (GASP) produces data in 30-minute intervals with 1 km resolution, and the Multiangle Imaging Spectroradiometer (MISR) produces nearly continuous AOD data but with 17.6 km resolution. Additionally, AOD can be estimated at the earth's surface by the Aerosol Robotic Network (AERONET), which measures AOD from the ground surface and has sites distributed globally. AERONET AOD measurements may provide some validation of satellite AOD measurements.

The many factors that impact the relationship between AOD and $PM_{2.5}$ concentrations lead to widely varying and sometimes relatively low, correlations when linear relationships are developed. In the Hoff and Christopher (2009) review, the correlation (R) (not specified as Spearman or Pearson) ranged from 0.4 to 0.98 across cited studies. Errors in satellite data may occur because the retrievals are sensitive to the aerosol vertical distribution and the optical properties of the particles, which in turn are determined by their morphology and composition, whether they are internally or externally mixed, and the surface contribution to satellite measured reflectance. Hu (2009) observed a Pearson $R = 0.67$ for the eastern U.S. and $R = 0.22$ for the western U.S. The authors attributed poor retrieval in the western U.S. to variation in topography and meteorology. Moreover, satellite data are obtained during brief overpass, and can't be integrated over the longer averaging times used in ground-based measurements. Satellite observations have been compared with AERONET to determine how remote sensing influences measurements of

AOD. Kim et al. (2015) compared AOD for the southeastern U.S. from AERONET with that from MODIS and MISR and found correlations of 0.83 and 0.74, respectively. Normalized mean biases were −18% for MODIS and 1.5% for MISR compared with AERONET. The amplitudes of seasonal peaks were larger in satellite observations compared with the surface data. Kim et al. (2015) suggested that two main factors contribute to this finding: in summer, the mixed layer is deeper, which allows for vertical mixing to greater heights where the sensitivity of the satellite measurements is greater, and there is biogenic SOA production from isoprene oxidation; conversely in winter, the shallower mixed layer depth restricts the extent of vertical mixing, and SOA formation is greatly reduced compared to summer.

The influence of surface reflectance on the relationship between estimated $PM_{2.5}$ and AOD depends on the wavelength range of the retrieval system. The most commonly used algorithm for retrieving AOD from MODIS uses reflected sunlight in the 470 to 2,110 nm wavelength range and is more reliable over dark surfaces than over bright surfaces, because bright surfaces typically show high reflectivity in the red and near-infrared frequencies, resulting in low signal to noise ratios over bright surfaces. However, retrievals of AOD over bright surfaces are possible by making use of reflected sunlight measured in the 412−470 nm channels (Sorek-Hamer et al., 2015). R^2 was determined between retrievals of AOD over the San Joaquin Valley using a mixed effects model. In this model fixed effects represent average relationship between AOD and $PM_{2.5}$ over all monitors in the study area for the study period (2005−2008) and random effects reflect daily variability in the relationship between $PM_{2.5}$ and AOD. R^2 was 0.69, root mean square predicted error (RMSPE) was 9.1 ± 1.2 μg/m^3 and normalized RMPSE was 0.44 ± 0.05.

Spatial resolution of the satellite image influences the relationship between estimated $PM_{2.5}$ and AOD. More recently, Chudnovsky et al. (2013b) used the Multiangle Implementation of Atmospheric Correction (MAIAC) AOD, derived from MODIS radiances with a 1 km resolution over New England from 2002 to 2008 to assess how AOD resolution impacted the coefficient of determination with $PM_{2.5}$ using a simple linear fit. The 1 km resolution retrievals displayed greater spatial variability over New England than did the 10 km resolution with an increase in the sample of cloud free cells. They found that, in their application, the R^2 decreased as the resolution was decreased (from a median of about 0.5 at 1 km resolution to about 0.2 at 10 km), suggesting that higher resolution AOD products can provide increased spatial detail and higher accuracy. Using the same data from New England from 2002 to 2008, Chudnovsky et al. (2013a) also compared the correlation between AOD and fixed-site $PM_{2.5}$ concentration derived from 10 km resolution MODIS data and 1 km resolution MAIAC data with concentration from 84 fixed-site $PM_{2.5}$ monitors. Correlations (not stated whether Pearson or Spearman) were similar (R = 0.62 for MODIS and 0.65 for MAIAC) across all data and when broken down by region and season. The 1 km resolution MAIAC data were found to have valid AOD measures for a larger fraction of the monitoring sites compared with 10 km MODIS data. Chudnovsky et al. (2013a) noted that comparisons between AOD and fixed-site monitor $PM_{2.5}$ concentration data can sometimes produce inverse relationships. The AOD averaged over an area can be lower or higher than the $PM_{2.5}$

concentration measured at a fixed-site monitor depending on the spatial distribution of primary $PM_{2.5}$ sources.

To summarize, satellite-based measurements are becoming more widely used for estimating $PM_{2.5}$ to provide more extensive spatial coverage than can be obtained with $PM_{2.5}$ monitoring network data. The satellite based instruments measure radiance to provide information on AOD, and computational algorithms are then used to estimate $PM_{2.5}$ from AOD. These algorithms can be complex, and there is considerable uncertainty in the $PM_{2.5}$ estimated from AOD. This is because of the many factors that influence the relationship between $PM_{2.5}$ and AOD, including boundary layer thickness, cloud presence, humidity, PM composition and size distribution, and ground reflectivity. Satellite based $PM_{2.5}$ estimates are more accurate over dark surfaces on days without clouds than over bright surfaces or with clouds present, but they can also be used effectively in hybrid models that may incorporate other data sources, including CMAQ model output, surface measurements, and land use variables (Section 3.3.3).

2.4.6 Monitoring Networks

Objectives for PM monitoring include: (1) supporting air quality analyses used to conduct assessments of exposure, health risks, and welfare effects, (2) characterizing air quality status, including providing the public with timely reports and forecasts of the air quality index (AQI), (3) determining compliance with the NAAQS, (4) developing and evaluating air pollution control strategies, and (5) measuring trends and overall progress for air pollution control programs. Federal rules that regulate monitoring programs and details of the various sampling networks relevant for PM measurement are described in the 2009 PM ISA (U.S. EPA, 2009) and updated in the 2016 PM IRP (U.S. EPA, 2016b). Data from U.S. EPA's ambient air monitoring network are available from two national databases. The AirNow database provides data used in public reporting and forecasting of the AQI and the Air Quality System (AQS) database is the U.S. EPA's long-term repository of ambient air monitoring data. The current $PM_{2.5}$ network as of May 2018 is shown in Figure 2-10. As of May 2018, there are 738 FRM monitors and 839 continuous mass FEM monitors.

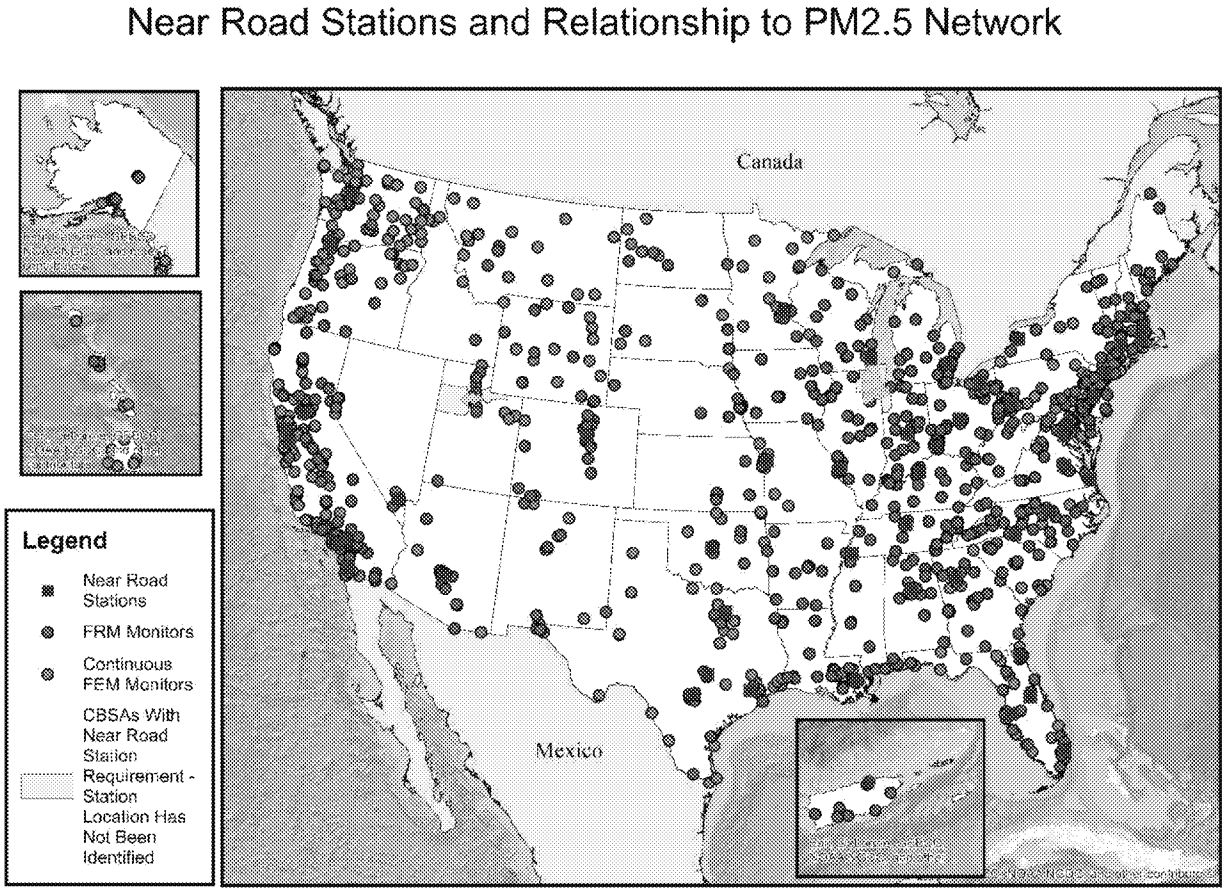

Source Permission pending: U.S. Environmental Protection Agency 2016 analysis of data from monitoring networks.

Figure 2-10 $PM_{2.5}$ Network Including Near Road Monitors.

There are a number of other major national monitoring networks for PM that have been in place for multiple decades. PM_{10} is also monitored in a national network for comparison of PM_{10} data to the NAAQS. As of May 2018, there are 420 FRM monitors and 351 continuous FEM monitors in the PM_{10} network. $PM_{2.5}$ components are measured in two monitoring networks, the Chemical Speciation Network (CSN), and the Interagency Monitoring of Protected Visual Environments (IMPROVE) network, which was implemented to better understand the relationship between PM composition and properties with atmospheric visibility (U.S. EPA, 2016b). As of May 2018, there are 153 CSN stations and 152 IMPROVE stations. The field and laboratory approaches used in the CSN and IMPROVE network as well as their historical evolution, measurement errors and uncertainties, and differences between them have been thoroughly reviewed (Solomon et al., 2014). Monitor locations and number of monitors required for the $PM_{2.5}$, PM_{10}, CSN, and IMPROVE networks are discussed in the 2016 PM IRP (U.S. EPA, 2016b) and monitor siting criteria are described in CFR 40 Part 58 Appendix D and the

SLAMS/NAMS/PAMS Network Review Guidance (U.S. EPA, 1998). Maps of these other national monitoring networks are not included in this ISA, but have been presented along with extensive discussion of PM monitoring networks in the 2009 PM ISA (U.S. EPA, 2009).

Extensive new PM monitoring efforts now complement these long-standing networks by providing additional data supporting multiple objectives, including for PM research. These new monitoring efforts include near road monitoring for $PM_{2.5}$, and the National Core (NCore) network for multipollutant measurement, as well as monitoring of additional PM measurements that are associated with special projects or are complementary to other networks, including particle number, black carbon, and continuous component monitoring (U.S. EPA, 2016b).

$PM_{2.5}$ near road monitors located within 50 meters of roads with heavy traffic are identified in Figure 2-10. By January 1, 2015 22 core based statistical areas (CBSAs) with a population of 2.5 million or more were to have a $PM_{2.5}$ monitor operating at a near road location and by January 1, 2017 30 CBSAs with a population between 1 million and 2.5 million were to have a $PM_{2.5}$ monitor at a near road location.

The NCore network in Figure 2-11 is a relatively new national air quality monitoring network that has been operating since January 1, 2011 and has 78 monitoring sites designed for measurement of multiple pollutants, including $PM_{10-2.5}$ (Weinstock, 2012). The purpose of the NCore network is to support long-term science and policy objectives by contributing data from the latest monitoring technology over a wide range of representative urban and rural locations (Weinstock, 2012). $PM_{10-2.5}$ is measured nationwide in both the NCore and IMPROVE networks. The number of monitoring locations for $PM_{10-2.5}$ is considerably smaller than the number of $PM_{2.5}$ or PM_{10} monitors. As of May 2018, $PM_{10-2.5}$ was being monitored at 140 IMPROVE stations in addition to the 78 NCore monitoring sites.

Another new development is the routine monitoring of particle number at several sites in the U.S. Hourly particle number monitoring data over a period of several years has been reported to AQS from an urban and a rural site in New York state, and additional monitors reported data for shorter periods. At least three near road network monitoring sites will also include particle number measurements (U.S. EPA, 2016b).

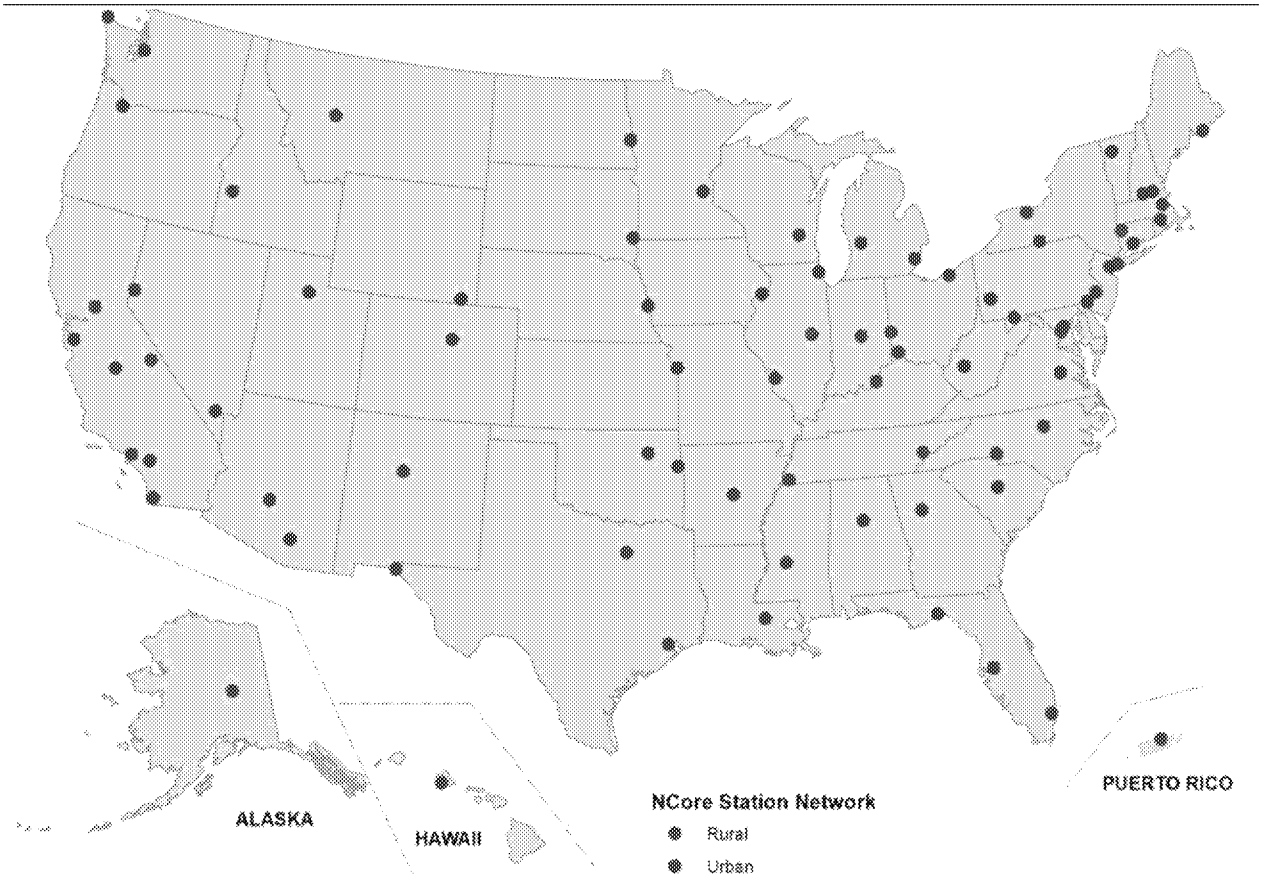

Source Permission pending: U.S. Environmental Protection Agency 2016 analysis of data from monitoring networks.

Figure 2-11 National Core (NCore) Multipollutant Monitoring Network.

2.4.7 Chemistry-Transport Models

This section briefly reviews scientific advances in chemistry-transport models (CTMs)—numerical models of atmospheric transport, chemistry, and deposition of PM. The 2009 PM ISA (U.S. EPA, 2009) provided a description of the relevant processes and numerical methods. Key observations were that the largest errors in photochemical modeling were still thought to arise from the meteorological and emissions inputs to the model (Russell and Dennis, 2000) and that additional uncertainty was introduced by the parameterization of meteorological and chemical processes (U.S. EPA, 2009). Alternative approaches to modeling these processes were discussed and compared (U.S. EPA, 2009). Most major regional-scale air-related modeling efforts at U.S. EPA use the Community Multiscale Air Quality modeling system (CMAQ) (Byun and Schere, 2006; Byun and Ching, 1999). Recent updates to CTM model design, and in particular to CMAQ, are described below. Use of CTMs for exposure assessment studies, including combination of CTMs with other models or data to increase spatial resolution of the concentration field, are described in Section 3.3.2.4.

Numerous advances in atmospheric science have been codified in CTMs, including improved algorithms that better simulate long-chain alkanes important for urban aerosol (Woody et al., 2016), biogenic secondary organic aerosol from isoprene and terpenes (Pye et al., 2017), aging of organic aerosols from combustion (Ciarelli et al., 2017), chemistry within cloud droplets and aerosol water (Fahey et al., 2017), gas-phase oxidant chemistry relevant for the formation of aerosol precursors, and dry deposition by gravitational settling (Nolte et al., 2015). Many processes that influence $PM_{2.5}$ are strongly affected by the weather, and accordingly considerable scientific effort has focused on improving the representation of meteorological processes in CTMs and interactions with aerosols (Tuccella et al., 2015). Improved algorithms for understanding the influence of weather on emissions of $PM_{2.5}$ from sources such as sea spray (Grythe et al., 2014), wind-blown dust (Foroutan et al., 2017), and emissions of precursors such as VOCs from plants (Bash et al., 2016) and ammonia from agricultural lands (Bash et al., 2013; Flechard et al., 2013; Pleim et al., 2013), have also advanced the capabilities of CTMs.

All of these improvements in specific processes work in concert to improve the CTM's performance at quantifying the spatial and temporal distribution of $PM_{2.5}$. CTMs are rigorously evaluated using $PM_{2.5}$ observations from extensive monitoring networks. Figure 2-12 shows the pattern of seasonal mean bias in $PM_{2.5}$ in CMAQ Version 5.1, which is the most recently published in the peer-reviewed literature (Appel et al., 2017). Compared to the prior version of CMAQ (v. 5.02), seasonal variability is generally improved as simulated concentrations decrease during winter and increase during summer, especially for organic carbon. Other CTMs that have reported comparisons between $PM_{2.5}$ simulated over North America and measurements of ambient $PM_{2.5}$, updated since the previous review, include the Comprehensive Air-quality Model with Extensions (Koo et al., 2014) and the Weather Research and Forecasting model coupled with Chemistry (Crippa et al., 2016).

A number of chemical transport models have been configured to conduct their simulations online with the meteorological model. This may include feedbacks between the physical and optical properties of aerosols, solar radiation, and clouds (Forkel et al., 2015; Gan et al., 2015; Yu et al., 2014b; Wong et al., 2012). The modeling community has sought to evaluate these models as part of the Air Quality Model Evaluation International Initiative (AQMEII-2)—an effort "to promote policy-relevant research on regional air quality model evaluation across the atmospheric modeling communities" (Im et al., 2015b). Five modeling groups submitted results for North America which were compared against observations of $PM_{2.5}$ at 659 stations (Im et al., 2015a). The study reported the root mean squared error for WRF-CMAQ v5.0.1 simulations of 24-hour averaged $PM_{2.5}$ as 3.08 $\mu g/m^3$ at urban monitoring sites, although another study reported larger errors for individual seasons (Hogrefe et al., 2015).

Since CTMs are often used to estimate the impact of a change in emissions, it is also important to evaluate the ability of the modeling system to respond correctly to emission perturbations. While it is challenging to isolate the impact of a single emission change in ambient observations, a few studies have conducted decade-long simulations to examine the modeling system's (both the model and the inputs) ability to capture long-term trends. Over the U.S. and Europe, substantial reductions in sulfur dioxide and

nitrogen oxides have created an opportunity to compare the model results with the trends in ambient observations (Banzhaf et al., 2015; Xing et al., 2015; Cohan and Chen, 2014; Civerolo et al., 2010). Studies have shown that CMAQ is skilled at capturing the seasonal and long-term trends in sulfate $PM_{2.5}$, in part because the emission changes are large and well quantified. CMAQ also captures the long-term trend in nitrate $PM_{2.5}$; however, the model has less skill for seasonal variability in nitrate $PM_{2.5}$, owing to uncertainties in ammonia emission trends (Banzhaf et al., 2015; Xing et al., 2015).

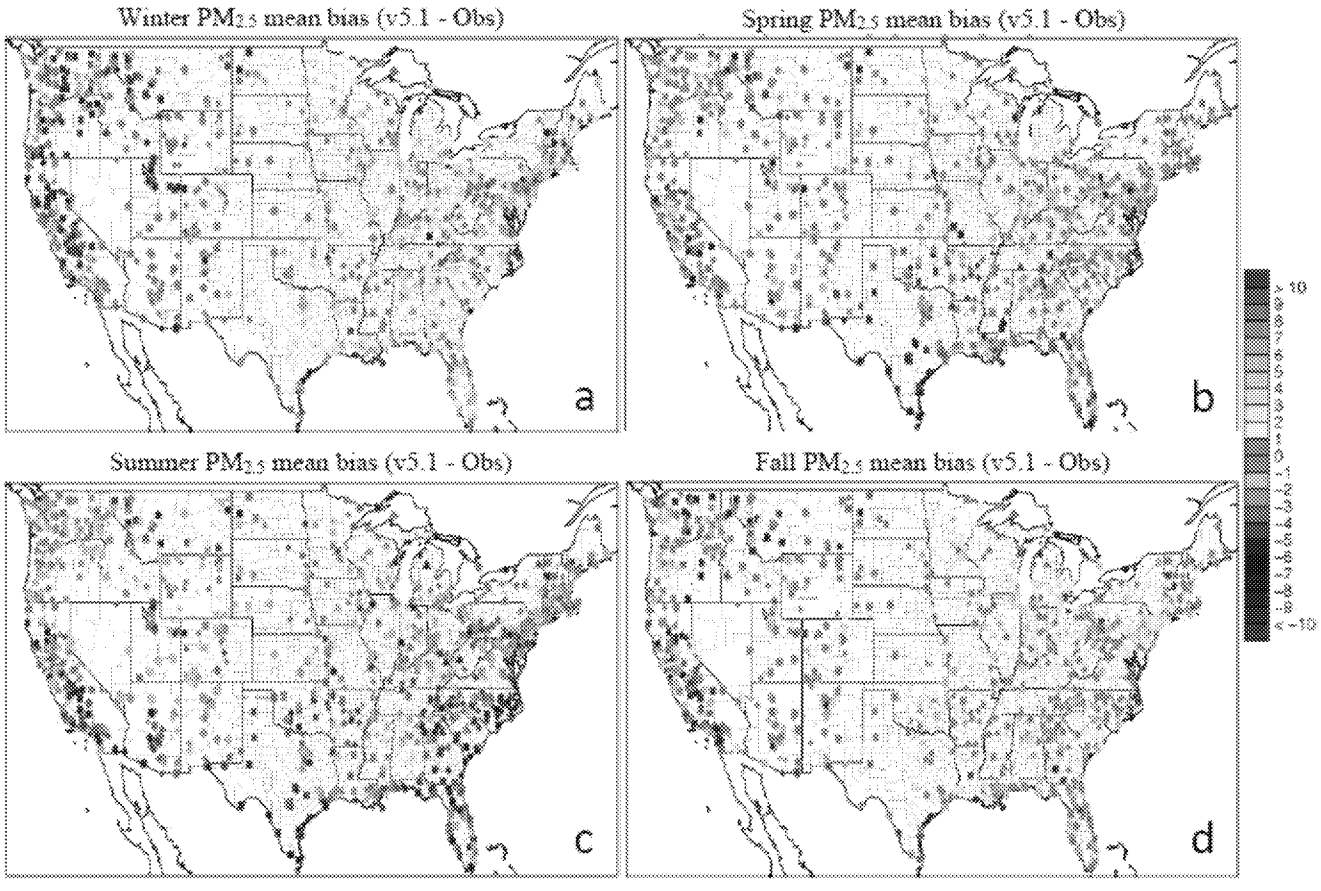

[a]DJF = December + January + February, MAM = March + April + May, JJA = June + July + August, SON = September + October + November.

Source Permission pending: Appel et al. (2017).

Figure 2-12 Seasonal average $PM_{2.5}$ mean bias (µg m^{-3}) in Community Multiscale Air Quality (CMAQ) simulations for 2011 at Interagency Monitoring of Protected Visual Environments (IMPROVE) (circles), Chemical Speciation Network (CSN) (triangles), air quality system (AQS) hourly (squares) and AQS daily (diamonds) sites for (a) winter (DJF)[a], (b) spring (MAM)[a], summer (JJA)[a] and fall (SON)[a].

2.5 Ambient Concentrations

2.5.1 Spatial Distribution

This section focuses on two spatial scales, the regional scale and urban/neighborhood scale. The regional scale is useful for understanding geographic differences between regions, especially with respect to PM concentrations, composition, and size. The urban and neighborhood scales are useful for understanding primary $PM_{2.5}$, $PM_{10-2.5}$, and UFP, because there are usually numerous sources, and PM concentrations can decrease steeply with distance from sources, resulting in considerable variation in PM concentrations over relatively short distances. The urban scale refers to citywide conditions with dimensions on the order of 4 to 50 km. The neighborhood scale refers to an extended area of a city with dimensions on the order of 0.5 to 4 km (CFR 40 Part 58 Appendix E, 2018).

Much of our understanding of spatial and temporal variation in PM concentrations is based on observations from PM monitoring networks. Spatial and temporal differences in $PM_{2.5}$ concentrations have also been predicted from models based on covariate data for both fine and large spatial scales (Yanosky et al., 2014; Paciorek and Liu, 2009; Yanosky et al., 2009). In general, stronger cross-validation agreement and greater precision for $PM_{2.5}$ than for PM_{10} or $PM_{10-2.5}$ have been observed for predictive models of PM concentration, probably because $PM_{10-2.5}$ concentrations exhibited greater spatial variability (Yanosky et al., 2014; Yanosky et al., 2009). Regionally predictive capability in one study was best for the Northeast and Midwest and poorest in the Northwest and Central Plains, with intermediate performance in the Southeast, South Central and Southwest (Yanosky et al., 2014). Pang et al. (2010) compared two computational estimation methods, Bayesian maximum entropy and ordinary kriging, and concluded that lower $PM_{2.5}$ estimation errors and error variances were obtained with a Bayesian maximum entropy approach.

2.5.1.1 Variability Across the U.S.

2.5.1.1.1 $PM_{2.5}$

$PM_{2.5}$ concentrations have decreased considerably compared to those reported in the 2009 PM ISA (U.S. EPA, 2009). Figure 2-13 shows the 3-year mean of the 24-hour $PM_{2.5}$ concentrations for network monitoring sites across the U.S. from 2013–2015. Figure 2-14 shows the 98th percentile $PM_{2.5}$ concentrations over the 3-year period from 2013–2015 at monitors across the U.S. Although concentrations have decreased, the geographic distribution of average concentrations is similar to the period 2005–2007 reported in the 2009 PM ISA (U.S. EPA, 2009). Some of the highest 3-year average 24-hour $PM_{2.5}$ concentrations are in the San Joaquin Valley and the Los Angeles-South Coast Air Basin of California. Many sites in the Northwest, including Oregon, Idaho, Western Montana, and Utah

experienced 98th percentile $PM_{2.5}$ concentrations greater than 40 $\mu g/m^3$. Numerous sites in the Central Valley of California also reported 98th percentile $PM_{2.5}$ concentrations above 40 $\mu g/m^3$. In the Eastern U.S. there is a zone of elevated $PM_{2.5}$ with annual average concentrations greater than 10 $\mu g/m^3$ and 98th percentile concentrations greater than 25 $\mu g/m^3$ in the Ohio Valley, and stretching into to Eastern Pennsylvania. Both annual average and 98th percentile concentrations are generally lower than what was observed in the 2005–2007 period as reported in the 2009 PM ISA, continuing the downward trend reported there (U.S. EPA, 2009).

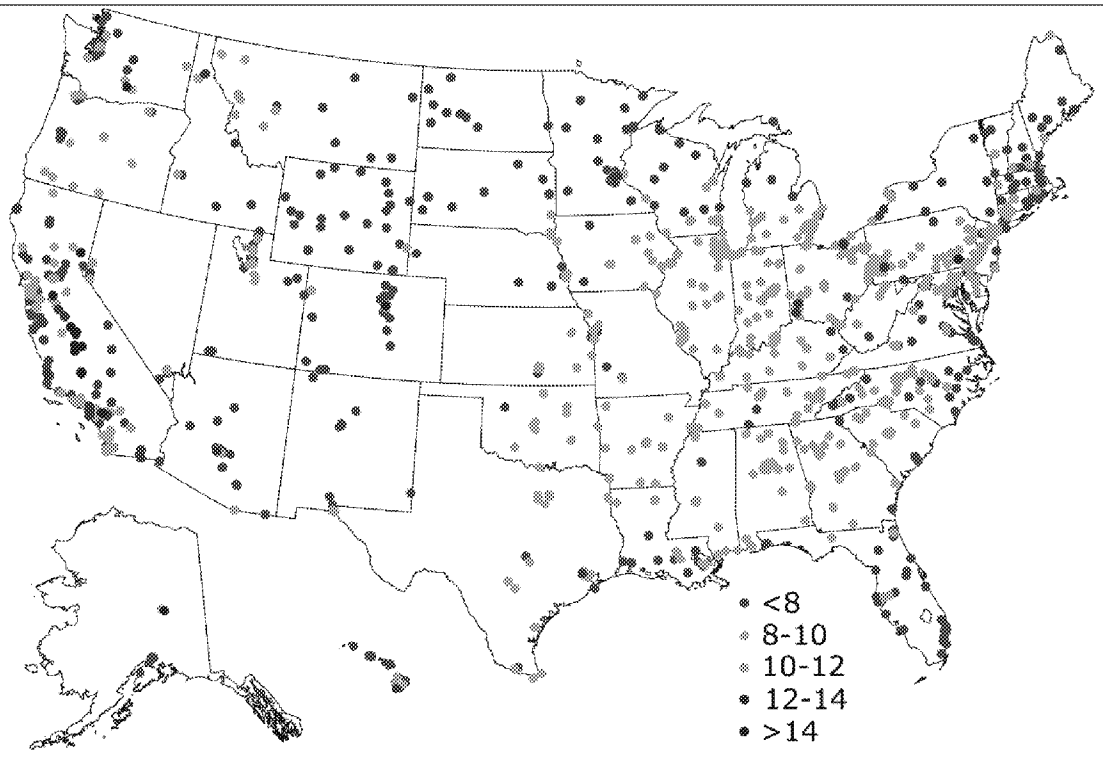

Source Permission pending: U.S. EPA 2016 analysis of Air Quality System network data 2013–2015.

Figure 2-13 Three-year average $PM_{2.5}$ concentrations 2013–2015.

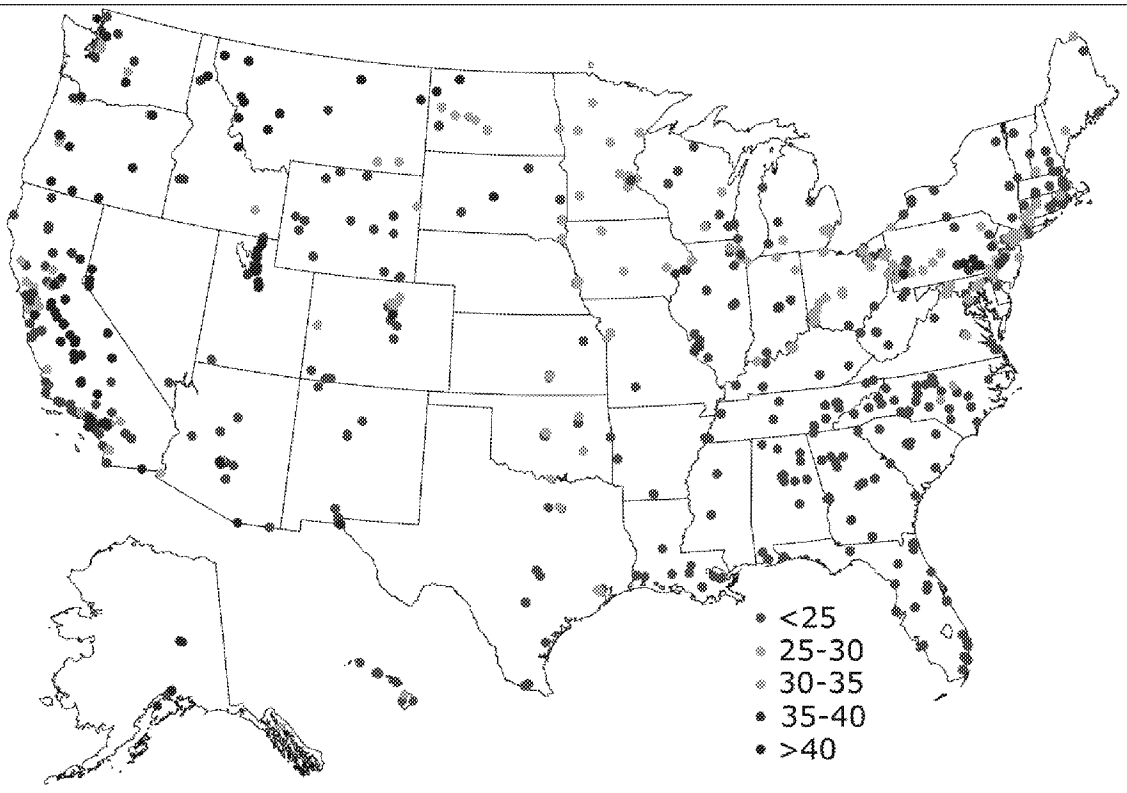

Source Permission pending: U.S. EPA 2016 analysis of Air Quality System network data 2013–2015.

Figure 2-14 98th percentile 24-hour $PM_{2.5}$ concentrations 2013–2015.

Specific regional concentration patterns are also evident from $PM_{2.5}$ data derived from satellites (see Section 2.4.5), including the higher average abundance in the eastern half than in the western half of the U.S., with especially high concentrations in the Ohio Valley; the Sonoran desert region, which extends from Mexico into Arizona and inland areas of Southern California and is subject to frequent dust storms; the Los Angeles urban area; the San Joaquin Valley; and the Big Bend area of Texas, which is also subject to dust storms (Lary et al., 2014).

Table 2-4 contains summary statistics for $PM_{2.5}$ reported to AQS for the period 2013–2015. The table provides a distributional comparison between annual, 24-hour and 1-hour averaging times, as well as between quarters. The mean of annual average concentrations based on 24-hour samples across all sites during the 3-year period was 8.6 $\mu g/m^3$. This compares to a mean of annual average concentrations of 12 $\mu g/m^3$ for 2005 to 2007 (U.S. EPA, 2009), a substantial decrease.

Table 2-4 Summary statistics for $PM_{2.5}$ 2013–2015 (concentrations in µg/m^3).

	N	Mean	1	5	10	25	50	75	90	95	98	99	2nd Highest	Max
Annual (FRM[a] + 24h FEM[b])	1,533	8.6	2.1	4.6	5.5	7.1	8.7	9.9	11.3	12.1	14.1	15.4	26.3	28.8
Daily (FRM[a])	328,881	8.9	1.5	2.7	3.5	5.1	7.6	11.2	15.4	18.7	23.9	28.9	161.0	167.3
Daily (24-h FEM[b])	350,293	8.5	0.0	1.6	2.5	4.4	7.1	10.9	15.6	19.3	25.1	30.8	231.7	270.1
Hourly (1-h FEM[c])	8,424,430	8.5	−2.1	0.0	1.1	3.7	6.9	11.0	17.1	22.0	30.0	37.4	985	1,167
Daily (FRM[a] + 24-h FEM[b])	679,104	8.7	0.4	2.1	3.0	4.8	7.4	11.0	15.5	19.0	24.5	29.9	231.7	270.1
1st quarter[d]	158,434	9.7	0.5	2.2	3.2	5.1	8.0	12.3	18.0	22.6	29.8	36.2	155.8	170.7
2nd quarter[d]	161,586	7.7	0.5	2.1	3.0	4.6	6.9	10.0	13.3	15.7	18.8	21.5	133.3	167.3
3rd quarter[d]	162,366	8.9	0.4	2.3	3.2	5.1	7.8	11.4	15.4	18.2	22.2	26.4	231.7	270.1
4th quarter[d]	160,851	8.4	0.3	1.9	2.7	4.4	6.9	10.7	15.5	19.5	26.0	32.2	150.1	161.0

[a]FRM refers to Federal Reference Method.

[b]24-h FEM refers to Federal Equivalence Method with a 24-h sampling period.

[c]1-h FEM refers to Federal Equivalence Method with a 1-h sampling period.

[d]1st Quarter = January + February + March, 2nd Quarter = April + May + June, 3rd Quarter = July + August + September, 4th Quarter = October + November + December. Quarterly data includes FRM, 24-h FEM, and 1-h FEM data.

Source: U.S. EPA 2016 analysis of Air Quality System network data 2013–2015.

1

Average $PM_{2.5}$ concentrations were somewhat higher in winter (January–March) than in other seasons. The higher winter average contrasts with results from the 2009 PM ISA, in which slightly higher concentrations in summer were reported (U.S. EPA, 2009). This replacement of summer with winter as the season with the highest national average concentration is analyzed in more detail in Section 2.5.2.2. Table 2-4 still shows higher average $PM_{2.5}$ concentrations in summer than in fall or spring. This pattern of elevated summer and winter average $PM_{2.5}$ concentrations with lower concentrations in fall and spring has been observed since the initiation of the $PM_{2.5}$ monitoring network, and is also explored in detail in Section 2.5.2.2. The 99th percentile $PM_{2.5}$ concentration was considerably higher in winter than other seasons. This observation was consistent with trends reported in the 2009 PM ISA, which were attributed to wintertime stagnation events (U.S. EPA, 2009). The impact of meteorology on seasonal $PM_{2.5}$ concentrations is discussed in Section 2.5.2.2.

The distribution of 24-hour and 1-hour average FEM data are comparable up to the 90th percentile. At the 95th percentile, the 1-hour average is about 3 $\mu g/m^3$ higher than the 24-hour average, and at the 98th percentile it is 6 $\mu g/m^3$ higher. These concentration differences are consistent with those observed in 2005–2007 data reported in the 2009 PM ISA, although actual concentrations are 4–5 $\mu g/m^3$ lower in 2013–2015 than for 2005–2007. The deviation between 1-hour and 24-hour averaging times results from short duration spikes in $PM_{2.5}$ that have more influence on the 1-hour distribution, than the 24-hour average distribution (U.S. EPA, 2009).

2.5.1.1.2 PM_{10}

PM_{10} mass includes all of the other PM mass size fractions considered in this chapter, i.e., $PM_{2.5}$, $PM_{10-2.5}$, and UFP. Like $PM_{2.5}$, geographic trends are very similar to those reported in the 2009 PM ISA (U.S. EPA, 2009). Figure 2-15 shows the 98th percentile of PM_{10} concentration at monitors across the U.S. The highest concentrations were observed in the Western U.S., including the San Joaquin Valley, Imperial Valley, and other areas of California, as well as the Southwest, including Arizona, New Mexico, Colorado, and El Paso, TX. In contrast, throughout the Northeast and Southern U.S. 98th percentile PM_{10} concentrations are generally below 100 $\mu g/m^3$. In the Midwest, Oklahoma, Texas, and Florida, concentrations between these extremes were generally observed for 98th percentile PM_{10}.

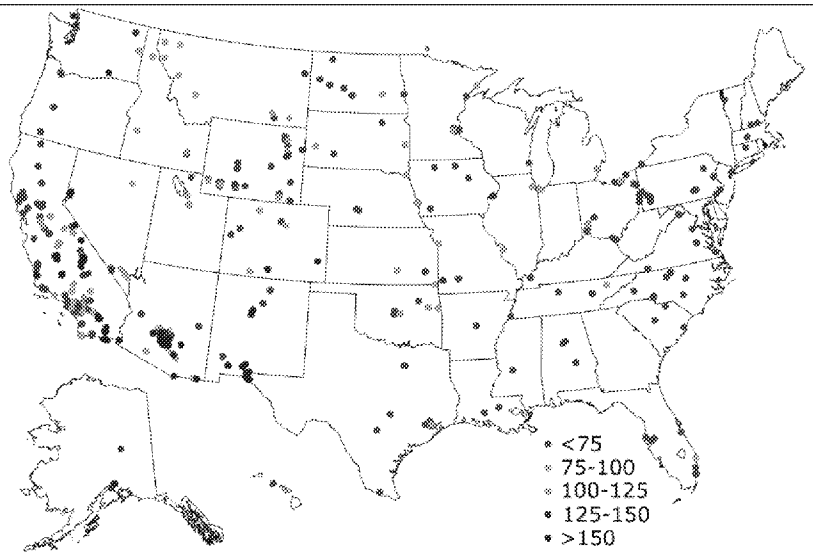

Source Permission pending: U.S. EPA 2016 analysis of Air Quality System network data 2013–2015.

Figure 2-15 98th percentile PM_{10} concentrations (2013–2015).

Table 2-5 gives summary statistics for PM_{10} for the period 2013–2015. The national average concentration based on FRM was 21.1 μg/m^3, which is 15% lower than the average for 2005–2007 reported in the 2009 PM ISA (U.S. EPA, 2009). However, at the 99th percentile, PM_{10} concentrations were almost identical to 2005–2007 data, with a FRM 99th percentile concentration of 91 μg/m^3 in 2005–2007 and 92 μg/m^3 in 2013–2015. Table 2-5 does not exclude any data for exceptional events and many of the areas with increasing trends are in California (fires) and Arizona (dust). These sporadic natural events could have a more important impact on the trends of the upper percentiles than the average.

While some concentrations exceeded 150 μg/m^3, 99th percentile concentration was well below this concentration for all monitor types and averaging periods, and 98th percentile concentrations were below 100 μg/m^3. Summer concentrations appear to be typically higher than other seasons, with the highest average concentration as well as the highest concentration at all percentiles up to the 95th percentile for summer. However, the most extreme events appear to be more likely in the spring, as indicated by the highest 98th and 99th percentile concentrations. Winter concentrations are the lowest at all percentiles, with average concentrations 6 μg/m^3 lower in winter than in summer.

Table 2-5 Summary statistics for PM_{10} 2013–2015 (concentrations in µg/m^3).

	N	Mean	1	5	10	25	50	75	90	95	98	99	2nd Highest	Max
Daily (FRM[a])	186,552	21.1	2	5	6	10	17	25	37	49	69	92	3,916	3,972
Daily (24-h FEM[b])	311,632	23.8	3	5	7	11	18	29	43	57	80	106	1,739	1,739
Daily (1-h FEM[c])	7,341,950	23.8	1	2	5	9	17	28	45	62	93	127	12,445	13,304
Daily (FRM[a] + 24-h FEM[b])	498,184	22.8	2	5	7	11	18	27	41	54	76	101	3,916	3,972
1st quarter[d]	123,249	19.3	2	4	5	9	14	23	37	49	69	89	1,482	1,488
2nd quarter[d]	125,605	24.0	2	5	7	11	18	28	42	55	83	122	3,284	3,916
3rd quarter[d]	124,999	25.3	4	8	10	14	20	30	44	56	78	102	1,006	1,265
4th quarter[d])	124,331	22.4	2	5	7	11	17	27	42	55	76	96	2,187	3,972

[a]FRM refers to Federal Reference Method.

[b]24-h FEM refers to Federal Equivalence Method with a 24-hour sampling period.

[c]1-h FEM refers to Federal Equivalence Method with a 1-hour sampling period.

[d]1st quarter = January + February + March, 2nd quarter = April + May + June, 3rd quarter = July + August + September, 4th quarter = October + November + December. Quarterly data includes FRM, 24-h FEM, and 1-h FEM data.

Source: U.S. EPA 2016 analysis of Air Quality System network data 2013–2015.

1

2.5.1.1.3 $PM_{10-2.5}$

As described in Section 2.4.2 and Section 2.4.6, $PM_{10-2.5}$ measurement capabilities and availability of $PM_{10-2.5}$ ambient concentration data have greatly increased since the 2009 PM ISA. At that time $PM_{10-2.5}$ concentrations were not routinely monitored, other than in the IMPROVE program, and $PM_{2.5}$ and PM_{10} measurements could only be compared between different types of samplers with different designs and flow rates (U.S. EPA, 2009).

Figure 2-16 shows the 98th percentile concentrations for $PM_{10-2.5}$ between 2013–2015. 98th percentile concentrations greater than 40 $\mu g/m^3$ were observed in multiple locations, not only in California and the Southwestern states of Nevada, Arizona, and New Mexico, but also in Texas, Oklahoma, Missouri, Iowa, and Alaska. St. Louis, Cleveland, south Florida also stand out as urban areas with some of the highest $PM_{10-2.5}$ concentrations.

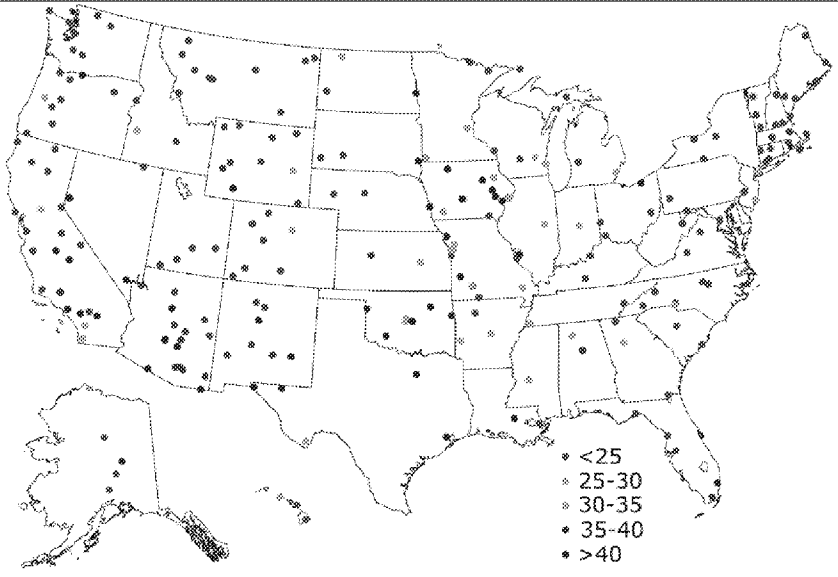

Source Permission pending: U.S. EPA 2016 analysis of Air Quality System network data 2013–2015.

Figure 2-16 98th percentile concentrations for $PM_{10-2.5}$ between 2013–2015.

Table 2-6 shows summary statistics on national $PM_{10-2.5}$ concentrations from 2013–2015. Data for FRMs and IMPROVE national mean and percentile concentrations are quite different than FEM, typically a factor of 2 or more higher for FEM data than the filter-based FRM and IMPROVE data, probably because of differences in site locations such as the urban-rural mix. Concentrations of several hundred micrograms per cubic meter were occasionally observed, but 98th percentile concentrations were

under 50 μg/m^3 regardless of method or averaging period. Concentrations were typically higher in summer than in other seasons on average, and at all percentiles up to the 95th percentile. However, 98th and 99th percentile concentrations for $PM_{10-2.5}$ are highest in the fall rather than the spring, although the very highest concentration was observed in the spring.

These observations are supported by additional studies showing that the highest concentrations of $PM_{10-2.5}$ were generally observed in the Southwestern U.S. (Li et al., 2013). They are also consistent with urban data from the 2009 PM ISA (U.S. EPA, 2009)showing $PM_{10-2.5}$ comprised most of PM_{10} in Denver and Phoenix, but not in other major cities (U.S. EPA, 2009). At two urban sites in Denver and two comparatively rural sites in Greeley, CO, average $PM_{10-2.5}$ concentrations over the course of a year averaged 9.0 to 15.5 μg/m^3, with the highest values in Northeast Denver (Clements et al., 2012). $PM_{10-2.5}$ concentrations up to 5 times higher than $PM_{2.5}$ concentrations were reported (Clements et al., 2014b). $PM_{10-2.5}$ concentrations in Denver were highest when winds were coming from the urban core, and highest in Greeley when winds were coming from Denver and other large communities (Clements et al., 2012).

Table 2-6 Summary statistics for $PM_{10-2.5}$ 2013–2015 (concentrations in µg/m^3).

	N	Mean	1	5	10	25	50	75	90	95	98	99	2nd Highest	Max
Daily (FRM[a] + IMPROVE[b])	74,095	5.7	0	0.3	0.6	1.6	3.8	7.4	12.7	17.3	24.8	31.5	178.7	178.7
Daily (24-h FEM[c])	34,619	12.4	−0.6	1.2	2.3	4.7	9.0	15.9	25.5	33.6	45.2	56.4	695.5	858.6
Daily (FRM[a] + 24-h FEM[c] + IMPROVE[b])	108,714	7.8	0	0.4	0.8	2.2	5.0	10.0	17.6	24.3	34.6	43.2	695.5	858.6
1st quarter[d]	26,760	5.7	−0.4	0.1	0.3	1.0	2.9	7.0	14.0	20.0	30.0	38.8	301.5	341.8
2nd quarter[d]	27,737	8.2	−0.1	0.5	0.9	2.3	5.3	10.4	18.1	24.3	35.4	45.5	695.5	858.6
3rd quarter[d]	27,238	9.2	0.5	1.4	2.1	3.7	6.7	11.5	19.0	25.3	33.9	40.3	227.4	295.0
4th quarter[d]	26,979	8.2	0	0.5	0.9	2.3	5.1	10.5	18.9	26.3	38.2	47.7	180.0	185.1

[a]FRM refers to Federal Reference Method.

[b]IMPROVE refers to IMPROVE sampler used for PM measurement in the IMPROVE network (see Section 2.4.6).

[c]24-h FEM refers to Federal Equivalence Method with a 24-hour sampling period.

[d]1st quarter = January + February + March, 2nd quarter = April + May + June, 3rd quarter = July + August + September, 4th quarter = October + November + December. Quarterly data includes FRM, 24-h FEM, and 1-h FEM data.

Source: U.S. EPA 2016 analysis of Air Quality System network data 2013–2015.

1

2.5.1.1.4 $PM_{2.5}/PM_{10}$

In numerous earlier studies summarized in the 2009 PM ISA (U.S. EPA, 2009) as well as in an extensive analysis of data reported in the 1996 PM AQCD (U.S. EPA, 1996), the ratio of $PM_{2.5}$ to PM_{10} was higher in the East than in the West in general. Crude estimates of the fraction of PM_{10} accounted for by $PM_{2.5}$ were obtained by dividing the 3-year average $PM_{2.5}$ concentration by the 3-year average PM_{10} concentration for 15 cities in the 2009 PM ISA (U.S. EPA, 2009, 179916}. PM_{10} was estimated to contain less $PM_{2.5}$ than $PM_{10-2.5}$ in Phoenix and Denver (3-year mean $PM_{2.5}/PM_{10}$ ratios of 0.19 and 0.32, respectively), but more $PM_{2.5}$ than $PM_{10-2.5}$ in Philadelphia ($PM_{2.5}/PM_{10}$ = 0.74), New York ($PM_{2.5}/PM_{10}$ = 0.68) and Pittsburgh ($PM_{2.5}/PM_{10}$ = 0.67) (U.S. EPA, 2009). By comparison, in Europe $PM_{2.5}$ usually accounts for 50 to 90% of PM_{10} and ratios are fairly constant for individual sites, but vary between sites (Putaud et al., 2010).

A more current and comprehensive comparison of the relative contributions of $PM_{2.5}$ and $PM_{10-2.5}$ to PM_{10} by region and season using data from the NCore Network is now possible. Figure 2-11 (Section 2.4.6) shows a map of NCore monitors in operation on a routine basis. Table 2-7 provides average $PM_{2.5}/PM_{10}$ ratios from the NCore network based on a FRM designed specifically for $PM_{10-2.5}$ (see Section 3.4.3) averaged over the entire period of monitoring site operation at 28 locations distributed throughout the U.S. The data indicate roughly equivalent amounts of $PM_{2.5}$ and $PM_{10-2.5}$ at most urban sites, with $PM_{2.5}/PM_{10}$ ratios ranging from 41 to 61% for all urban sites except Dayton, OH and Columbia, SC, and from 61 to 66% for rural sites in the Northeast. Although the Dayton, OH monitor is located within a defined CBSA, it is on the property of a rural county high school. In general, the $PM_{2.5}/PM_{10}$ ratios observed from the new NCore data are considerably lower than the $PM_{2.5}/PM_{10}$ ratios for Eastern U.S. sites reported in the 2009 PM ISA (U.S. EPA, 2009) and other earlier studies.

Table 2-7 $PM_{2.5}/PM_{10}$ ratios from National Core network (NCore).

Location	Landscape	Years	Avg $PM_{2.5}$	Avg $PM_{10-2.5}$	$PM_{2.5}/PM_{10}$
Dayton, OH	Rural	2011–2015	9.5	4.7	0.66
Litchfield, CT	Rural	2012–2015	5.3	2.8	0.66
Peterborough, NH	Rural	2011–2015	4.4	2.2	0.66
Columbia, SC	Urban	2011–2015	9.2	5.0	0.65
Beltsville, MD	Rural	2011–2015	8.1	4.3	0.64
McFarland Hill, ME	Rural	2015	4.2	2.1	0.64
Londonderry, NH	Rural	2011–2015	6.1	4.0	0.61
Raleigh, NC	Urban	2011–2015	8.7	5.7	0.61
Charlotte, NC	Urban	2011–2015	9.3	6.2	0.60
Providence, RI	Urban	2011–2015	7.2	4.6	0.59
Cincinnati, OH	Urban	2011–2015	10.6	7.7	0.58
Little Rock, AR	Urban	2011–2015	10.5	8.2	0.58
Louisville, KY	Urban	2014–2015	9.6	7.0	0.58
Philadelphia, PA	Urban	2014–2015	10.2	7.2	0.58
Wilmington, DE	Urban	2011–2015	10.0	7.4	0.57
Portland, OR	Urban	2011–2015	7.6	5.3	0.56
Seattle, WA	Urban	2005–2015	6.5	5.3	0.56
Grand Rapids, MI	Urban	2011–2015	9.2	7.4	0.55
Birmingham, AL	Urban	2012–2015	11.3	11.1	0.53
Davenport, IA	Urban	2013–2015	8.3	7.7	0.53
Jackson, MS	Urban	2015	9.4	9.7	0.53
New Haven, CT	Urban	2012–2015	8.3	7.2	0.53
Newark, NJ	Urban	2015	9.1	8.0	0.53
Boston, MA	Urban	2011–2015	7.2	7.2	0.52
Fairbanks, AK	Urban	2012–2015	12.2	10.1	0.52

Table 2 7 (Continued): $PM_{2.5}/PM_{10}$ ratios from National Core network (NCore).

Location	Landscape	Years	Avg $PM_{2.5}$	Avg $PM_{10-2.5}$	$PM_{2.5}/PM_{10}$
Memphis, TN	Urban	2013–2015	8.4	9.4	0.51
St. Louis, MO	Urban	2011–2015	10.9	11.3	0.50
Detroit, MI	Urban	2011–2015	10.0	11.0	0.48
San Jose, CA	Urban	2011–2015	9.9	10.7	0.47
Tulsa, OK	Urban	2011–2015	9.2	11.4	0.46
Albuquerque, NM	Urban	2011	7.1	9.4	0.45
Cleveland, OH	Urban	2013–2015	11.9	18.8	0.42
Denver, CO	Urban	2015	7.1	11.1	0.41

Source: U.S. EPA 2016 analysis of Air Quality System network data 2011–2015.

The lower $PM_{2.5}/PM_{10}$ ratios indicate a generally higher fraction of $PM_{10-2.5}$ in the Eastern U.S. than was reported in the 2009 PM ISA. The trend of a greater $PM_{2.5}$ fraction in the East and greater $PM_{10-2.5}$ fraction in the West (U.S. EPA, 2009) is generally preserved, but the data in Table 2-7 show $PM_{2.5}$ contributing only slightly more to PM_{10} mass than $PM_{10-2.5}$ in urban sites of the Northeast. $PM_{10-2.5}$ made a greater contribution to PM_{10} not only at most western sites, but also in the Midwest (Cleveland, Detroit). Important exceptions to lower $PM_{2.5}/PM_{10}$ ratios in the Western U.S. were the major cities of the Pacific Northwest (Seattle, Portland), where $PM_{2.5}$ accounted for most of PM_{10} and $PM_{2.5}/PM_{10}$ ratios were similar to Eastern locations. $PM_{2.5}$ was 60% or more of PM_{10} at only 9 of 33 NCore stations. All of these were either rural Northeastern (Litchfield, CT, Peterborough, NH, Beltsville, MD, McFarland Hill, ME, Londonderry, NH) or urban Southeastern (Charlotte, NC, Raleigh, NC, Columbia, SC) sites. It appears that PM_{10} in the U.S. has become considerably coarser than observed in the 2009 PM ISA (U.S. EPA, 2009), and that in many urban areas $PM_{10-2.5}$ mass makes a similar or greater contribution to PM_{10} mass than does $PM_{2.5}$ mass.

2.5.1.1.5 Ultrafine Particles

Key atmospheric science related uncertainties identified in the 2009 PM ISA for linking measurable particle number concentration with adverse UFP effects were the lack of data on UFP concentrations, lack of data on UFP composition, lack of data on spatial and temporal evolution of UFP size distribution and chemical composition, the lack of a UFP network in the U.S., and the lack of information on spatial and temporal variability in UFP concentration. There are few long-term average data on particle number concentrations in the U.S. Annual average particle number concentrations reaching 22,000 cm^{-3} for particles from 0.003 to 0.5 μm in Pittsburgh (Stanier et al., 2004) and monthly

average concentrations exceeding 30,000 cm^{-3} for particles from 0.017 to 0.1 μm (Hughes et al., 1998) and from 0.014 to 0.7 μm (Singh et al., 2006) in Los Angeles have been reported. The 2009 PM ISA (U.S. EPA, 2009) described several ambient UFP characteristics. Number concentrations dropped off quickly with distance from a road, and greater spatial variability occurred for UFP than $PM_{2.5}$ on an urban scale. Traffic was described as a major source, but high number concentrations during new particle formation events were also described. OC was identified as the major UFP component in several studies, along with substantial contributions from EC and sulfate. Higher winter than summer concentrations were reported in several northern locations. UFP concentration peaks during rush hour in urban areas were described, and broad midday peaks in summer were also noted in some instances, possibly due to NPF after photochemical reactions (U.S. EPA, 2009).

Results from a number of field studies reported in the 2009 PM ISA (U.S. EPA, 2009) described spatial and temporal variations in total particle number concentrations used as an estimate of UFP number concentration. In general, spatial variability of total particle number concentration increased with increasing distance between measurements, increasing source variation in the area studied, and increasing particle size within the UFP size range. Figure 2-17 shows three sites in the state of New York where UFP measurements have been initiated. Hourly results over several years from these sites are presented in Figure 2-18 and provide a much larger data set for comparing spatial and temporal variability than has been previously available (NYDEC, 2016). Figure 2-18 shows the average particle count of each location at each hour of the day, beginning and ending at midnight. The Buffalo data are averaged over three sites. There is a pronounced difference in particle number concentration between locations, with urban particle number counts several times higher than the background site. Not shown in Figure 2-18, the highest particle number counts at three sites in Buffalo were observed at a near road site.

The particle numbers remain fairly constant throughout the day at the Steuben County background site, although particle number counts are slightly elevated on average during the midday hours. In contrast, particle numbers display daily trends, peaking around 8:00 a.m. in Buffalo and New York City (NYC), and remain high into the evening hours, with distinct rush hour and early afternoon peaks. These results are consistent with spatial and temporal results reported in the 2009 PM ISA, but are based on a much larger data set. The state of New York is continuing to analyze the data for seasonal differences in the frequency of high particle number counts and nucleation events, and neighborhood scale differences in a near road environment (NYDEC, 2016).

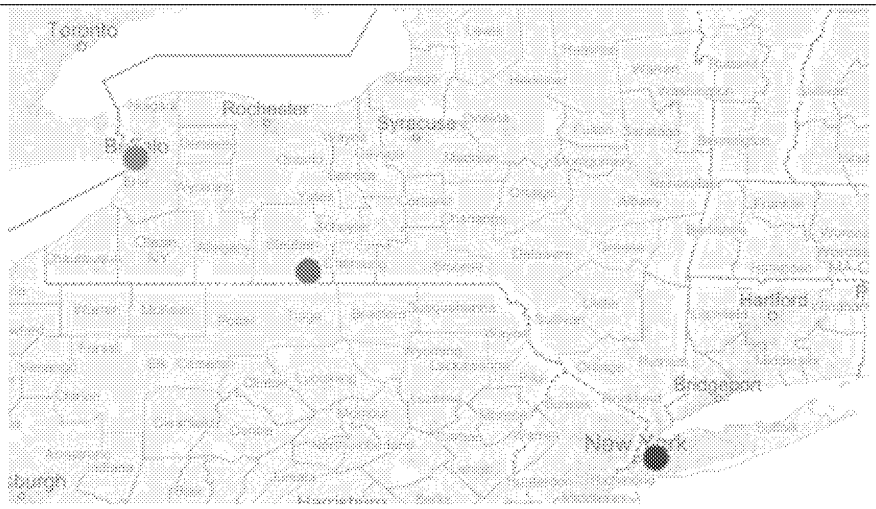

Source Permission pending: U.S. EPA 2016 analysis of Air Quality System network data.

Figure 2-17 Sites in New York state which reported particle number counts to air quality system (AQS).

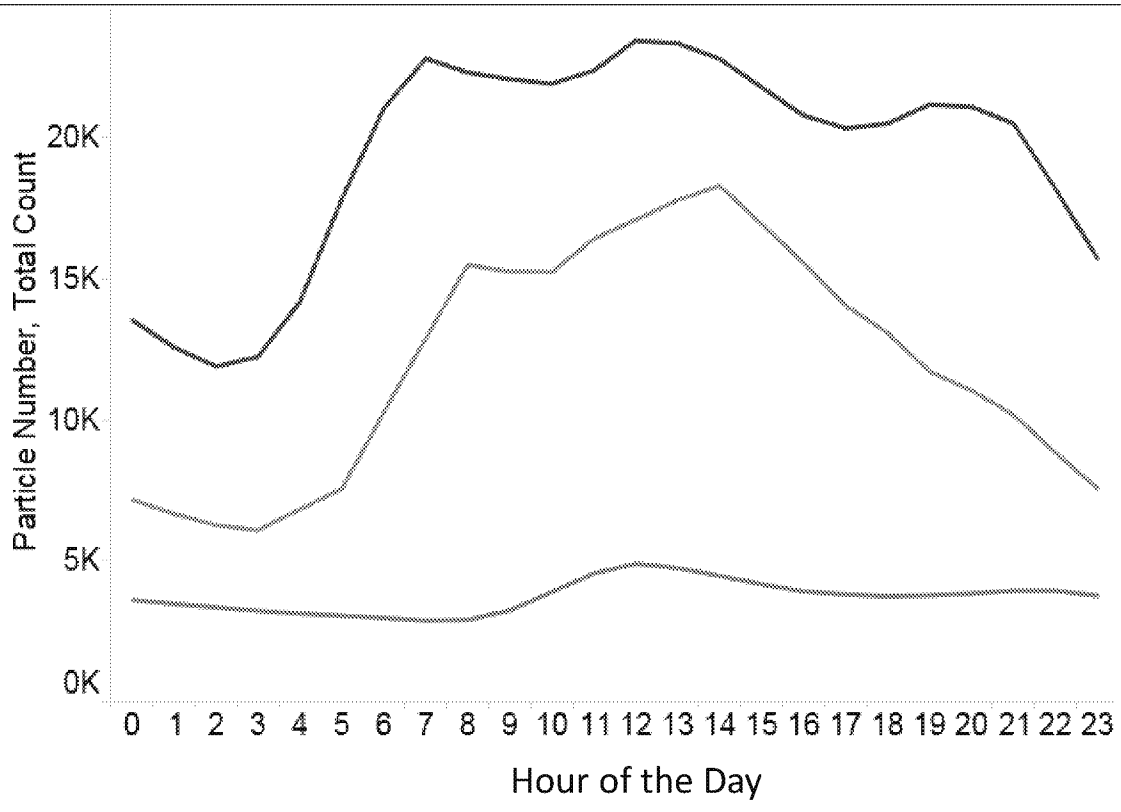

Line colors in the graph correspond to the colors of the sites on the map, i.e., orange data was collected in Buffalo, green data was collected in Steuben County, and red data was collected in NYC.

Source Permission pending: U.S. EPA 2016 analysis of Air Quality System network data 2012–2015.

Figure 2-18 Average hourly particle number concentrations from three locations in New York state for 2014–2015.[39]

Routine monitoring to obtain long-term average particle number distributions is a relatively recent development (Wiedensohler et al., 2012) using electromobility and electrometer based methods developed for the European UFP monitoring network (Section 2.3.4.1). Average particle concentrations classified by size from 24 European monitoring sites over a period of 2 years were recently described (Asmi et al., 2011). As one example, at the Ispra, Italy site number concentrations averaged 1,341 cm^{-3} for 0.03 to 0.05 μm, 4,448 cm^{-3} for 0.05 to 0.1 μm, and 2,129 cm^{-3} for 0.1 to 0.5 μm, corresponding to an average of 73% of airborne particles smaller than 0.1 μm (Asmi et al., 2011). This is an upper limit value because a substantial number of particles can be smaller than the 0.03 μm lower size limit for these data

[39] NYC and Steuben County also include 6 months in 2012. Buffalo data are from three different sites, with the sampler moved between sites over the 2-year period. Data for the orange line depicting Buffalo are all from Buffalo, but not all from the same site within Buffalo.

(Stanier et al., 2004). For all 24 European locations, the average upper limit percentage of particles smaller than 0.1 μm ranged from 67 to 85%.

No such large-scale summary of U.S. data is possible, because there are few long-term data on number size distributions in the U.S. Number size distribution data have been reported for an 8-year period from 2002 to 2009 in Rochester, and number concentrations averaged 4,730 cm^{-3} for 0.01 to 0.05 μm particles, 1,838 cm^{-3} for 0.05 to 0.1 μm, and 1,033 cm^{-3} for 0.1 to 0.5 μm (Wang et al., 2011). This corresponds to 90% of total particles smaller than 0.1 μm. This is a larger fraction than the European range, but the lower size limit was 0.01 μm, compared to 0.03 μm for the European network data (Wang et al., 2011). Long-term trends for this period are summarized in Section 2.5.2.1.4. These data can also be compared to earlier observations of particle number concentrations for eight size ranges for a full year from the Pittsburgh Air Quality study (Stanier et al., 2004). Using their data, it is possible to calculate that 90% of the number of particles were also smaller than 0.1 μm and that 98% were smaller than 0.2 μm.

2.5.1.1.6 $PM_{2.5}$ Components

It is useful to distinguish between bulk PM components and more finely speciated components. The term bulk component refers to a large component category like OC, sulfate, or nitrate, which is monitored in networks like CSN or IMPROVE and usually makes up a substantial portion of PM mass. It is also used to differentiate broad categories of components like OC and crustal material, which are considered bulk components, from more finely speciated components like individual organic compounds and elements, which are usually present in lower amounts.

Figure 2-19 shows contributions of sulfate, nitrate, OC, EC, crustal material, and sea salt to $PM_{2.5}$. A major change in $PM_{2.5}$ composition compared to the 2009 PM ISA (U.S. EPA, 2009) is the reduction in sulfate concentrations, resulting in a smaller sulfate contribution to $PM_{2.5}$ mass in 2013–2015 compared to what was reported for 2005–2007 in the 2009 PM ISA, especially in the Eastern U.S. As a result, at many locations sulfate has been replaced as the greatest single contributor to $PM_{2.5}$ mass by organic material or nitrate. This long-term trend demonstrating a reduction in sulfate concentrations is described in more detail in Section 2.5.2.1.4.

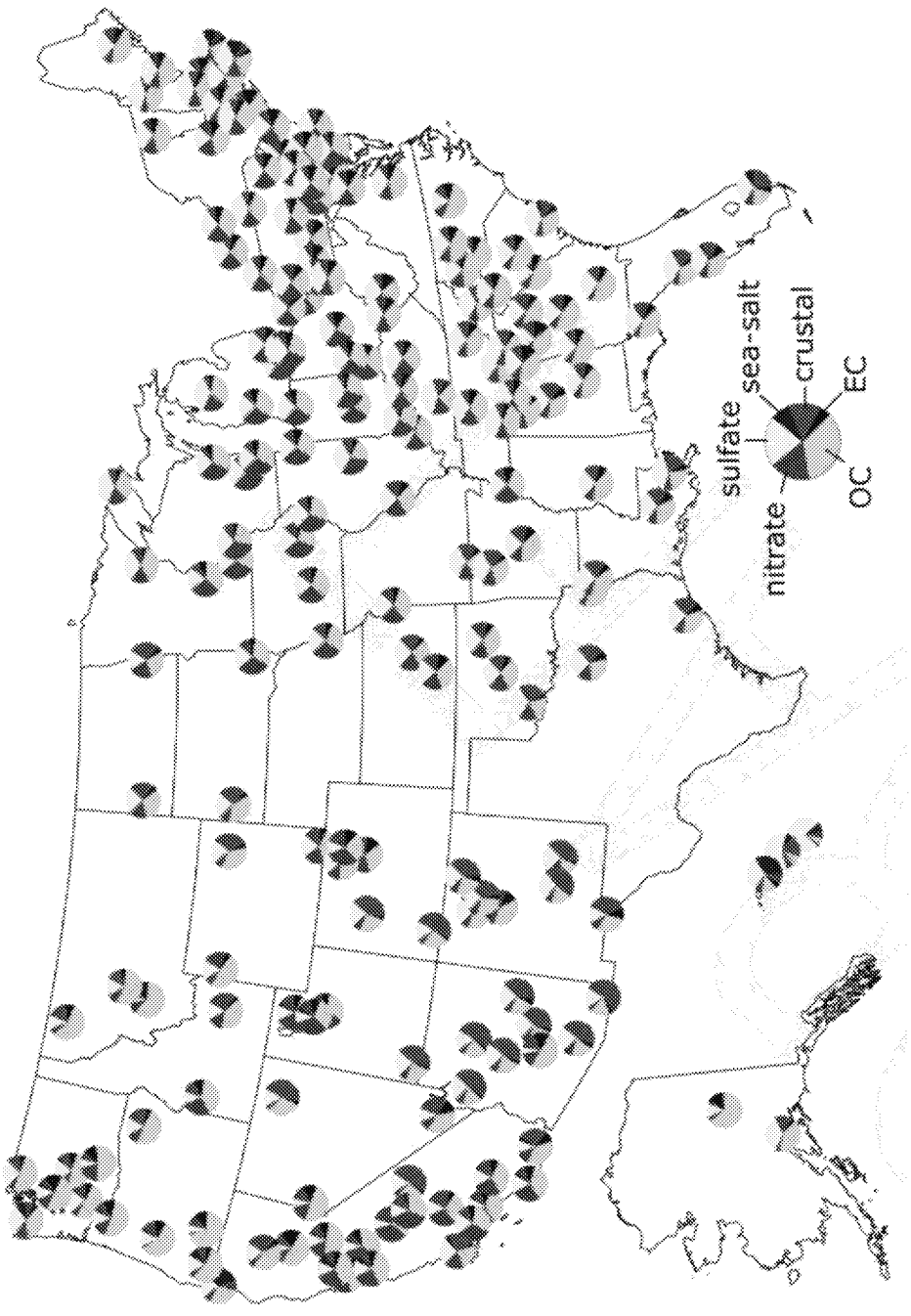

Source Permission pending: U.S. EPA 2016 analysis of Air Quality System network data 2013−2015.

Figure 2-19 Contributions of sulfate, nitrate, organic carbon (OC), elemental carbon (EC), crustal material, and sea salt to $PM_{2.5}$.

Regional patterns of component contributions to $PM_{2.5}$ in Figure 2-19 are similar to those reported in the 2009 PM ISA (U.S. EPA, 2009). Sulfate and OC are the species with the highest

contribution to total mass in most eastern locations and OC usually makes the greatest contribution to $PM_{2.5}$ mass in the west, although sulfate, nitrate, and crustal material can also be abundant (U.S. EPA, 2009). Urban and rural sulfate are both substantially higher in the East than in the West (Hand et al., 2012c). The highest nitrate concentrations are found in the west, particularly in California, but with some elevated concentrations in the upper Midwest. Larger contributions of OC to $PM_{2.5}$ mass observed in the Southeast and the West than in the Central and Northeastern U.S. are consistent with larger OC concentrations in those regions described in the 2009 PM ISA (U.S. EPA, 2009). The ratio of organic mass to OC mass depends on source and aerosol age, and was discussed in detail in the 2009 PM ISA (U.S. EPA, 2009). Based on speciation data from 15 cities reported in the 2009 PM ISA, EC contributed a smaller fraction of $PM_{2.5}$ mass than sulfate, nitrate, or OC, but consistently accounted for 4−11% of $PM_{2.5}$ (U.S. EPA, 2009).

Nationally, higher urban than rural OC and EC concentrations were reported by (Hand et al., 2013) and differences in urban and rural seasonal patterns for OC and EC were also observed. They also reported the highest rural OC and EC concentrations were in the Northwest and Southeast (Hand et al., 2012c). On average, OC and EC concentrations were both more uniformly distributed in the eastern U.S., but more localized in the West, with the highest urban concentrations in the West during fall and winter (Hand et al., 2013). However, EC concentrations were more consistent across cities regardless of region in the 2009 PM ISA (U.S. EPA, 2009). In the Southeastern U.S., annual average primary OC concentrations were estimated to exceed annual average secondary OC concentrations, but secondary OC could exceed primary OC at rural sites during the warmest months, and secondary OC concentration also showed little difference between urban and rural sites (Blanchard et al., 2013).

A large fraction of organic PM can be water soluble (Mwaniki et al., 2014). During the summer CalNex 2010 campaign (Kelly et al., 2014), water soluble $PM_{2.5}$ was at a maximum in the morning and in the evening in the San Joaquin Valley of California. In the same study, nitrate was present at higher concentrations than sulfate or ammonium, averaging 0.8 $\mu g/m^3$ and there were hourly average concentrations greater than 25 $\mu g/m^3$ during the winter 2013 DISCOVER-AQ campaign (Kelly et al., 2018).

Fine soil concentrations are higher in the Southwest than in other parts of the U.S., and also exhibit seasonal patterns for urban and rural sites (Hand et al., 2012c). High PM concentrations in urban desert areas were associated with a substantial contribution from crustal material from both coarse and fine PM (Wagner and Casuccio, 2014). Soil related PM also contributes substantially to $PM_{2.5}$ in populated areas of other parts of the world (Satsangi and Yadav, 2014). The pattern of higher crustal material contributions to $PM_{2.5}$ in drier areas of the Western U.S. can also be seen in Figure 2-19 with the examples of Phoenix and Denver.

There are a few new results to add to the body of literature on elemental composition, concerning both ambient observations and sources. In Southern California the most abundant elemental species was sulfur, followed by Si, Fe, Ca, and Al, with soil related elements accounting for 51% of total elemental

mass measured. New research to investigate sources further explored the importance of brake wear, lubricating oils, gasoline and diesel combustion, secondary sulfates, sea salts, and biomass burning as sources of trace elements (Na and Cocker, 2009). New research on atmospheric iron indicate that extent of aqueous solubility of iron present in PM is related to sulfur content of the PM (Oakes et al., 2012b). In Atlanta, iron concentrations exhibit considerable fluctuation, and reach up to 300 to 400 ng/m^3 for a few hours at time, (Oakes et al., 2012b). In Atlanta Fe(II) accounted for between 5 and 35%, or an average of about 25% of total soluble iron (Oakes et al., 2012a). In rural samples copper and zinc were found to be mainly present as sulfates and also nitrates in $PM_{2.5}$ in rural samples, but copper and zinc compounds found in larger particles were similar to copper and zinc compounds found in soil (Osan et al., 2010).

2.5.1.1.7 $PM_{10-2.5}$ Components

It was noted in the 2004 AQCD (U.S. EPA, 2004) that concentrations of most elements differed between $PM_{2.5}$ and $PM_{10-2.5}$, but that concentrations of some metals were similar between the two size fractions. It was also noted that this contrasted with earlier years with less controlled combustion, when Pb and other metals were much higher in $PM_{2.5}$.

Components of $PM_{10-2.5}$ are not routinely monitored like they are for $PM_{2.5}$, and information on $PM_{10-2.5}$ composition is largely limited to specific local studies. In the Southeast, OC and nitrate made similar fractional contributions to $PM_{2.5}$ and $PM_{10-2.5}$, but there was much less sulfate and EC in $PM_{10-2.5}$ than $PM_{2.5}$, and much more major metal oxides (U.S. EPA, 2009). In Los Angeles, crustal material and trace elements accounted for 47.5% of total reconstructed coarse PM mass, with secondary ions (sulfate, nitrate, ammonium, 22.6%) and organic matter (19.7%) also making important contributions, and elemental carbon was a less significant component, accounting for less than 2% of the mass (Cheung et al., 2011). Los Angeles crustal materials had low water solubility, but Ba and Cu were modestly water soluble and activity due to reactive oxygen species was most highly associated with water soluble elements, V, Pd, Cu and Rh in Los Angeles (Cheung et al., 2012a).

In the desert southwest, crustal material is the dominant component of $PM_{10-2.5}$, sometimes accounting for more than half of the mass, followed by organic matter, accounting for 15% (Clements et al., 2014a, 2013). High correlations between $PM_{2.5}$ and PM_{10} indicated that a large component of the fine fraction was derived from dust (Clements et al., 2013). In Denver and Phoenix, $PM_{10-2.5}$ made a greater contribution to total ambient PM_{10} mass than in other cities (U.S. EPA, 2009). PM in Denver has been studied in more detail since then. Coarse PM concentrations were attributed to crustal material, road salt, vehicle abrasion and sulfate (Clements et al., 2014b).

While crustal material often makes the greatest contribution to $PM_{10-2.5}$ mass, the organic fraction also makes a substantial contribution. In the Southeast, organic and elemental carbon accounted for approximately 30% of $PM_{10-2.5}$. Primary biological aerosol particles (PBAP), which consist of microorganisms and fragments of living things, can account for a large fraction of $PM_{10-2.5}$ mass (U.S.

EPA, 2009). These have been measured by treating collected PM with a dye which only reacts with protein containing material (Matthias-Maser et al., 2000). PBAP cannot be distinguished from other types of OC by methods used in monitoring networks. New research on sources of PBAP was summarized in Section 2.3.3. New information on the nature of bioaerosols and biological material associated with particles is well-described in the review by (Froehlich-Nowoisky et al., 2016). PBAP includes living and dead organisms, e.g., algae, archaea, bacteria and viruses, dispersal units, e.g., fungal spores and plant pollen, various fragments or excretions, e.g., plant debris and brochosomes. This class of material can range in size from 1 nm (individual proteins) to 5 millimeters (pollen grains). Summertime aerosols in Phoenix were abundant in biological compounds (e.g., sugars and fatty acids), present almost exclusively in the coarse size fraction (Cahill, 2013).

A pilot study on $PM_{10-2.5}$ species monitoring was carried out to develop target species, evaluate analytical methods and field performance, and to assess sampling and operational issues for routine measurement of $PM_{10-2.5}$ species (U.S. EPA, 2015). Samples collected in all seasons over a period of 1 year in both Phoenix and St. Louis indicated that soil oxides dominated $PM_{10-2.5}$ mass, with organic matter accounting for 10–20%. Sulfate and nitrate accounted for very little of the $PM_{10-2.5}$ mass, although they were substantial contributors to $PM_{2.5}$ mass. Soil oxides were by far the largest component in both locations throughout the year, except in St. Louis in winter, when soil and organic contributions were similar, but overall $PM_{10-2.5}$ concentrations were considerably lower (U.S. EPA, 2015).

2.5.1.1.8 Ultrafine Particle Components

There was little information on the composition of UFP presented in the 2009 PM ISA, although urban UFP was suspected to be rich in OC and EC, and sulfate was expected to be a substantial contributor in rural areas while new particle formation occurred (U.S. EPA, 2009). New research indicates that motor vehicles are a major, and frequently dominant, source of ultrafine particles in urban environments (Morawska et al., 2008). Chemical composition of these particles are determined by the composition of the used fuel and lubricating oil, driving conditions, and engine after-treatment system, as well as meteorological conditions, but generally PM from these sources consists mostly of agglomerates of solid-phase carbonaceous material, and can also contain metallic ash, adsorbed or condensed hydrocarbons and sulfur compounds, and liquid droplets consisting mainly of hydrocarbons and hydrated sulfuric acid that form very rapidly after the vehicle exhaust leaves a tailpipe (Liu et al., 2015; Saffaripour et al., 2015; Karjalainen et al., 2014; Rönkkö et al., 2014; Fushimi et al., 2011; Gidney et al., 2010; Heikkilä et al., 2009; Johnson, 2009).

The chemical composition of ultrafine particles originating from atmospheric NPF is tied heavily to their growth processes during their atmospheric aging. Direct observations during the period of atmospheric NPF show that the composition of particles originating from NPF is usually dominated by organic compounds, especially in forests (Han et al., 2014; Pennington et al., 2013; Pierce et al., 2012; Pierce et al., 2011), but also in many rural or urban environments (Bzdek et al., 2014; Setyan et al., 2014;

Bzdek et al., 2013; Ahlm et al., 2012; Smith et al., 2008). Exceptions for this pattern are environments exposed to major sulfur emissions, in which sulfate may explain up to about half of the ultrafine particle mass (Vakkari et al., 2015; Crilley et al., 2014; Bzdek et al., 2012; Zhang et al., 2011b; Wiedensohler et al., 2009).

2.5.1.1.9 Reactive Oxygen Species

Particle acidity, oligomer formation and the production of reactive oxygen species (ROS) are interrelated, aqueous phase processes with direct consequence for aerosol concentrations, chemical composition and toxicity (Weber et al., 2016). Polymerization reactions responsible for generating oligomers in atmospheric particles require relatively high concentrations of H^+. The reactive forms of the transition metals that play a central role in production of particle phase ROS primarily exist in low pH aqueous conditions.

Sulfate is often the main acid component of $PM_{2.5}$, and largely determines its acidity. Contrary to expectations, declining SO_2 emissions along with fairly stable NH_3 emissions (see Section 2.3.2.1), have led to little long-term change in pH of $PM_{2.5}$ (see Section 2.5.1.1.6). Low pH conditions facilitate the formation of oligomers and HULIS in aqueous particles. Upwards of 90% oligomeric/high molecular weight material has been found in SOA formed in the presence of NO_X, including a substantial fraction of organic nitrogen compounds (Nguyen et al., 2011). Humic-like substances and smaller organic compounds have been implicated in the production of particle-phase ROS, along with transition metal ions, especially Cu and Mn (Verma et al., 2015).

The 2009 PM ISA described early chamber work on identifying reactive oxygen species (ROS) in secondary organic PM by Docherty et al. (2005). Under the conditions of their experiment, they produced very high yields (47 and 85%) of organic peroxides by reacting O_3 with α- and β-pinene. Reactive oxygen species include hydroxyl radical, organic peroxides and hydroperoxides. A discussion of the role of particle-phase ROS in human health effects can be found in Section 5.1.1.

Identification of individual components that act as ROS in PM is incomplete and an active area of research. The extent to which an ambient particle can engage in oxidative reactions depends on the concentration of aqueous oxidants, such as the hydroxyl radical (OH), and whether or not reactants capable of producing additional oxidants are present within the particle. Oxidants, in addition to OH, can be taken up from the atmosphere or chemically formed from processes such as photolysis of nitrate, nitrite, or hydrogen peroxide (H_2O_2), or Fenton-type reactions between H_2O_2 and Fe(II) (McNeill, 2015; Arakaki et al., 2013; Ervens et al., 2011; Herrmann et al., 2010). Organic species, such as quinones, can act as transition ion reducing agents, which allow oxidized form of an aqueous transition metal ion to produce more ROS (Shirai et al., 2012). Tuet et al. (2017) found that the identities of available reactive precursors in the particle phase, humidity and the fate the reactive intermediate were important

determinants of particle reactivity. Atmospheric aging (oxidation) of organic aerosols has also been found to be an important indicator of ROS activity of ambient PM (Saffari et al., 2016; Verma et al., 2015).

2.5.1.2 Urban and Neighborhood Scale Variability

2.5.1.2.1 $PM_{2.5}$

Understanding spatial variation at the neighborhood and urban scale is important for interpreting data from community monitors. Because of its longer atmospheric lifetime (see Section 2.2), $PM_{2.5}$ is expected to exhibit less spatial variability on an urban scale than UFP or $PM_{10-2.5}$. In the 2004 PM AQCD (U.S. EPA, 2004) annual average $PM_{2.5}$ concentration differences between monitors within the urban area were compared for 17 urban areas. The difference in concentration between monitors with the highest and lowest concentrations ranged from less than 1 $\mu g/m^3$ (Baton Rouge, LA) to more than 8 $\mu g/m^3$ (Pittsburgh, PA). The difference exceeded 6 $\mu g/m^3$ in 6 of the 17 cities (Pittsburgh, Cleveland, Chicago, Detroit, St. Louis, Seattle), in 5 of which the highest $PM_{2.5}$ concentrations were between 20 and 22 $\mu g/m^3$. In the remaining city (Seattle) concentrations ranged from 6 to 12 $\mu g/m^3$.

The degree of spatial uniformity within urban areas also varied depending on location (U.S. EPA, 2004). Intra-urban spatial variability of $PM_{2.5}$ concentrations was discussed in considerable quantitative detail in the 2009 PM ISA, using a number of comparison statistics (U.S. EPA, 2009). In most metropolitan areas correlations between $PM_{2.5}$ monitoring sites up to a distance of 100 km from each other were greater than 0.75, with the notable exceptions of Denver, Los Angeles, and Riverside (U.S. EPA, 2009). However, while $PM_{2.5}$ concentrations at different sites within an urban area can be highly correlated, significant differences in concentration can occur on a given day (U.S. EPA, 2009).

Several recent publications have addressed urban scale spatial variability. Urban concentrations are often several $\mu g/m^3$ above regional background concentrations. For example, Indianapolis urban concentrations are on average 3.9 to 5. $\mu g/m^3$ higher than regional background (Sullivan and Pryor, 2014). Substantial spatial variation of $PM_{2.5}$ concentrations has been reported for New York City (Matte et al., 2013). Spatial variability was also demonstrated by a study indicating that $PM_{2.5}$ was present at significantly higher concentrations at urban sites than at upwind suburban sites in the greater New York area (Patel et al., 2009). Substantial differences in $PM_{2.5}$ concentrations between neighborhoods was also observed in Los Angeles (Fruin et al., 2014), but not in Boston (Patton et al., 2014). One of the contributing factors was that monitors are closer to each other in Boston, where more uniformity was observed. Sub-10 km spatial variability was identified as a contributor to poor results for satellite estimates of $PM_{2.5}$ from aerosol optical depth (AOD) using a 10 × 10 km grid (Lary et al., 2014; Chudnovsky et al., 2013b). In Indianapolis for time scales shorter than 1-day spatial variability was 2 to 3 times greater than temporal variability (Sullivan and Pryor, 2014). However, for 24-hour measurements

of PM components temporal variability accounted for 90% of the variance in Detroit (Bereznicki et al., 2012).

Spatial variability arises from source proximity, with motor vehicles accounting for 24 to 36% and secondary sulfate for 17 to 35% of $PM_{2.5}$ among different residential monitoring areas in Detroit, MI (Duvall et al., 2012). Diesel exhaust was also identified as a major and variable source of $PM_{2.5}$ in New York City (Patel et al., 2009). Land use regression modeling based on 155 city-wide street-level locations in New York City (Clougherty et al., 2013) indicated that concentrations of $PM_{2.5}$ and other pollutants varied by more than a factor of two, with highest concentrations near midtown Manhattan. They also reported that density of oil-burning boilers along with total and truck traffic density explained more than 80% of $PM_{2.5}$ spatial variability (Clougherty et al., 2013). However, in Dallas $PM_{2.5}$ exposure was only moderately associated with motor vehicles and weakly associated with industrial sources, but strongly associated with population density (Zou et al., 2009). Overall, recent observations indicate that uniform $PM_{2.5}$ concentrations can occur, but that substantial spatial variability is also common.

2.5.1.2.2 PM_{10}

PM_{10} concentrations vary by as much as a factor of five over urban scale distances of 100 km or less and by a factor of two or more over scales as small as 30 km (U.S. EPA, 2009; Alexis et al., 2001). Differences in PM_{10} measurements across 15 cities were summarized in the 2009 PM ISA (U.S. EPA, 2009). PM_{10} concentrations were less well correlated than $PM_{2.5}$, probably because of greater spatial variability of $PM_{10-2.5}$ (see Section 2.5.1.2.3). For monitors less than 4 km apart an average correlation of 0.93 between $PM_{2.5}$ monitors and 0.70 for PM_{10} monitors was observed (U.S. EPA, 2009). Spatial and temporal differences in PM_{10} concentrations have also been predicted from models based on the geographic information system; meteorological and copollutant data for both fine and large spatial scales and distance to road; elevation; and proportion of low-intensity residential, high-intensity residential, industrial, commercial, and transportation land use within 1 km have all been reported to be statistically significant predictors of measured PM_{10} (Blanchard et al., 2014; Paciorek et al., 2009; Yanosky et al., 2009); (Yanosky et al., 2014).

2.5.1.2.3 $PM_{10-2.5}$

As indicated in the 2004 PM AQCD (U.S. EPA, 2004), the shorter lifetime of $PM_{10-2.5}$ leads to lower spatial correlations for $PM_{10-2.5}$ than for either $PM_{2.5}$ or PM_{10} concentrations (U.S. EPA, 2009, 2004). Errors in measurement (see Section 2.4.4) can also contribute to lower spatial correlations of $PM_{10-2.5}$ (U.S. EPA, 2004). Recent observations from several cities indicate that there is often, but not always, considerable spatial variability in $PM_{10-2.5}$ concentrations in urban areas, that they are often related to specific industrial sources, and that concentrations of specific chemical components can be more variable than mass. In Detroit $PM_{10-2.5}$ was 5 $\mu g/m^3$ higher in two industrial areas, and 8 $\mu g/m^3$

higher in an area heavily impacted by traffic than average concentrations in other parts of the city, and not very consistent with central site monitor concentrations (Thornburg et al., 2009). Poor correlations between monitors were also observed in Los Angeles (Pakbin et al., 2010) and between industrial and suburban sites in Cleveland (Sawvel et al., 2015). In Rochester, NY, where major coarse particle sources were road dust and biological particles, considerable heterogeneity in both composition and concentrations were also observed between different sites (Lagudu et al., 2011).

2.5.1.2.4 Ultrafine Particles

As described in Section 2.5.1.1, UFP spatial variability increased with increasing distance between measurements, increasing source variation in the area studied, and increasing particle size within the UFP size range. (U.S. EPA, 2009). Particularly high spatial variabilities have been observed near roads with heavy traffic, where numerous observations of UFP number concentration declining sharply with distance from roadways have been reported (U.S. EPA, 2009).

More recently, spatial variability of UFP was compared between studies of two locations, Los Angeles, CA (Hudda et al., 2010; Krudysz et al., 2009; Moore et al., 2009) and Rochester, NY (Wang et al., 2012). These two studies provide an interesting comparison because the two studies were similar in domain size. The comparison is summarized in Table 2-8. It should be noted that the Los Angeles studies employed SMPS for particle size distribution measurements, while the Rochester study used a FMPS. Both Krudysz et al. (2009) and Hudda et al. (2010) indicated that regionally transported PM from upwind urban areas of Los Angeles lowered spatial variability by acting as a "homogenizing" factor during favorable meteorological conditions. This effect was not noticeable in Rochester, NY (Wang et al., 2012). Nevertheless, significant variability among sites was observed in both studies.

Table 2-8 Comparison between two urban-scale studies of UFP seasonal and spatial variability.

	Los Angeles, CA (Krudysz et al., 2009)	Rochester, NY (Wang et al., 2012)
Area	11 × 11 km, urban	9 × 9 km, urban
Sites	13 sites	12 sites
Instrumentation	SMPS (14–793 nm), CPC (>7 nm)	FMPS (with one SMPS in a fixed site), 5.6 to 560 nm
Levels of average total number concentrations	5,300 to 27,000 particles/cm^3	9,025 (summer), 10,939 (winter), 4,955 (spring), and 14,485 (fall) particles/cm^3
Seasonal variability	Relatively higher levels observed in the fall/winter than in the summer	Relatively higher levels observed in the fall/winter than in the spring; Relatively high 100–500 mode in the summer
Coefficient of divergence (COD)	>0.2 on average for all particles measured, 0.25 to 0.6 for size-dependent average COD	No clear overall pattern
Size-dependency	Number concentrations of smaller particles (<40 nm) differ from site to site, whereas larger particles tended to have similar concentrations at various sampling locations.	No clear overall pattern

Source: Krudysz et al. (2009).

2.5.1.2.5 Chemical Components

A detailed analysis of 15 urban locations in the 2009 PM ISA (U.S. EPA, 2009) indicated a generally fair degree of spatial uniformity in bulk $PM_{2.5}$ components. Exceptions were noted in one or two cities for crustal material, nitrate, elemental carbon, organic carbon and nickel (U.S. EPA, 2009). More recent observations have focused mainly on carbonaceous components across urban areas. Black carbon (BC) concentrations were 2 to 3 times higher at urban locations than at suburban locations in the greater New York area (Patel et al., 2009). There were several reports of higher concentrations of some PM components near roads with heavy traffic than other urban locations. For example, carbonaceous aerosols exhibited substantial intra-urban variability in Detroit, MI and Cleveland, OH that was consistent with local sources, with EC higher at sites adjacent to freeways and busy surface streets (Snyder et al., 2010). Site to site variability in OC was approximately 7% at distances from 0.5 to 4 km, but between 4–27% at distances 4 to 100 km. However, more finely speciated organic components differed by as much as 60% at the 0.5 to 4 km scale and up to 200% at the 4–100 km scale (Snyder et al., 2010). PAHs and steranes

along with OC and EC were found to be higher near roads with heavy traffic than in other urban locations (Xie et al., 2012). Differences of a factor of 2 to 3 between concentrations on major streets and at background locations in the same city in the Netherlands were also observed for chromium, copper, and iron, elements that were mainly present in the coarse fraction, as well as for black carbon and particle number count (Boogaard et al., 2011).

2.5.2 Temporal Variability

2.5.2.1 Regional Trends

Differences in national average concentrations and regional variability between data from immediately prior to this assessment and the 2009 PM ISA (U.S. EPA, 2009) were discussed in Section 2.5.1.1, which demonstrated substantial decreases in PM concentrations since publication of the 2009 PM ISA (U.S. EPA, 2009). This section expands on those observations by exploring long-term trends that extend back as far as 2000, when widespread network measurements of urban $PM_{2.5}$ began, in order to provide more complete assessment of trends.

2.5.2.1.1 $PM_{2.5}$

Figure 2-20 show how $PM_{2.5}$ concentrations have decreased substantially at almost all $PM_{2.5}$ monitoring sites between the periods 2003–2005 and 2013–2015, with especially large decreases in the Eastern U.S. Figure 2-21 also shows a decreasing trend of $PM_{2.5}$ concentrations as a time series using national data from network monitoring sites throughout the U.S. Overall, $PM_{2.5}$ concentrations have decreased substantially nationwide since the 2003–2005 period, especially in the Eastern U.S. $PM_{2.5}$ concentrations derived from satellite data also exhibit a decreasing trend, of $-0.39 + 0.10$ $\mu g/m^3$ per year averaged over a 1 by 1 degree grid (Boys et al., 2014).

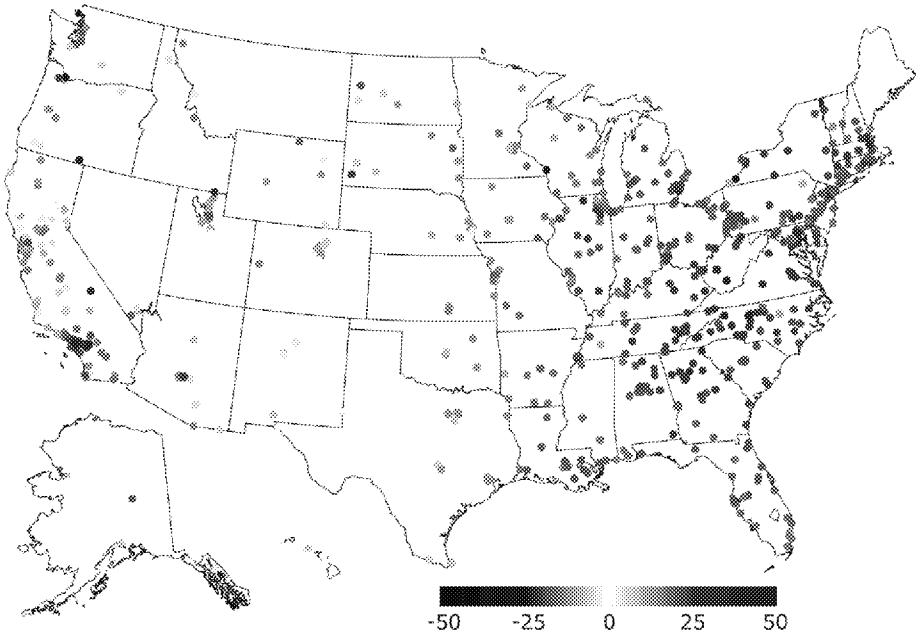

Blue indicates a decrease and red indicates an increase. Percentage increase or decrease is indicated by color intensity of the circle.

Source Permission pending: U.S. EPA 2016 analysis of Air Quality System network data 2003−2005 and 2013−2015.

Figure 2-20 Increase or decrease in 3-year annual average $PM_{2.5}$ concentrations between 2003−2005 and 2013−2015.

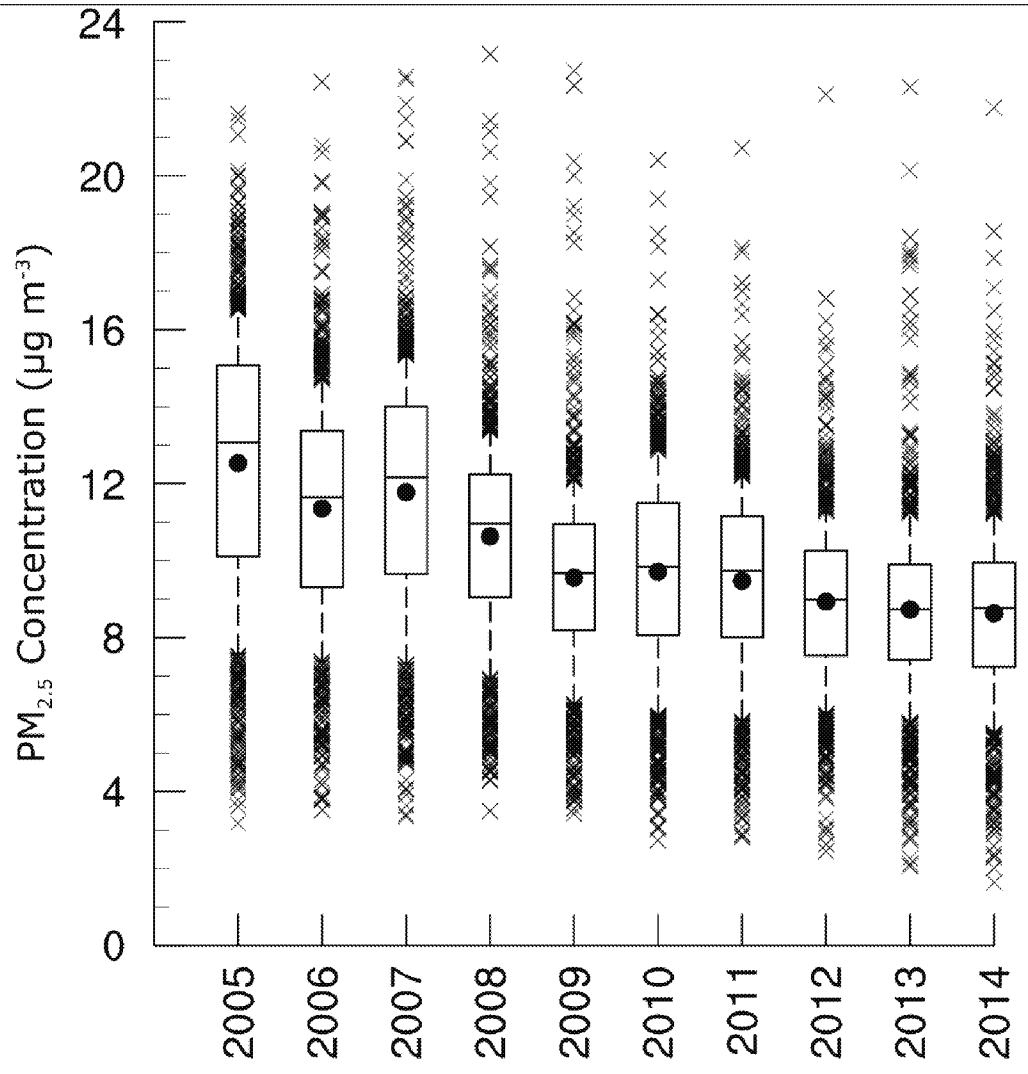

Source Permission pending: U.S. EPA 2016 analysis of Air Quality System network data 2005–2014.

Figure 2-21 Average $PM_{2.5}$ concentration trends 2005–2014

The predominant downward trends shown in Figure 2-21 are a continuation of the decreasing trend in $PM_{2.5}$ concentration reported in the 2009 PM ISA (U.S. EPA, 2009), in which a 10% decrease in annual average $PM_{2.5}$ concentrations between the 3-year period from 1999–2001 and the 3-year period from 2005–2007 was described. Figure 2-22 shows an overall decrease in monthly and annual $PM_{2.5}$ average and 90th percentile concentrations over the 16-year period from 2000–2015, as well as a steadily shrinking summer peak, across all reporting FRM site-level monitors in the U.S. (Chan et al., 2018). Over this period $PM_{2.5}$ concentration averaged over the entire network decreased by 5 $\mu g/m^3$ and 90th percentile concentrations decreased by 9 $\mu g/m^3$ (Figure 2-22). It is evident from Figure 2-22 that the sharpest decrease occurred in 2008–2010.